

Modeling the prion aspect of cerebral β -amyloidosis in organotypic slice cultures and mice

Dissertation

zur Erlangung des Grades
eines Doktors der Naturwissenschaften

der Mathematisch-Naturwissenschaftlichen Fakultät
und
der Medizinischen Fakultät
der Eberhard-Karls-Universität Tübingen

vorgelegt

von

Renata Michaela Werner
geb. Novotný
aus Freiburg im Breisgau, Deutschland

März 2016

Tag der mündlichen Prüfung: 14.07.2016

Dekan der Math.-Nat. Fakultät: Prof. Dr. W. Rosenstiel
Dekan der Medizinischen Fakultät: Prof. Dr. I. B. Autenrieth

1. Berichterstatter: Prof. Dr. M. Jucker
2. Berichterstatter: Prof. Dr. B. Heimrich

Prüfungskommission:
Prof. Dr. M. Jucker
Prof. Dr. B. Heimrich
Prof. Dr. O. Riess
Prof. Dr. S. Di Giovanni


Erklärung

Ich erkläre, dass ich die zur Promotion eingereichte Arbeit mit dem Titel:

“Modeling the prion aspect of cerebral β -amyloidosis in organotypic slice cultures and mice”

selbständig verfasst, nur die angegebenen Quellen und Hilfsmittel benutzt und wörtlich oder inhaltlich übernommene Stellen als solche gekennzeichnet habe. Ich versichere an Eides statt, dass diese Angaben wahr sind und dass ich nichts verschwiegen habe. Mir ist bekannt, dass die falsche Angabe einer Versicherung des Eides statt mit Freiheitsstrafe bis zu drei Jahren oder mit Geldstrafe bestraft wird.

Tübingen, 16.03.2016


.....
Unterschrift

For my family

Acknowledgements

First and foremost I would like to express my special appreciation and gratitude to Prof. Mathias Jucker for giving me the opportunity to pursue my PhD in his department at the Hertie Institute for Clinical Brain Research in Tübingen. I would like to thank him for his supervision as well as his support and advice during my PhD work.

My sincere thanks also go to the members of my Advisory Board, Prof. Olaf Riess and Prof. Simone Di Giovanni for their insightful comments and scientific ideas concerning my projects.

Special thanks go to Prof. Bernd Heimrich, who had a decisive influence on my scientific career, not merely as a collaboration partner, but also as a mentor. In this context I would like to express my appreciation for the members of the Department of Anatomy and Cell Biology at the Institute of Neuroanatomy at the University of Freiburg, for many years of fruitful collaboration. In particular, I would like to thank Simone Zenker, Aileen Koch, Sigrun Nestel, Stephanie Kraft and Birgit Egle for their kind support and encouragement. It was a pleasure to work with you!

I would like to thank all my colleagues of the Jucker group for contributing immensely to the quality of my professional and personal time at the Hertie Institute: Mehtap Bacioglu, Frank Baumann, Andrea Bosch, Isolde Breuer, Anika Bühler, Karoline Degenhardt, Simone Eberle, Yvonne Eisele, Timo Eninger, Sarah Fritschi, Petra Füger, Bernadette Graus, Jasmin Hefendehl, Götz Heilbronner, Michael Hruscha, Stephan Käser, Christian Krüger, Marius Lambert, Franziska Langer, Carina Leibssle, Sonia Mazzitelli, Amudha Nagarathinam, Jonas Neher, Ulrike Obermüller, Jörg Odenthal, Jay Rasmussen, Claudia Resch, Juliane Schelle, Manuel Schweighauser, Angelos Skodras, Matthias Staufenbiel, Nicholas Varvel, Bettina Wegenast-Braun, Ulla Welzel, Ann-Christin Wendeln, Jan Winchenbach and Lan Ye.

I would like to express my gratitude in particular to Franziska Langer, Sarah Fritschi and Ulrike Obermüller for the introduction into surgical methods and into other scientific techniques; Angelos Skodras for the introduction into imaging techniques; Carina Leibssle, Christian Krüger and Jörg Odenthal for their help with organizing animal work and handling laboratory mice; the animal caretakers of the FORS, especially Vera Pichler and to the veterinarians of the University of Tübingen.

My time in the laboratory of Prof. Jucker was enriched by my PhD companions and friends who became a part of my life: Mehtap Bacioglu, Manuel Schweighauser and Juliane Schelle – I thank you for the time we spent together, your support in hard times and your friendship.

Lastly, I would like to express my gratefulness to my family, my father Jaroslav, my sister Alexandra and my husband Philipp who supported and encouraged me during my time as a PhD student. I would like to thank my closest friends, Melanie and Nina, for their years of encouragement and help. You all have inspired and motivated me and for that I am deeply grateful.

Table of contents

1. Summary	7
2. Synopsis	10
2.1 Introduction	10
2.1.1 Brief history of Alzheimer's disease	10
2.1.2 The neuropathological hallmark lesions of Alzheimer's disease	11
2.1.3 Amyloid- β peptide – the root cause of Alzheimer's disease	12
2.1.4 The amyloid cascade hypothesis – A β accumulation as the primary driver	14
2.1.5 Inflammation in Alzheimer's disease	15
2.1.6 Alterations in neuronal structure and function in Alzheimer's disease	17
2.1.7 Proteinopathies – neurodegenerative diseases with abnormal protein deposition	17
2.1.8 Misfolded propagation – the common denominator in proteinopathies	18
2.2 Analogy between prions and assemblies of amyloid-β peptide	20
2.2.1 <i>In vitro</i> and <i>in vivo</i> approaches to study A β aggregation and plaque formation	20
2.2.2 Prion-like properties of amyloid- β seeds	22
2.2.3 Propagation of amyloid- β strains by prion-like seeding	23
2.2.4 Amyloid- β peptide – a prion?	24
2.3 Organotypic hippocampal slice culture models of cerebral β-amyloidosis	26
2.3.1 Organotypic slice cultures – the interface of <i>in vitro</i> and <i>in vivo</i> approaches	26
2.3.2 Organotypic slice cultures in AD research	28
2.3.3 A new powerful model to study biologically active synthetic A β conformers	28
2.4 Applicability of organotypic slice cultures in modeling α-synucleinopathies	30
2.5 Concluding remarks and outlook	31
2.6 References	33
3. Publications	47
3.1 Description of personal contribution	47
3.2 Seeded strain-like transmission of β-amyloid morphotypes in APP transgenic mice	48
3.3 Conversion of synthetic Aβ to <i>in vivo</i> active seeds and amyloid plaque formation in a hippocampal slice culture model	64
3.4 Organotypic hippocampal slice cultures as a new tool to study α-synuclein lesions	96
4. Appendix	106
4.1 Abbreviations	106
4.3 Bibliography	108

1. Summary

The aggregation of specific proteins within the nervous system is generally assumed to be a crucial element in the pathogenesis of a plethora of age-related neurodegenerative diseases. These diseases are often referred to as proteinopathies, with Alzheimer's disease (AD) and Parkinson's disease (PD) being the two most common neurodegenerative diseases of the elderly. In AD, amyloid- β peptides ($A\beta$) are the main component of insoluble aggregates forming senile plaques; in PD the α -synuclein protein (α -syn) is the main component of Lewy bodies (LBs) and Lewy neurites (LNs). Recent findings have shown that $A\beta$ aggregates as well as α -syn aggregates, can initiate the conversion of the same properly-folded protein into the misfolded, disease-associated aggregated state. This has led to the suggestion of a prion-like mechanism of disease pathogenesis. Moreover, abnormally folded proteins may adopt a range of structurally different morphologies. Such protein conformers (strains) have been described to harbor different biological activities. The objective of this thesis was to elucidate the prion-like aspects of $A\beta$ in mouse models and in organotypic slice cultures.

This thesis is divided into three sections: The first section describes the results of a study aiming to elucidate the strain-like transmission of $A\beta$ morphotypes in mouse models of cerebral β -amyloidosis. In the second section, organotypic slice cultures were developed as a versatile tool to model cerebral β -amyloidosis and gather mechanistic insights into prion-like misfolding of $A\beta$. The last section is dedicated to our effort to adopt the organotypic slice cultures to model LB and cell-to-cell transmission of misfolded α -syn aggregates.

The first study of this thesis was initiated to further examine the hypothesis that different $A\beta$ morphotypes ($A\beta$ strains) may exist. The strain-like properties of misfolded $A\beta$ aggregates after seeded transmission were investigated in two $A\beta$ -precursor protein (APP) transgenic (tg) mouse models, APP23 and APPPS1. Influenced by differences in the ratios of the two main $A\beta$ isoforms, $A\beta_{40}$ and $A\beta_{42}$, the two models develop $A\beta$ plaques of different morphology. Amyloid-laden brain extracts of either an aged APP23 or an aged APPPS1 mouse were intracerebrally injected into young pre-depositing APP23 or APPPS1 recipient mice. Similar to the strain concept described in prion diseases, the intrinsic characteristics of the source material could be stably propagated in the recipient mice, confirming a mechanism of seeded strain-like transmission. This study was performed in collaboration with K.P.R. Nilsson from the

University of Linköping in Sweden and was published in *EMBO Reports* (Heilbronner et al., 2013).

In the second study of this thesis, we established a new hippocampal slice culture (HSC) model of cerebral β -amyloidosis. The A β plaque formation in HSCs was induced by a single treatment of A β -laden brain extract from aged APP tg mice on top of the culture and the continuous supply of synthetic A β into the culture medium. This HSC model reproduces many aspects of cerebral β -amyloidosis such as A β -deposit-induced microglia response and neuronal alterations. Notably, the morphological appearance and the conformational structure of the induced A β deposits in HSCs depended again on both, the extract and the synthetic A β species used, resembling the results found in APP tg mice. The new HSC model of cerebral β -amyloidosis hence demonstrates the seeded conversion of synthetic A β in HSCs. To provide evidence for the synthetic nature of induced A β aggregates on HSCs, we used in addition HSCs from *App*-null mice and showed that endogenously expressed A β is not necessary for the A β plaque formation. However, induced A β plaque formation requires a living cellular environment since fixation of the HSC prior to treatment largely prevented amyloid plaque formation. Given that synthetic A β aggregates generated *in vitro* show less seeding activity *in vivo* and are therefore distinct from biological A β , we tested the biological efficiency of HSC-derived synthetic A β aggregates *in vivo*. Remarkably, we were the first to succeed in converting synthetic A β into biologically functional seeds by using the HSC model. Our result leads to the inference that the diversity of factors in the HSC influences the intrinsic characteristics of the synthetic peptide, rendering it more biologically-active than *in vitro*-generated synthetic A β aggregates. This study was performed in collaboration with Prof. B. Heimrich from the University of Freiburg in Germany and is in press in *The Journal of Neuroscience* (Novotny et al., 2016).

The success of the HSC model to mimic cerebral β -amyloidosis encouraged us to utilize HSCs to investigate other proteinopathies. The third part of this thesis outlines that LB- and LN-like α -syn inclusions can be induced in HSCs. Indeed, we succeeded in inducing α -syn lesions in cultures from wildtype mice and mice overexpressing human mutated α -syn by one-time application of tg brain extract containing α -syn aggregates on top of the HSCs. The same treatment yielded no inclusions on HSCs derived from α -syn-deficient mice, indicating that

culture-derived α -syn is necessary for the induction of α -syn inclusions. This study is ongoing and results are presented as unpublished data in the last part of this thesis.

In summary, the results of the first two studies presented here support the concept of prion-like-templated misfolding of A β . By using HSCs we succeeded for the first time to convert synthetic A β into *in vivo* seeding-active seeds. Furthermore, we emphasize that the involvement of cellular processes in a living HSC is crucial for the conversion to biologically-active synthetic A β aggregates. Consequently this new HSC model for cerebral β -amyloidosis is suitable to explore the contribution of cellular and molecular cofactors to achieve seeding-active A β aggregates. Additionally, our last study shows that the HSC model could also be applicable to other proteinopathies. We are the first to show inducible LB- and LN-like α -syn inclusions in slice cultures. This model can be used to investigate the cell-to-cell transmission of α -syn and could shed light on how misfolded α -syn spreads to healthy cells.

2. Synopsis

2.1 Introduction

2.1.1 Brief history of Alzheimer's disease

I'll just go to the end of the road [...]. I won't go far [...]. The street is empty. Did I reach the end of the road and turn around already? Am I going to or from, and to where? The houses on either side of the road look the same. I stand very still. I left my home less than two minutes ago, and now I am not sure where it is. [...] I didn't bring my phone and anyway I can't always remember how to use it any more. I've lost numbers [...].

Excerpt from the book: *The Memory Book* by Rowan Coleman, p.13 (Coleman, 2014)

The protagonist in “The Memory Book” written by Rowan Coleman is suffering from early onset familial Alzheimer's disease (EO-FAD). Based on a gene mutation inherited by the protagonist's father the family is now confronted with this devastating disease. AD with genetic/familial origin (familial Alzheimer's disease, FAD) can appear either at an unusually early age (> 65 years) or affect individuals after 65 years (early onset or late onset familial Alzheimer's disease, EO-FAD or LO-FAD, respectively). In contrast, the majority of sporadic AD cases is of unknown/idiopathic origin and can have either a late (< 65 years, LOAD) or an early (> 65 years, EOAD) disease onset (<http://www.alzforum.org/early-onset-familial-ad>).

Alois Alzheimer has described the first and most famous case of EOAD in 1907 (Alzheimer, 1907). He followed the case of Auguste Deter, a 51-year-old woman who had been admitted to the mental institution. He thoroughly described her clinical symptoms, including progressive cognitive decline and disorientation. Dementia at that time was generally considered as part of normal aging and was designated as “senile dementia”. The fact that Auguste Deters dementia appeared before she was 50 years old set her case apart. Alzheimer examined her brain after her death in 1906 and described the characteristic features of the disease: changes in neurofibrils (today referred to neurofibrillary tangles) and deposition of an unknown substance all over the cortex (today known as deposits of the amyloid- β peptide).

In order to distinguish this mid-life dementia from dementia occurring with ageing Alzheimer's mentor, Kraepelin introduced the eponym Alzheimer's disease in 1910 (Kraepelin, 1910). This distinction was abandoned in the 1975 when Robert Katzman declared that senile dementia and Alzheimer's disease (AD) were one and the same entity and therefore seen as one single

disease (Katzman and Karasu, 1975; Katzman, 1976). Initially, AD did not receive widespread public interest. The major landmark for public awareness of AD was achieved 1976 by the redefinition of AD from a rare disease, effecting only a small number of people, into a disease affecting numerous aged individuals becoming a major public health issue in the aging society (Katzman, 1976). This had an enormous impact on public opinion and awareness of AD. Today, the number of people living with dementia worldwide is estimated at 46.8 million and will increase to an estimated 74.7 million in 2030 (<http://www.worldalzreport2015.org>). Age is the main known risk factor for AD, with the incidence of dementia increasing exponentially with age. Due to advanced medical care, the global prevalence of AD will continuously escalate especially in industrialized nations. Therefore, AD not only counts as the most common form of dementia, it is also one of the most burdensome health conditions worldwide.

In summary, it is of outstanding interest and absolute necessity to our society to interfere with this devastating disease and the rapid increase of AD cases worldwide. Therefore, enhancing AD research is of particular importance in order to better understand the origin and the pathology of the disease and certainly to finally find an effective therapeutic strategy that delays or even prevents onset and progression of AD.

2.1.2 The neuropathological hallmark lesions of Alzheimer's disease

Alois Alzheimer's description of neurofibrillary tangles (NFTs) and extracellular amyloid plaques as one of the characteristic pathological hallmark lesions of AD has been unvalued until the technological breakthroughs in the 1960s. Using the electron microscope, Michael Kidd and Robert Terry were able to observe the paired helical filament (PHF) structure of AD-NFTs and the amyloid nature of the nucleus of neuritic plaques (Kidd, 1963; Terry et al., 1963; Wisniewski et al., 1976). Decades after these important findings, the major component of the deposits, a 39-43 amino acid peptide referred to β -amyloid (now known as amyloid- β peptide, A β), was purified from cerebral blood vessels (Glenner and Wong, 1984b) and cerebral plaques (Masters et al., 1985b), both from AD cases and from a brain of a trisomy 21 patient (Glenner and Wong, 1984a, b; Masters et al., 1985a).

Almost simultaneous to the breakthroughs achieved with A β , the microtubule associated protein tau (MAPT), a protein initially discovered by the group of Marc Kirschner (Weingarten et al., 1975; Cleveland et al., 1977), was finally identified as the main constituent of the PHF that form the NFT in AD (Grundke-Iqbal et al., 1986a; Kosik et al., 1986; Goedert et al., 1988). In the same year, it was shown that the tau protein contains abnormal hyperphosphorylation in

AD (Grundke-Iqbal et al., 1986b; Iqbal et al., 1986), depressing its binding to microtubules (Alonso et al., 1994). Altogether, each of the above-mentioned hallmark lesions has a characteristic distribution enabling the postmortem classification in different stages of AD progression (Braak and Braak, 1991; NIA-RI Consensus, 1997). The relationship between these two major pathological hallmark lesions of AD is complex. It seems that A β is not the only culprit, but rather appears to be the initiator of a diversity of pathological changes involving tau and resulting in a cascade of events proposed in the amyloid cascade hypothesis (further discussed in subsection 2.1.4.). Besides the already mentioned extracellular deposits of A β in amyloid plaques and the intracellular accumulation of hyperphosphorylated tau in NFTs, neuropil threads (Braak et al., 1986), cerebral amyloid angiopathy (Etienne et al., 1998; Jellinger, 2002), reactive microglia and astrocytes (Beach et al., 1989; Itagaki et al., 1989; Prokop et al., 2013) and neuronal and synaptic loss (DeKosky and Scheff, 1990; Jobst et al., 1994; West et al., 1994) also display characteristic features of AD. The controversial role of the immune system in AD with the main focus on microglia cells will be further discussed in subsection 2.1.5.

2.1.3 Amyloid- β peptide – the root cause of Alzheimer’s disease

In 1984 Glenner and Wong succeeded in isolating A β from cerebral blood vessels of AD cases and later from the brains of Trisomy 21 patients (Glenner and Wong, 1984a, b). The ultimate linkage between AD and Trisomy 21 was obtained by cloning the gene encoding the A β sequence and localizing it to chromosome 21 (Goldgaber et al., 1987; Kang et al., 1987; Robakis et al., 1987). The discovery and mapping to chromosome 21 also demonstrated that the 4.2 kDa A β peptide is encoded as part of the large β -amyloid precursor protein (APP), a type 1 integral membrane protein, from which shorter isoforms can be generated by alternative splicing (Kang et al., 1987; Kitaguchi et al., 1988; Ponte et al., 1988; Tanzi et al., 1988). The three major splice isoforms generated are: APP695 (predominantly expressed in the central nervous system, CNS), APP751 and APP770 (both ubiquitously expressed in non-neuronal tissue) (Kitaguchi et al., 1988; Ponte et al., 1988; Tanaka et al., 1988). A role for APP has been suggested in regulating the synapse function, synaptic transmission, plasticity and memory formation, but the precise physiological function of APP is still under debate (Dawkins and Small, 2014).

Sequential proteolytic cleavage of APP can follow two pathways: the non-amyloidogenic pathway or the amyloidogenic pathway. In the non-amyloidogenic APP processing pathway the

cleavage of APP by the α -secretase (ADAM) results in a long, secreted form of APP (APPs α) and a remaining membrane-bound carboxyterminal (C-terminal) fragment (CTF α /C83). The subsequent cleavage of CTF α by the γ -secretase complex results in the release of the C-terminal fragments, AICD and p3. The alternative amyloidogenic APP processing pathway is initiated by the cleavage of APP by the β -secretase (BACE1) resulting in the generation of secreted APP β (APPs β). The cleavage of the remaining membrane-bound part (CTF β /C99) by the γ -secretase complex results in the liberation of AICD and A β . Compelling evidence indicates that cleavage of A β by the γ -secretase complex is taking place sequentially, initially releasing A β peptides with different carboxyl endings, either A β_{1-49} or A β_{1-48} , depending on the exact cleavage site of the γ -secretase (Takami et al., 2009). These two major precursors are subsequently processed along two different production lines (either A β_{1-49} →A β_{1-46} →A β_{1-43} →A β_{1-40} or A β_{1-48} →A β_{1-45} →A β_{1-42} →A β_{1-38}) releasing distinct intermediate A β isoforms. A β_{1-40} and A β_{1-42} are the most abundant isoforms of A β with A β_{1-42} being much more prone to aggregate into amyloid fibrils than A β_{1-40} (Yan and Wang, 2006). A β fibrils may further aggregate and deposit as A β plaques. A detailed description of the APP processing is illustrated in Fig. 1.

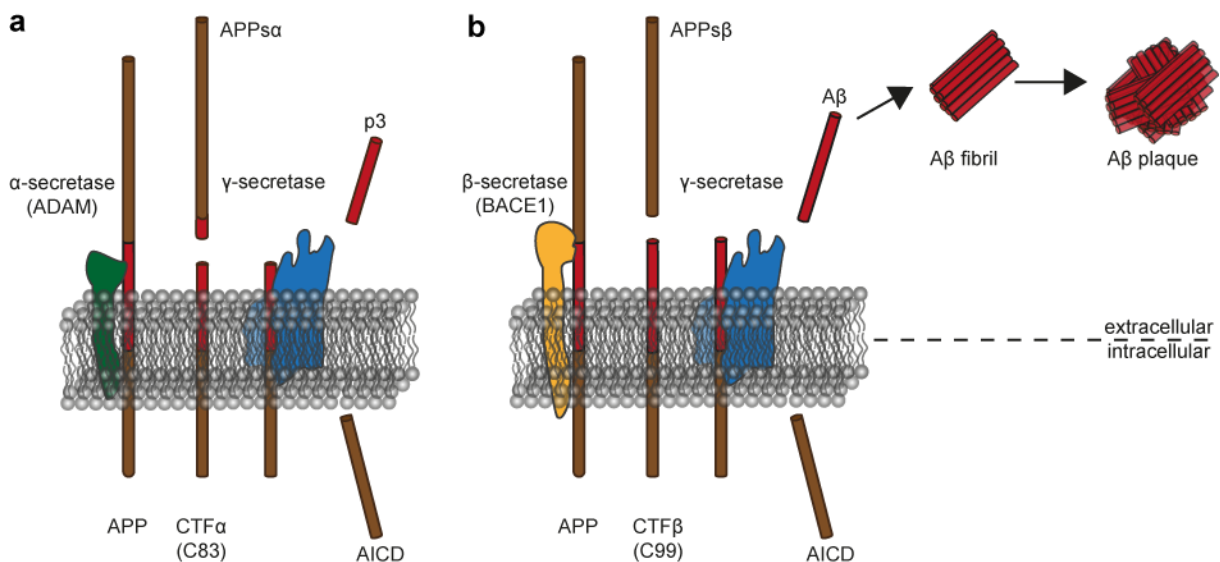


Fig. 1 Processing of the β -amyloid precursor protein (APP). **(a)** In the non-amyloidogenic pathway initial cleavage of APP by the α -secretase (ADAM) results in the generation of a long secreted form of APP (APPs α). The remaining C-terminal part (CTF α /C83) is further processed by the γ -secretase generating the products p3 and AICD. **(b)** The amyloidogenic APP processing pathway is initiated by cleaving APP by the β -secretase (BACE1) generating the long secreted form of APP (APPs β) and the remaining membrane bound CTF β /C99. Subsequent cleavage by the γ -secretase results in A β and AICD. Extracellularly secreted A β peptides tend to oligomerize and fibrillize, ultimately leading to the production of large aggregates or A β plaques (adapted from Thinakaran and Koo, 2008).

2.1.4 The amyloid cascade hypothesis – A β accumulation as the primary driver

The announcement of the exact amino acid sequence of A β by Glenner and Wong in 1984 (Glenner and Wong, 1984a) opened the scientific floodgates: in the following years A β was isolated from senile plaques (Masters et al., 1985b) and the APP gene was mapped to chromosome 21 (Goldgaber et al., 1987; Kang et al., 1987; Robakis et al., 1987). This can be considered the cornerstone of the amyloid cascade hypothesis: the deposition of A β in amyloid plaques is assumed to be the result of an imbalance between A β generation and clearance. This initial step is followed by neuroinflammation, tau tangle formation and hence leading to neuron loss and finally to the manifestation of the disease (Hardy and Allsop, 1991; Hardy and Higgins, 1992). Therefore, according to the amyloid cascade hypothesis, a sequence of events initiated by the deposition of A β in the brain leads ultimately to AD (Hardy and Selkoe, 2002). Genetic linkage of AD to chromosome 21 was reported for four large EO-FAD pedigrees (St George-Hyslop et al., 1987). The first pathogenic mutation in APP (Levy et al., 1990) linked to chromosome 21 was revealed in a Dutch family, causing hereditary cerebral hemorrhage with amyloidosis (human hereditary cerebral hemorrhage with amyloidosis of the Dutch type: HCHWA-D; Dutch E693Q) (Van Broeckhoven et al., 1990). Additional mutations were subsequently found in APP: Goate and colleagues described an EO-FAD mutation in APP (London mutation APP V717I) (Goate et al., 1991). The identical mutation was found in the same year in several families affected by FAD (Hardy, 1991). Additional mutations were discovered by other research groups including the Swedish M670/671NL (Mullan et al., 1992), Indiana V717F (Murrell et al., 1991) and Arctic E693G (Kamino et al., 1992) mutations (for more details on mutations, please see <http://www.alzforum.org/mutations>). Encouraged by these findings, soon two other genes – presenilin 1 (PSEN1) and presenilin 2 (PSEN2) – were reported as novel EO-FAD genes on chromosome 14 and chromosome 1, respectively (Schellenberg et al., 1992; St George-Hyslop et al., 1992). Mutations in any of these three genes (APP, PSEN1 and PSEN2) are fully penetrant and result in FAD. Intriguingly, researchers found that the increased genetic expression of APP alone, without the involvement of any mutations, is already sufficient to lead to AD (Cabrejo et al., 2006; Rovelet-Lecrux et al., 2006; Sleegers et al., 2006). APP locus duplication as well as mutations in any of these three genes result in EOAD due to the increased production of the highly amyloidogenic A β ₁₋₄₂ species.

The discovery of mutations in APP offered a treasure trove of strategies for the generation of tg mouse models of cerebral β -amyloidosis and amyloid pathology in the 1990s (Games et al., 1995; Hsiao et al., 1996; Sturchler-Pierrat et al., 1997). However, the presence of negative

linkage results obtained from EO-FAD families showed that mutations in APP were only present in a small number of families. The majority (99%) of people suffering from AD do not have a family history of AD and have an average disease onset of 65 years (late onset Alzheimer's disease, LOAD). Genetic variants, in combination with lifestyle and environmental exposure factors are considered to increase the susceptibility for LOAD (Reitz et al., 2011). A well-established genetic risk factor for LOAD is the ϵ 4-allele of the apolipoprotein E gene (APOE) (Schmechel et al., 1993; Strittmatter et al., 1993): already one copy of the ϵ 4-allele of the APOE (APOE4) increases AD risk by 4-fold and 2 copies by 12-fold (Corder et al., 1993). ApoE is a lipoprotein highly expressed in the liver and in the brain where it is in the latter secreted mainly by astrocytes and microglial cells (Xu et al., 2000; Xu et al., 2006). ApoE is essential for efficient intracellular clearance of soluble A β by microglia and promotes A β degradation in an isoform-dependent manner. The increased risk of AD by APOE4 is hence mediated by impaired and consequently less efficient removal of A β peptides from the brain by the ApoE4 isoform (Jiang et al., 2008).

The search for additional genetic risk factors was further enabled by the technological breakthrough in the development of genome-wide association studies (GWAS) (<http://www.alzgene.org/largescale.asp>). GWAS led to the identification of several genetic risk loci for LOAD with the involvement in lipid processing (APOE, ABCA7), endocytosis (PICALM, BIN1) and immunity (CR1, CD33) suggesting a pathogenic role for inflammatory processes in AD (Karch et al., 2014). Taken together, these new insights achieved by GWAS underline the importance of inflammation to AD pathogenesis and additionally justify attributing a more significant role of the immune system in AD progression (Gandy and Heppner, 2013; Prokop et al., 2013). The following section is devoted to the current view of brain-specific immune cells and their function in AD.

2.1.5 Inflammation in Alzheimer's disease

AD pathology is characterized by an inflammatory response mediated by the immune cells of the brain, primarily by CNS-resident cells like microglia, astrocytes and perivascular myeloid cells (Prinz et al., 2011). In brain tissue from AD patients or from mouse models of AD, activated microglia closely accumulate around A β plaques interacting through their processes with A β fibrils (Itagaki et al., 1989; Stalder et al., 1999). The tight clustering of microglial cells around A β plaques indicated early on that the immune system might have an important role in AD pathogenesis (Perlmutter et al., 1990; Aisen, 1997).

Microglia fulfill a panoply of tasks such as scanning the brain for pathogens, removing cellular debris and supporting CNS homeostasis and plasticity by continuously shaping and remodeling synapses (reviewed in: Prinz and Priller, 2014). However, the role of microglia as helpful actors in AD seems to be only one side of the coin. New preclinical and genetic data strongly suggests that the activation of the immune system not only accompanies AD pathology, but also drives AD pathogenesis (Prokop et al., 2013; Zhang et al., 2013a). Microglia can take up soluble A β via macropinocytosis (Mandrekar et al., 2009), whereas fibrillar forms of A β are phagocytosed after initiating a highly complex intracellular signaling cascade via complement receptor-mediated binding (Akiyama et al., 2000). Furthermore, A β activates microglia by binding to the receptor for advanced glycation end products (RAGE, Yan et al., 1996) and to other scavenger receptors (Paresce et al., 1996; Bamberger et al., 2003), ultimately leading to a proinflammatory response (El Khoury et al., 2003; Stewart et al., 2010) accompanied by a phenotypic change of microglia (Kreutzberg, 1996). Paradoxically, the release of pro-inflammatory cytokines and chemokines seems to impair microglial mediated clearance of A β long-term and may ultimately lead to the loss of protective functions (Akiyama et al., 2000; Heneka and O'Banion, 2007; Hickman et al., 2008). Early activation of microglia in AD may restrict A β plaque formation, but chronic microglial activation may contribute to a more severe disease progression (Holmes et al., 2009).

The role of the immune system in AD therefore is puzzling, but inflammation has recently become a pivotal topic since GWAS have revealed variants of immune-related genes as risk factors for LOAD (Lambert et al., 2013; Neumann and Daly, 2013). Among them, variants of the triggering receptor expressed on myeloid cells 2 (TREM2) have been found to triple the risk of developing AD (Guerreiro et al., 2013; Jonsson et al., 2013) and therefore provide strong evidence that inflammation is integral to the AD disease process. TREM2 is expressed in the brain by myeloid cells and is an important modulator of immune cell function. Recent publications underscore the role of TREM2 in AD by showing that TREM2 detects damage-associated lipid patterns, sustaining the microglial response to A β accumulation, while TREM2 deficiency reduces phagocytic activities of microglia mainly by promoting the survival of activated microglia (Kawabori et al., 2015; Wang et al., 2015).

In summary, recent work has accentuated the capacity of the brain's immune cells to influence AD pathophysiology. It has been suggested that immune cells act in a beneficial way at early disease stages while influencing AD pathophysiology in a more detrimental way at late stages. This suggests that the change of underlying immune events during disease course has to be

carefully taken into account when developing new drugs to therapeutically target inflammatory pathways.

2.1.6 Alterations in neuronal structure and function in Alzheimer's disease

Anatomical changes in the AD brain are characterized by massive neuronal cell and synapse loss. These changes correlate much better with the clinical manifestation of AD than the extracellular deposition of aggregated A β in plaques (DeKosky and Scheff, 1990; Terry et al., 1991; Sze et al., 1997). It has been suggested that changes in the expression of synaptic proteins might manifest already early in synaptic damage and are therefore identifiable in patients with mild cognitive impairment (MCI) or early stages of AD (Masliah et al., 2001; Scheff et al., 2007). Recent studies suggest that soluble intracellular A β – in particularly oligomeric forms – interfere with synaptic function leading to cognitive decline and dementia (Takahashi et al., 2002; Shankar and Walsh, 2009; Gouras et al., 2010). Nevertheless, the order of events leading to alterations in neuronal structures is under controversial debate: One study published by Meyer-Luehmann and colleagues provided new possible insights into the temporal sequence of these events, showing that amyloid plaque formation led to activation and recruitment of microglia followed by the appearance of dystrophic neurites (Meyer-Luehmann et al., 2008). However, the final proof that only extracellular A β plays a role in the formation of A β plaques and neuritic dystrophy is still missing. Another study is rather in support of the theory that intraneuronal A β is causing neuritic dystrophy, suggesting that ruptured neurons form the core of neuritic plaques by releasing intranuclear A β , ultimately leading to A β plaques (Pensalfini et al., 2014).

2.1.7 Proteinopathies – neurodegenerative diseases with abnormal protein deposition

Structurally misfolded proteins are grouped under the term proteinopathy and mostly display the physiological and chemical properties of amyloid. Despite different amino acid sequences, amyloid fibrils share certain features, such as a β -pleated-sheet secondary structure and a characteristic cross- β diffraction pattern when isolated from tissue and analyzed by X-ray diffraction (Eanes and Glenner, 1968). Furthermore, the amyloid fibrils bind Congo red and show green birefringence under polarized light (Divry and Florkin, 1927; Buxbaum and Linke, 2012; Sipe et al., 2014). Non-branching fibrils usually have a diameter of approximately 10 nm (Cohen and Calkins, 1959). To date, more than 31 extracellular fibril proteins and their clinical manifestation in amyloidosis are described in humans and classified by the International Society of Amyloidosis (Sipe et al., 2014). Furthermore, due to the existence of intracellular

protein inclusions that fulfill the criteria of amyloid protein fibrils, the initial definition of a mainly extracellular depositing amyloid fibril has been expanded and now also includes 'intracellular' amyloid (Westermarck et al., 2007; Sipe et al., 2014). Intracellular inclusions of the tau protein for example fulfill the criteria of an 'intracellular amyloid', whereby inclusions of the protein α -synuclein only display some of the amyloid features. Protein misfolding and the presence of abnormally enriched β -sheets is a common feature of amyloids, including prions. In the following subsection the self-propagation of disease-causing misfolded structures by templated misfolding will be discussed.

2.1.8 Misfolded propagation – the common denominator in proteinopathies

In 1966 Gajdusek and colleagues (Gajdusek et al., 1966) showed for the first time the transmissibility of a human disease called Kuru that shared remarkable similarities to scrapie, a disease of sheep and goats. Stanley Prusiner and colleagues identified in 1982 (Prusiner, 1982) the pathogenic particle responsible for this disease and assigned the term prion (proteinaceous infectious particle). Prion diseases, also termed transmissible spongiform encephalopathy (TSE), include bovine spongiform encephalopathy (BSE) in cows, scrapie in sheep and Creutzfeldt-Jakob disease (CJD) in humans. The common feature of TSE is the conversion of the cellular natively folded prion protein (cellular prion protein, PrP^C) into a β -sheet-rich pathological isoform termed PrP^{Sc} ("scrapie" form of the prion protein, Prusiner, 1998). The latter interact with physiological PrP^C converting it into toxic PrP^{Sc} and thereby accelerating the formation of aggregates and fibrils. The precise molecular mechanism of the conversion of PrP^C into PrP^{Sc} remains elusive. However, the current prion paradigm suggests that infectious oligomeric PrP^{Sc} acts as a seed that interacts with PrP^C and converts it into PrP^{Sc} (Pan et al., 1993; Prusiner, 1998). The converted PrP^{Sc} is incorporated into a growing polymer, which at some point breaks into smaller pieces and initiates a crystallization-like process known as 'seeded-nucleation' (Come et al., 1993; Jarrett and Lansbury, 1993). The rate-limiting step is the formation of the initial stable oligomeric nucleus that is also called 'seed'. Omitting the process of nucleus forming by the addition of preformed PrP^{Sc} seeds therefore accelerates protein aggregation (Jarrett and Lansbury, 1993). Although the mechanism of protein propagation and seeded aggregation of proteins was first revealed in prion disease, it soon emerged to apply to other non-prion neurodegenerative disease proteins (Prusiner, 2012; Jucker and Walker, 2013). A schematic illustration of the processes involved in the seeded-nucleation is depicted in Fig. 2. Multiple lines of evidence indicate common characteristics of

PrP^{Sc} and A β seeds (Goedert, 2015; Walker and Jucker, 2015). In the following section we have further investigated the prion-like properties of amyloid- β seeds.

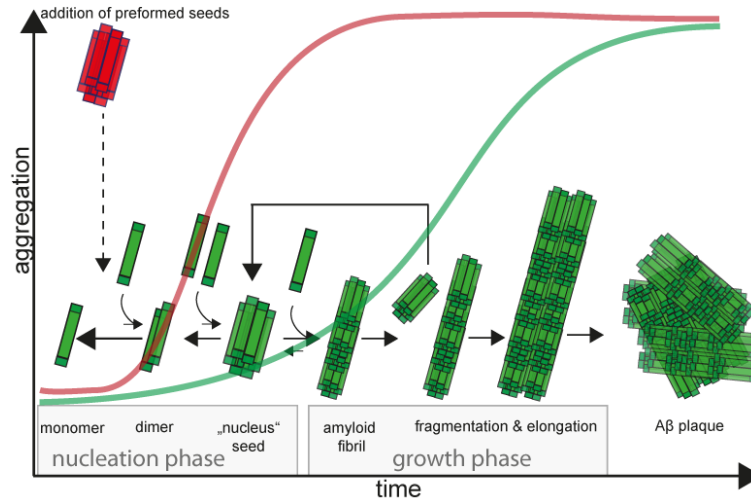


Fig. 2 Nucleation-dependent amyloid aggregation. In the slow nucleation phase monomers misfold and self-associate to form an oligomeric nucleus (seed). Once a seed is formed, larger aggregates assemble and the amyloid fibril elongates rapidly. The kinetics of the slow nucleation phase followed by a rapid growth phase is well presented by a sigmoidal shaped curve (green curve). The aggregation of misfolded monomers into seeds is the rate limiting step since a critical concentration of seeds has to be formed before entering into the growth phase. The addition of preformed seeds can shorten the nucleation phase by inducing faster aggregate formation (red curve). Aggregated fibrils can deposit as intracellular (NFTs, LBs) or extracellular (A β plaques) lesions (adapted and modified from Kumar and Walter, 2011).

2.2 Analogy between prions and assemblies of amyloid- β peptide

In reference to:

Seeded strain-like transmission of β -amyloid morphotypes in APP transgenic mice

Götz Heilbronner, Yvonne S. Eisele, Franziska Langer, Stephan A. Kaeser, **Renata Novotny**, Amudha Nagarathinam, Andreas Åslund, Per Hammarström, K. Peter R. Nilsson & Mathias Jucker (2013). *EMBO Reports*; 14(11):1017-1022.

2.2.1 *In vitro* and *in vivo* approaches to study A β aggregation and plaque formation

The knowledge of mechanisms of fibril formation and the understanding of fundamental processes that cause and underlie proteinopathies are seen as a prerequisite for the development of efficient diagnostic and therapeutic means. In 1993 a nucleation-dependent polymerization process for A β aggregation was proposed (Jarrett and Lansbury, 1993; Harper and Lansbury, 1997) and several cell-free *in vitro* aggregation studies of synthetic or recombinant A β peptides in solution supported this idea (Meinhardt et al., 2007; DaSilva et al., 2010; Du et al., 2011). Furthermore, a molecular modeling approach to understand the ability of peptides to self-aggregate into β -sheet structures in solution was described (Lopez De La Paz et al., 2002). Simultaneously, detailed structural information about A β fibrils was obtained using solid-state nuclear magnetic resonance (NMR) measurements of synthetic A β peptides aggregated *in vitro* (Petkova et al., 2002). Results from the same group additionally displayed that fibrils that grow from seeds inherit their morphological and molecular traits from the initial seed and demonstrated the self-propagation of amyloid structure (Petkova et al., 2005). Another widely used *in vitro* approach are cell lines and primary cultures to study A β cytotoxicity and investigate the mechanism of amyloid plaque formation. Thus, several research groups investigated the toxic function of different A β species by suggesting A β oligomers to be the potentially most toxic form of the peptide (Lambert et al., 1998; Walsh et al., 2002). The cell culture system was used as a method to investigate the possible involvement of the cellular environment on A β aggregation (Friedrich et al., 2010), solidifying previous studies claiming that A β plaque formation may have an intracellular basis (Takahashi et al., 2002; Rajendran et al., 2007; Hu et al., 2009). Recently, stem-cell technology has advanced to the point of induced pluripotent stem cells (iPSCs) being used to model AD pathology (Choi et al., 2014).

Cellular models are a powerful system enabling detailed studies of AD pathogenesis, but unfortunately single cell lines do not efficiently reflect the complexity of the brain. The generation of several tg mouse models recapitulating nearly all aspects of A β amyloid pathology bolstered the understanding and therapeutic approaches of AD (Jucker, 2010). The widely used mouse models of amyloid pathology are based on the overexpression of human APP bearing mutations associated with FAD (Games et al., 1995; Hsiao et al., 1996; Sturchler-Pierrat et al., 1997). Tg mice overexpressing mutant presenilin (PS) were also generated, but although their production of the aggregation prone isoform A β ₁₋₄₂ is increased (Duff et al., 1996), they do not exhibit cerebral amyloid deposits. However, double tg mice co-expressing human mutated APP and PS were generated to further investigate the impact of mutant PS on APP processing (Borchelt et al., 1996; Citron et al., 1997). In the following years our laboratory has used APP tg mouse models for experiments aiming to explore the nucleation dependent polymerization of A β aggregates by prion-like seeding (Meyer-Luehmann et al., 2006; Eisele et al., 2009; Hamaguchi et al., 2012) with the main purpose to gain insights about the amyloid-inducing A β species (Langer et al., 2011) and to investigate the routes of A β induction (Eisele et al., 2010). Although each mouse model provides unique features, APP tg mice for instance only show moderate neuronal loss (Calhoun et al., 1998; Rupp et al., 2011) and are lacking tau pathology, hence modeling disease aspects and not reflecting the whole spectrum of the disease. A triple tg mouse model (3xtg-AD) with mutations in APP, PS1 and tau, recapitulates most closely the proteopathic alterations seen in AD and is suggested to more completely model AD pathology (Oddo et al., 2003).

In summary, high accessibility for manipulations is an important advantage of *in vitro* approaches, especially when used for initial screenings in high-throughput tests to determine e.g. the most promising drug, prior testing *in vivo*. However, the outcome of drugs tested *in vitro* might differ dramatically from the *in vivo* efficacy due to the fact that different cell types and cell connectivity cannot be taken in account *in vitro*. The outstanding strength of animal models is the possibility to investigate relevant aspects of the disease in the context of cell diversity and connectivity, albeit the complex mechanisms involved in the disease process are not directly accessible.

2.2.2 Prion-like properties of amyloid- β seeds

A plethora of research has aimed to characterize the similarities of PrP^{Sc} and A β seeds. Baker and colleagues (Baker et al., 1993) performed one of the first experimental studies reporting the exogenous induction of senile plaques after intracerebral injection of AD brain homogenates into marmosets (*Callithrix jacchus*). The conclusion of the authors that A β and associated factors can initiate and accelerate plaque formation was further confirmed by seeding experiments performed in APP tg mouse models (Kane et al., 2000; Walker et al., 2002; Meyer-Luehmann et al., 2006; Eisele et al., 2009). Work from our laboratory showed that not only intracerebral injection of A β -rich brain extract (seeding extract), but also peripherally applied seeding extract could hasten amyloid deposition in mice (Eisele et al., 2010; Eisele et al., 2014) similar to the findings made in prion diseases in rodents (Kimberlin and Walker, 1986; Aguzzi and Calella, 2009). Furthermore, we could show that in particular, small, soluble and proteinase K resistant A β aggregates are highly potent seeds (Langer et al., 2011) and prion-like seeding of A β aggregation is possible even with subattomolar amounts of brain-derived A β (Fritschi et al., 2014b). These A β seeds do (partially) resist heat (Meyer-Luehmann et al., 2006) and formaldehyde inactivation (Fritschi et al., 2014a) as it has been shown before for prions (Pattison, 1965; Prusiner, 1982). A very intriguing aspect of prion disease is that the disease protein acquires different protein conformations targeting specific brain regions (Bruce et al., 1989; Hecker et al., 1992) and causing unique clinical characteristics (Fraser and Dickinson, 1973; Mastrianni et al., 1999), hence representing distinct prion strains. The biological activity harbored by a particular prion strain is hereby enciphered in the conformation of the protein (Peretz et al., 2001). The strain phenomenon was further supported by producing *de novo* PrP^{Sc} *in vitro* (Saborio et al., 2001) in the absence of any brain-derived starting material but with unique clinical, neuropathological and biochemical characteristics *in vivo* (Legname et al., 2006; Deleault et al., 2007; Barria et al., 2009). Approaches to identify the minimal requirements necessary for *de novo* prion formation further led to the identification of polyanions (RNA) and lipids (Geoghegan et al., 2007; Deleault et al., 2012). The generation of various synthetic prion strains provided the ultimate evidence in support of the prion paradigm (Barria et al., 2009). The potential to form distinct strains leading to clinical and pathological heterogeneity in patients is also considered in AD (Lu et al., 2013; Knowles et al., 2014; Watts et al., 2014) and is the subject of the next subsection.

2.2.3 Propagation of amyloid- β strains by prion-like seeding

Amyloid fibrils are polymorphic, meaning that the amino acid sequence is not necessarily determining the molecular structure of amyloid fibrils. The presumption that amyloid- β can form distinct strains was a seminal finding in the AD field. Petkova and colleagues (Petkova et al., 2005) were one of the first to describe structural variations of A β *in vitro*. These different variations of A β depend on aggregation conditions and structural properties of the initial seeds and revealed significantly different toxicities in neuronal culture. Note that differences in neurotoxicity might also have biological implications, correlating structural variations with disease severity. In addition, this study gave the first evidence for self-propagating molecular polymorphism in amyloid fibrils: newly formed A β fibers retained the structural identity of the starting material – the initial seed.

The first approaches to assess the existence of A β strains *in vivo* were performed by Meyer-Luehmann and colleagues (Meyer-Luehmann et al., 2006). In this fundamental experiment, it was shown that the morphology and composition of exogenously induced cerebral β -amyloidosis depends on both, the host and the donor material. Extract from two different aged, plaque-laden APP tg mice (APPPS1 or APP23) were injected into young APP23 and APPPS1 mice, respectively. These two tg mouse lines show differences in plaque morphology (large, diffuse deposits in APP23 tg mice; small and coarse deposits in APPPS1 tg mice) as well as in the endogenous expression of A β isoforms (A β ₁₋₄₀ > A β ₁₋₄₂ in APP23 tg mice; A β ₁₋₄₂ > A β ₁₋₄₀ in APPPS1 tg mice) (Sturchler-Pierrat et al., 1997; Radde et al., 2006). We initiated a new study where we expand the previous results by additionally determining the biochemical composition and the intrinsic conformational differences of induced morphotypes. We reproduced the results from the previous published study showing that the morphology of the induced deposition is dependent on the amyloid inducing agent and the recipient. Furthermore, there is a preference in incorporating the host A β isoform that resembles the isoform predominantly available in the initial extract. In addition, we were able to demonstrate the ability of the exogenously applied seeds to impose their conformational properties to the recruited A β peptides of the host by applying luminescent conjugated polythiophenes (LCPs). LCPs have been used before to discriminate various prion strains (Sigurdson et al., 2007) and heterogeneous A β deposits *in vitro* and *in vivo* (Nilsson et al., 2007) and they have been proven to be a powerful and elegant tool to discriminate between distinct protein conformations.

In summary, these results show that the intrinsic properties of the initial seeds were able to alter the morphology and conformation of induced deposits by shifting the A β ₄₀/A β ₄₂ ratio in

seeded plaques. These results give strong evidence for transmissible amyloid conformers in AD mouse models and draw parallels to the seeded conversion described in prion disease.

2.2.4 Amyloid- β peptide – a prion?

There are great commonalities between A β seeds and prions, but the definitive proof for the formation of a self-propagating A β aggregate – by excluding auxiliary factors for the conversion of A β into a prion state – was long overdue. For a long time experiments to prove that A β alone is the amyloid-inducing agent were not successful, since synthetic A β peptides failed to induce A β deposition *in vivo* (Meyer-Luehmann et al., 2006). It was not until 2012 that Stohr and colleagues (Stohr et al., 2012) provided the final proof that A β is sufficient for the formation of a self-propagating assembly and hence is the amyloid-inducing agent. However, the specific biological seeding activity of the aggregated synthetic A β used in this study was much less than the one of brain-derived A β . It can be speculated that – given the fact that brain extracts contain much more than only A β – additional cofactors are needed to enhance the seeding potential of synthetic material (Xiao et al., 2015). A similar conclusion was also drawn in the prion field where researchers from different groups were able to spontaneously generate and propagate PrP^{Sc} when PrP^C was associated with nucleic acid or lipid molecules (Deleault et al., 2007; Deleault et al., 2012; Zhang et al., 2013b). Cell-specific cofactors might not only support the conversion of PrP^C into PrP^{Sc}, but also be responsible for the formation of distinct conformations (strains) consequently leading to variations in lesion profiles in prion diseases (Aguzzi et al., 2007). Recently, two studies suggested that clinically distinct disease progressions observed in AD patients have most probably their origin in the given shape of A β (Stohr et al., 2014; Watts et al., 2014). The heritable trait might hereby be conserved within the protein-shape as it was proposed before for prions. Remarkably, the researchers showed that specific strain-like conformational variants of synthetic A β exist and these can seed more aggregates of that same conformation *in vivo* (Stohr et al., 2014).

Nevertheless, the question whether A β is a prion is still under debate, since one defining feature of prions is being infectious (Gajdusek et al., 1966; Prusiner, 1982). A recently published study raises the possibility that A β may be transmissible between humans under certain rare circumstances (Jaunmuktane et al., 2015). This assumption is based on the finding that some patients that received cadaver-derived human growth hormone in their youth died from CJD as a result of these injections and additionally developed extensive A β deposition in the brain and vasculature. Notably, these patients were between 36 and 51 years of age – way

too early to develop AD pathology. It is therefore assumed that A β seeds were already present in the injected material and induced A β aggregation in these patients after an incubation time of about 30 years (Jaunmuktane et al., 2015). Recently, another study revealed A β pathology in patients that died from CJD after receiving dural grafts (Frontzek et al., 2016). However, it is important to emphasize that under other conditions, there is no evidence that AD pathology is transmissible between humans.

2.3 Organotypic hippocampal slice culture models of cerebral β -amyloidosis

In reference to:

Conversion of synthetic A β to *in vivo* active seeds and amyloid plaque formation in a hippocampal slice culture model

Renata Novotny*, Franziska Langer*, Jasmin Mahler, Angelos Skodras, Andreas Vlachos, Bettina M. Wegenast-Braun, Stephan A. Kaeser, Jonas J. Neher, Yvonne S. Eisele, Marie J. Pietrowski, K. Peter R. Nilsson, Thomas Deller, Matthias Staufenbiel, Bernd Heimrich and Mathias Jucker (2016). In press in *The Journal of Neuroscience*.

* contributed equally

2.3.1 Organotypic slice cultures – the interface of *in vitro* and *in vivo* approaches

Organotypic slice cultures (OSCs) are an innovative and potent *in vitro* method and slices from different brain regions are currently an important tool to study the structural connectivity as well as physiological properties and pharmacological applications. The term ‘organotypic’ implies that the original tissue organization is maintained and interactions between different cell types are fundamentally preserved in a fashion close to the *in vivo* situation. In the following, a brief outline of two commonly used techniques of slice culture cultivation will be introduced – the latter being used in this work.

In 1981 Gähwiler presented a new technique to cultivate brain slices long-term in contrast to the commonly used short living “acute” slices, which were used as an alternative to *in vivo* electrophysiology studies. In Gähwiler’s roller tube technique the OSCs were embedded in a chicken plasma clot on coverslips and cultivated in medium by using a roller-drum to assure a continuous changing of the liquid-gas interface by rotation with an appropriate angle (Gähwiler, 1981). The brain slices retained many essential architectural features of the host tissue, such as neuronal connectivity and glial-neuronal interactions (Gähwiler et al., 1997). This technique is quite difficult to handle and bears high experimental variability due to tissue thinning through abrasion processes. However, the resulting non-physiological monolayer of cells makes it possible to visualize individual cells directly with phase contrast microscopy without the necessity of re-slicing the cultures. Furthermore, exogenously applied substances to the media are in direct contact with the culture avoiding time consuming diffusion. Unfortunately, this method does not allow repeated morphological observations during culturing, since an embedding material covers the tissue. To overcome this limitation, Stoppini

et al. introduced a new and much simpler culturing method: the membrane interface culture method (Stoppini et al., 1991). This technique generates brain slices that maintain viability during long-term cultivation, successfully preserves the tissue architecture, provides good experimental access and allows the precise control of the extracellular environment. The slices are placed on semipermeable membranes, obtaining nutrition via capillary action from medium on the bottom side and kept alive inside a thin film of fluid at the air-liquid interface at the upper side (Bergold and Casaccia-Bonnel, 1997). OSCs are typically prepared from animals at postnatal days 3-9 since tissue from young animals shows a high degree of plasticity and resistance to mechanical trauma during slice preparation (Gähwiler et al., 1997; Lossi et al., 2009). Slice cultures from a variety of different brain regions – including the hippocampus, striatum, cortex, spinal cord and cerebellum – have been established over the past years (reviewed in Lossi et al., 2009). Nevertheless, the hippocampus is by far the best-characterized brain area in slice cultures: all neuronal types (the granule cells, the pyramidal neurons and the interneurons) are well preserved in HSCs, albeit shortly after preparation the density of synaptic contacts decreases due to traumatic injury by preparation. After a few days the slice culture recovers and neurite outgrowth and reactivated synaptogenesis can be observed (Stoppini et al., 1993; Bahr, 1995). In a study from De Simoni and colleagues cultivation time of slice cultures and the age of postnatal animals was matched by comparing the status of the development of neurons and synaptic changes. The significant finding in this study was that after 1 week *in vitro* the changes were established to a degree that the following development proceeded almost in parallel to the development *in vivo* (De Simoni et al., 2003). This is the reason why in experimental settings the treatment of slice cultures is generally started at the earliest after 1 week of cultivation to ensure stable culturing conditions. Remarkably, the recovery of the slice cultures is taking place without additional external stimuli, since afferent fibers are cut during preparation and thereafter degenerate (De Simoni et al., 2003). OSCs have become a popular tool to bridge the gap between *in vitro* and *in vivo* approaches. In the following subsection we give a brief outline of the application of OSCs in the field of AD research.

2.3.2 Organotypic slice cultures in AD research

The first study published in the context of AD was aiming to investigate the toxic effect of A β (Malouf, 1992). In this study synthetic A β fragments of various lengths were directly injected into different regions of the HSC, but without a notable effect. Studies followed where synthetic A β was either injected (Harrigan et al., 1995) or applied directly under or on top of the culture (Allen et al., 1995), reaching a slightly toxic effect. Finally, a study by Bruce et al. succeeded in showing that treatment of mature cultures with A β results in neuronal injury in a time- and concentration dependent manner (Bruce et al., 1996). Follow up studies were aiming to explore the involved cell signaling pathways by which the A β peptide induces toxicity in HSCs (Dineley et al., 2001; Nassif et al., 2007) as well as exploring the influence of human synthetic and naturally secreted cell-derived A β ₁₋₄₂ on the induction of long-term potentiation (Wang et al., 2004). The first plaque-like A β aggregates in HSCs were induced by the application of synthetic A β to the culture media after adding modulating pro-inflammatory stimuli (Harris-White et al., 1998). In 2006 Johansson et al. characterized in HSCs the consequences of induced lesions on neuronal and glial cell populations after exposure to synthetic A β ₂₅₋₃₅ and A β ₁₋₄₂ peptides (Johansson et al., 2006b). Furthermore, exposure to synthetic A β ₂₅₋₃₅ lead to increased tau phosphorylation in HSCs providing the first evidence for a link between A β and tau phosphorylation in HSCs (Johansson et al., 2006a). OSC contain several cell populations and retain the general cytoarchitecture, revealing possibilities for *in vitro* studies bridging to *in vivo* systems. The application of HSCs to investigate mechanisms underlying the prion-like behavior of A β will be outlined in the next subsection.

2.3.3 A new powerful model to study biologically active synthetic A β conformers

In a newly described *ex vivo* hippocampal slice culture (HSC) model we induced A β deposition and recapitulated many aspects of AD-associated β -amyloid induced lesions. HSCs were treated once with seeding extract from aged APP tg mice and continuously with synthetic A β to induce A β deposition. The induction of A β deposition required both, the seeding extract and the synthetic A β , suggesting that deposition in HSCs occurs via seeded conversion of synthetic A β . In fact, by using HSCs from *App*-null mice it has been proofed that amyloid plaque formation in HSCs is indeed independent from endogenously expressed A β , hence providing evidence for the synthetic nature of induced A β aggregates. Nevertheless, since fixation of the culture prior to treatment largely prevented amyloid plaque formation, a living cellular environment is necessary for amyloid plaque formation in HSCs. Furthermore, by applying seeding extract

from two different APP tg mice (APP23 and APPPS1) in combination with two different isoforms of synthetic A β (A β ₁₋₄₀ and A β ₁₋₄₂) we found that morphological and conformational differences of A β deposits depend on both, the source of the seed and the nature of synthetic A β . The differences in the conformation of induced A β deposits were assessed by applying luminescent conjugated oligothiophenes (LCOs, Klingstedt et al., 2011). To test the biological efficiency of the synthetic HSC-amyloid, extract from HSCs with induced A β deposition was injected into young APP tg mice. Although, *in vitro* aggregated synthetic A β can act as seed *in vivo* (Stohr et al., 2012; Stohr et al., 2014), it's seeding efficacy is much lower than the one from brain-derived aggregated A β (Meyer-Luehmann et al., 2006; Stohr et al., 2012; Stohr et al., 2014). Remarkably and in contrast these studies, this innovative HSC model for β -amyloidosis shows for the first time that *in vitro* HSC-aggregated synthetic A β is seeding active *in vivo* in the same order of magnitude as the brain derived aggregated A β . Therefore, our study favors that the living slice culture may contain factors that confers the synthetic A β peptide's prion-like properties. The important finding of the seeded conversion of synthetic A β into biologically-active A β aggregates in HSCs should consequently ease further studies targeting the factors responsible for its conversion. The involvement of cofactors like polyanions and lipids has been described before in prion propagation and thus may also have an impact on A β aggregation (Geoghegan et al., 2007; Deleault et al., 2012).

Expanding our scientific knowledge about the factors involved in the aggregation process of A β will drive the AD field forward by exposing possible points of attack to slow-down and combat disease progression. Furthermore, HSCs combine the advantages of maintained structural and functional properties of the hippocampus *in vivo* with a high accessibility for manipulation to accomplish the demands of a powerful *in vitro* tool. We therefore emphasize that slice cultures may become a suitable model to study other proteinopathies as well. In the following section we discuss in more detail the application of HSCs to study α -syn inclusions.

2.4 Applicability of organotypic slice cultures in modeling α -synucleinopathies

In reference to:

Organotypic hippocampal slice cultures as a new tool to study α -synuclein lesions

Renata Novotny*, Mehtap Bacioglu*, Manuel Schweighauser, Jasmin Mahler, K. Peter R. Nilsson, Bernd Heimrich and Mathias Jucker. *Unpublished data.*

* contributed equally

Neurodegenerative diseases defined as α -synucleinopathies include Parkinson's disease (PD), Dementia with Lewy Bodies (DLB) and Multiple System Atrophy (MSA). PD is the second most common neurodegenerative disease after AD and characterized by the accumulation of misfolded α -synuclein (α -syn) protein (Spillantini et al., 1998a). The α -syn protein in its native state is unfolded, but can become misfolded forming aggregates rich in β -sheet structures (Conway et al., 2000; Serpell et al., 2000). Intracellular deposits of aggregated α -syn are the main components of Lewy bodies (LBs) and Lewy neurites (LNs) (Spillantini et al., 1998b) and are a prominent neuropathological hallmark of PD. LBs and LNs appear in the brain over time, following a stereotypical pattern, suggesting a cell-to-cell transmission within interconnected neurons (Braak et al., 2003). Motor symptoms of PD manifest later during the disease and are caused by the degeneration of dopaminergic neurons. Transplantations of human embryonic dopaminergic neurons into the brains of patients with PD were performed with the hope to improve the motor control of these patients by replenishing the missing neurotransmitter dopamine (Lindvall et al., 1990; Freed et al., 2001). Surprisingly, several studies showed that α -syn positive LBs appeared in the grafted tissue decades after transplantation (Kordower et al., 2008; Li et al., 2008; Kurowska et al., 2011). To explain this unexpected finding a mechanism of prion-like transmission of α -syn was proposed. Albeit a diversity of α -syn tg mouse models has been developed and confirmed the host-to-graft transfer of α -syn *in vivo* (Desplats et al., 2009; Hansen et al., 2011) the underlying mechanisms of the cell-to-cell transmission are still under investigation. Given the benefits of OSCs with its maintained *in vivo* cellular interactions and preserved three-dimensional structure, OSCs may help in unrevealing how misfolded α -syn moves between cells, thereby complementing current mouse work (reviewed in Dehay et al., 2016). Therefore, we aimed to establish a slice culture model to study α -syn inclusions. Unpublished data of this ongoing project is presented in subsection 3.4.

2.5 Concluding remarks and outlook

Proteinopathies are clinically heterogeneous with a progressive disease pathogenesis. A possible explanation for the phenotypic variations in AD patients might be that different strains of A β aggregates exist. Therefore, the aim of this PhD was to evaluate the hypothesis that A β strains exist by using APP tg mouse models and a newly established HSC model. Furthermore, we aim to provide a deeper understanding of the prion-like aspects of A β aggregation and propagation.

From the present study the transmission of characteristic strain-like features, such as an alteration of the A β ratio and the imprint of the intrinsic conformation of the source brain material to the induced A β deposits became apparent. We can now conclude from these results that strain-like characteristics of A β are transmitted to the host by seeded conversion and hence our results point to the existence of prion-like A β strains. Nevertheless, experiments focusing on serial passaging of the induced material are required to add to the growing body of evidence that A β strains exist. Further experiments have to be performed to show that distinct A β strains harbor different biological functions that finally result in distinct disease phenotypes.

It is suggested that cofactors may be involved in the conversion of A β into biologically active A β assemblies. Therefore, we established a new HSC model for cerebral β -amyloidosis where we succeeded to convert synthetic A β into biologically active *in vivo* seeds. The present finding favors the idea that the biological activity of synthetically derived A β aggregates indeed relies on a suitable chemical and physical environment, which is provided by the living HSC. Future experiments could be targeted towards the identification of the underlying cellular and molecular factors that promote the conversion to a pathological, biologically functional A β conformation. A recommended approach could be to use potent inhibitors to block endocytic pathways in the HSC to rule certain pathways either in or out.

In general, our results add to the growing body of evidence that A β strains exist by displaying the transmission and propagation of intrinsic properties of A β seeds in APP tg mice and HSCs. The new HSC model for cerebral β -amyloidosis additionally assigns an important role to living cells and cofactors for the conversion of synthetic A β into biologically functional protein conformations. Further research on the mechanistic cellular functions and the nature of the cofactors involved in A β plaque formation are major challenges that can be overcome with the

new HSC model. The identification of the nature of these cofactors could help to target β -amyloidosis therapeutically.

The application of HSCs as a model to study α -syn lesions is ongoing and we aim to further elucidate the α -syn cell-to-cell transmission in this model. Furthermore, mechanisms underlying the seeded aggregation of α -syn can be investigated in slice cultures. The HSC system offers the opportunity to study the consequences of α -syn lesions for the surrounding tissue as well as on neuronal circuits. Consequently, we see a lot of potential in this new model of α -synucleinopathies.

2.6 References

- Aguzzi A, Calella AM. Prions: protein aggregation and infectious diseases. *Physiol. Rev.*, 2009; 89: 1105-52.
- Aguzzi A, Heikenwalder M, Polymenidou M. Insights into prion strains and neurotoxicity. *Nat. Rev. Mol. Cell Biol.*, 2007; 8: 552-61.
- Aisen PS. Inflammation and Alzheimer's disease: mechanisms and therapeutic strategies. *Gerontology*, 1997; 43: 143-9.
- Akiyama H, Barger S, Barnum S, Bradt B, Bauer J, Cole GM, et al. Inflammation and Alzheimer's disease. *Neurobiol. Aging*, 2000; 21: 383-421.
- Allen YS, Devanathan PH, Owen GP. Neurotoxicity of beta-amyloid protein: cytochemical changes and apoptotic cell death investigated in organotypic cultures. *Clin. Exp. Pharmacol. Physiol.*, 1995; 22: 370-1.
- Alonso AC, Zaidi T, Grundke-Iqbal I, Iqbal K. Role of abnormally phosphorylated tau in the breakdown of microtubules in Alzheimer disease. *Proc. Natl. Acad. Sci. U. S. A.*, 1994; 91: 5562-6.
- Alzheimer A. Über eine eigenartige Erkrankung der Hirnrinde. *Allgemeine Zeitschrift für Psychiatrie und psychisch-gerichtliche Medizin*, 1907; 64: 146-8.
- Bahr BA. Long-term hippocampal slices: a model system for investigating synaptic mechanisms and pathologic processes. *J. Neurosci. Res.*, 1995; 42: 294-305.
- Baker HF, Ridley RM, Duchen LW, Crow TJ, Bruton CJ. Evidence for the experimental transmission of cerebral beta-amyloidosis to primates. *Int. J. Exp. Pathol.*, 1993; 74: 441-54.
- Bamberger ME, Harris ME, McDonald DR, Husemann J, Landreth GE. A cell surface receptor complex for fibrillar beta-amyloid mediates microglial activation. *J. Neurosci.*, 2003; 23: 2665-74.
- Barria MA, Mukherjee A, Gonzalez-Romero D, Morales R, Soto C. De novo generation of infectious prions in vitro produces a new disease phenotype. *PLoS Pathog.*, 2009; 5: e1000421.
- Beach TG, Walker R, McGeer EG. Patterns of gliosis in Alzheimer's disease and aging cerebrum. *Glia*, 1989; 2: 420-36.
- Bergold PJ, Casaccia-Bonofil P. Preparation of organotypic hippocampal slice cultures using the membrane filter method. *Methods Mol. Biol.*, 1997; 72: 15-22.
- Borchelt DR, Thinakaran G, Eckman CB, Lee MK, Davenport F, Ratovitsky T, et al. Familial Alzheimer's disease-linked presenilin 1 variants elevate Abeta1-42/1-40 ratio in vitro and in vivo. *Neuron*, 1996; 17: 1005-13.
- Braak H, Braak E. Neuropathological staging of Alzheimer-related changes. *Acta Neuropathol.*, 1991; 82: 239-59.
- Braak H, Braak E, Grundke-Iqbal I, Iqbal K. Occurrence of neuropil threads in the senile human brain and in Alzheimer's disease: a third location of paired helical filaments outside of neurofibrillary tangles and neuritic plaques. *Neurosci. Lett.*, 1986; 65: 351-5.

- Braak H, Del Tredici K, Rub U, de Vos RA, Jansen Steur EN, Braak E. Staging of brain pathology related to sporadic Parkinson's disease. *Neurobiol. Aging*, 2003; 24: 197-211.
- Bruce AJ, Malfroy B, Baudry M. beta-Amyloid toxicity in organotypic hippocampal cultures: protection by EUK-8, a synthetic catalytic free radical scavenger. *Proc. Natl. Acad. Sci. U. S. A.*, 1996; 93: 2312-6.
- Bruce ME, McBride PA, Farquhar CF. Precise targeting of the pathology of the sialoglycoprotein, PrP, and vacuolar degeneration in mouse scrapie. *Neurosci. Lett.*, 1989; 102: 1-6.
- Buxbaum JN, Linke RP. A molecular history of the amyloidoses. *J. Mol. Biol.*, 2012; 421: 142-59.
- Cabrejo L, Guyant-Marechal L, Laquerriere A, Verdelletto M, De la Fourniere F, Thomas-Anterion C, et al. Phenotype associated with APP duplication in five families. *Brain*, 2006; 129: 2966-76.
- Calhoun ME, Wiederhold KH, Abramowski D, Phinney AL, Probst A, Sturchler-Pierrat C, et al. Neuron loss in APP transgenic mice. *Nature*, 1998; 395: 755-6.
- Choi SH, Kim YH, Hebisch M, Sliwinski C, Lee S, D'Avanzo C, et al. A three-dimensional human neural cell culture model of Alzheimer's disease. *Nature*, 2014; 515: 274-8.
- Citron M, Westaway D, Xia W, Carlson G, Diehl T, Levesque G, et al. Mutant presenilins of Alzheimer's disease increase production of 42-residue amyloid beta-protein in both transfected cells and transgenic mice. *Nat. Med.*, 1997; 3: 67-72.
- Cleveland DW, Hwo SY, Kirschner MW. Purification of tau, a microtubule-associated protein that induces assembly of microtubules from purified tubulin. *J. Mol. Biol.*, 1977; 116: 207-25.
- Cohen AS, Calkins E. Electron microscopic observations on a fibrous component in amyloid of diverse origins. *Nature*, 1959; 183: 1202-3.
- Coleman R. *The Memory Book*. 2014: 13.
- Come JH, Fraser PE, Lansbury PT, Jr. A kinetic model for amyloid formation in the prion diseases: importance of seeding. *Proc. Natl. Acad. Sci. U. S. A.*, 1993; 90: 5959-63.
- Conway KA, Harper JD, Lansbury PT, Jr. Fibrils formed in vitro from alpha-synuclein and two mutant forms linked to Parkinson's disease are typical amyloid. *Biochemistry*, 2000; 39: 2552-63.
- Corder EH, Saunders AM, Strittmatter WJ, Schmechel DE, Gaskell PC, Small GW, et al. Gene dose of apolipoprotein E type 4 allele and the risk of Alzheimer's disease in late onset families. *Science*, 1993; 261: 921-3.
- DaSilva KA, Shaw JE, McLaurin J. Amyloid-beta fibrillogenesis: structural insight and therapeutic intervention. *Exp. Neurol.*, 2010; 223: 311-21.
- Dawkins E, Small DH. Insights into the physiological function of the beta-amyloid precursor protein: beyond Alzheimer's disease. *J. Neurochem.*, 2014; 129: 756-69.
- De Simoni A, Griesinger CB, Edwards FA. Development of rat CA1 neurones in acute versus organotypic slices: role of experience in synaptic morphology and activity. *J. Physiol.*, 2003; 550: 135-47.
- Dehay B, Vila M, Bezard E, Brundin P, Kordower JH. Alpha-synuclein propagation: New insights from animal models. *Mov. Disord.*, 2016; 31: 161-8.

- DeKosky ST, Scheff SW. Synapse loss in frontal cortex biopsies in Alzheimer's disease: correlation with cognitive severity. *Ann. Neurol.*, 1990; 27: 457-64.
- Deleault NR, Harris BT, Rees JR, Supattapone S. Formation of native prions from minimal components in vitro. *Proc. Natl. Acad. Sci. U. S. A.*, 2007; 104: 9741-6.
- Deleault NR, Piro JR, Walsh DJ, Wang F, Ma J, Geoghegan JC, et al. Isolation of phosphatidylethanolamine as a solitary cofactor for prion formation in the absence of nucleic acids. *Proc. Natl. Acad. Sci. U. S. A.*, 2012; 109: 8546-51.
- Desplats P, Lee HJ, Bae EJ, Patrick C, Rockenstein E, Crews L, et al. Inclusion formation and neuronal cell death through neuron-to-neuron transmission of alpha-synuclein. *Proc. Natl. Acad. Sci. U. S. A.*, 2009; 106: 13010-5.
- Dineley KT, Westerman M, Bui D, Bell K, Ashe KH, Sweatt JD. Beta-amyloid activates the mitogen-activated protein kinase cascade via hippocampal alpha7 nicotinic acetylcholine receptors: In vitro and in vivo mechanisms related to Alzheimer's disease. *J. Neurosci.*, 2001; 21: 4125-33.
- Divry P, Florkin M. Sur les proprietes optiques de l'amyloide. *Comptes Rendus de la Societe de Biologie*, 1927; 97: 1808-10.
- Du D, Murray AN, Cohen E, Kim HE, Simkovsky R, Dillin A, et al. A kinetic aggregation assay allowing selective and sensitive amyloid-beta quantification in cells and tissues. *Biochemistry*, 2011; 50: 1607-17.
- Duff K, Eckman C, Zehr C, Yu X, Prada CM, Perez-tur J, et al. Increased amyloid-beta42(43) in brains of mice expressing mutant presenilin 1. *Nature*, 1996; 383: 710-3.
- Eanes ED, Glenner GG. X-ray diffraction studies on amyloid filaments. *J. Histochem. Cytochem.*, 1968; 16: 673-7.
- Eisele YS, Bolmont T, Heikenwalder M, Langer F, Jacobson LH, Yan ZX, et al. Induction of cerebral beta-amyloidosis: intracerebral versus systemic A β inoculation. *Proc. Natl. Acad. Sci. U. S. A.*, 2009; 106: 12926-31.
- Eisele YS, Fritschy SK, Hamaguchi T, Obermuller U, Fuger P, Skodras A, et al. Multiple factors contribute to the peripheral induction of cerebral beta-amyloidosis. *J. Neurosci.*, 2014; 34: 10264-73.
- Eisele YS, Obermuller U, Heilbronner G, Baumann F, Kaeser SA, Wolburg H, et al. Peripherally applied A β -containing inoculates induce cerebral beta-amyloidosis. *Science*, 2010; 330: 980-2.
- El Khoury JB, Moore KJ, Means TK, Leung J, Terada K, Toft M, et al. CD36 mediates the innate host response to beta-amyloid. *J. Exp. Med.*, 2003; 197: 1657-66.
- Etiene D, Kraft J, Ganju N, Gomez-Isla T, Gemelli B, Hyman BT, et al. Cerebrovascular Pathology Contributes to the Heterogeneity of Alzheimer's Disease. *J. Alzheimers Dis.*, 1998; 1: 119-34.
- Fraser H, Dickinson AG. Scrapie in mice. Agent-strain differences in the distribution and intensity of grey matter vacuolation. *J. Comp. Pathol.*, 1973; 83: 29-40.
- Freed CR, Greene PE, Breeze RE, Tsai WY, DuMouchel W, Kao R, et al. Transplantation of embryonic dopamine neurons for severe Parkinson's disease. *N. Engl. J. Med.*, 2001; 344: 710-9.

- Friedrich RP, Tepper K, Ronicke R, Soom M, Westermann M, Reymann K, et al. Mechanism of amyloid plaque formation suggests an intracellular basis of Abeta pathogenicity. *Proc. Natl. Acad. Sci. U. S. A.*, 2010; 107: 1942-7.
- Fritschi SK, Cintron A, Ye L, Mahler J, Buhler A, Baumann F, et al. Abeta seeds resist inactivation by formaldehyde. *Acta Neuropathol.*, 2014a; 128: 477-84.
- Fritschi SK, Langer F, Kaeser SA, Maia LF, Portelius E, Pinotsi D, et al. Highly potent soluble amyloid-beta seeds in human Alzheimer brain but not cerebrospinal fluid. *Brain*, 2014b; 137: 2909-15.
- Frontzek K, Lutz MI, Aguzzi A, Kovacs GG, Budka H. Amyloid-beta pathology and cerebral amyloid angiopathy are frequent in iatrogenic Creutzfeldt-Jakob disease after dural grafting. *Swiss Med. Wkly.*, 2016; 146: w14287.
- Gahwiler BH. Organotypic monolayer cultures of nervous tissue. *J. Neurosci. Methods*, 1981; 4: 329-42.
- Gähwiler BH, Capogna M, Debanne D, McKinney RA, Thompson SM. Organotypic slice cultures: a technique has come of age. *Trends Neurosci.*, 1997; 20: 471-7.
- Gajdusek DC, Gibbs CJ, Alpers M. Experimental transmission of a Kuru-like syndrome to chimpanzees. *Nature*, 1966; 209: 794-6.
- Games D, Adams D, Alessandrini R, Barbour R, Berthelette P, Blackwell C, et al. Alzheimer-type neuropathology in transgenic mice overexpressing V717F beta-amyloid precursor protein. *Nature*, 1995; 373: 523-7.
- Gandy S, Heppner FL. Microglia as dynamic and essential components of the amyloid hypothesis. *Neuron*, 2013; 78: 575-7.
- Geoghegan JC, Valdes PA, Orem NR, Deleault NR, Williamson RA, Harris BT, et al. Selective incorporation of polyanionic molecules into hamster prions. *J. Biol. Chem.*, 2007; 282: 36341-53.
- Glenner GG, Wong CW. Alzheimer's disease and Down's syndrome: sharing of a unique cerebrovascular amyloid fibril protein. *Biochem. Biophys. Res. Commun.*, 1984a; 122: 1131-5.
- Glenner GG, Wong CW. Alzheimer's disease: initial report of the purification and characterization of a novel cerebrovascular amyloid protein. *Biochem. Biophys. Res. Commun.*, 1984b; 120: 885-90.
- Goate A, Chartier-Harlin MC, Mullan M, Brown J, Crawford F, Fidani L, et al. Segregation of a missense mutation in the amyloid precursor protein gene with familial Alzheimer's disease. *Nature*, 1991; 349: 704-6.
- Goedert M. NEURODEGENERATION. Alzheimer's and Parkinson's diseases: The prion concept in relation to assembled Abeta, tau, and alpha-synuclein. *Science*, 2015; 349: 1255555.
- Goedert M, Wischik CM, Crowther RA, Walker JE, Klug A. Cloning and sequencing of the cDNA encoding a core protein of the paired helical filament of Alzheimer disease: identification as the microtubule-associated protein tau. *Proc. Natl. Acad. Sci. U. S. A.*, 1988; 85: 4051-5.
- Goldgaber D, Lerman MI, McBride OW, Saffiotti U, Gajdusek DC. Characterization and chromosomal localization of a cDNA encoding brain amyloid of Alzheimer's disease. *Science*, 1987; 235: 877-80.

- Gouras GK, Tampellini D, Takahashi RH, Capetillo-Zarate E. Intraneuronal beta-amyloid accumulation and synapse pathology in Alzheimer's disease. *Acta Neuropathol.*, 2010; 119: 523-41.
- Grundke-Iqbal I, Iqbal K, Quinlan M, Tung YC, Zaidi MS, Wisniewski HM. Microtubule-associated protein tau. A component of Alzheimer paired helical filaments. *J. Biol. Chem.*, 1986a; 261: 6084-9.
- Grundke-Iqbal I, Iqbal K, Tung YC, Quinlan M, Wisniewski HM, Binder LI. Abnormal phosphorylation of the microtubule-associated protein tau (τ) in Alzheimer cytoskeletal pathology. *Proc. Natl. Acad. Sci. U. S. A.*, 1986b; 83: 4913-7.
- Guerreiro R, Wojtas A, Bras J, Carrasquillo M, Rogaeva E, Majounie E, et al. TREM2 variants in Alzheimer's disease. *N. Engl. J. Med.*, 2013; 368: 117-27.
- Hamaguchi T, Eisele YS, Varvel NH, Lamb BT, Walker LC, Jucker M. The presence of Abeta seeds, and not age per se, is critical to the initiation of Abeta deposition in the brain. *Acta Neuropathol.*, 2012; 123: 31-7.
- Hansen C, Angot E, Bergstrom AL, Steiner JA, Pieri L, Paul G, et al. alpha-Synuclein propagates from mouse brain to grafted dopaminergic neurons and seeds aggregation in cultured human cells. *J. Clin. Invest.*, 2011; 121: 715-25.
- Hardy J. Molecular classification of Alzheimer's disease. *Lancet*, 1991; 337: 1342-3.
- Hardy J, Allsop D. Amyloid deposition as the central event in the aetiology of Alzheimer's disease. *Trends Pharmacol. Sci.*, 1991; 12: 383-8.
- Hardy J, Selkoe DJ. The amyloid hypothesis of Alzheimer's disease: progress and problems on the road to therapeutics. *Science*, 2002; 297: 353-6.
- Hardy JA, Higgins GA. Alzheimer's disease: the amyloid cascade hypothesis. *Science*, 1992; 256: 184-5.
- Harper JD, Lansbury PT, Jr. Models of amyloid seeding in Alzheimer's disease and scrapie: mechanistic truths and physiological consequences of the time-dependent solubility of amyloid proteins. *Annu. Rev. Biochem.*, 1997; 66: 385-407.
- Harrigan MR, Kunkel DD, Nguyen LB, Malouf AT. Beta amyloid is neurotoxic in hippocampal slice cultures. *Neurobiol. Aging*, 1995; 16: 779-89.
- Harris-White ME, Chu T, Balverde Z, Sigel JJ, Flanders KC, Frautschy SA. Effects of transforming growth factor-beta (isoforms 1-3) on amyloid-beta deposition, inflammation, and cell targeting in organotypic hippocampal slice cultures. *J. Neurosci.*, 1998; 18: 10366-74.
- Hecker R, Taraboulos A, Scott M, Pan KM, Yang SL, Torchia M, et al. Replication of distinct scrapie prion isolates is region specific in brains of transgenic mice and hamsters. *Genes Dev.*, 1992; 6: 1213-28.
- Heilbronner G, Eisele YS, Langer F, Kaeser SA, Novotny R, Nagarathinam A, et al. Seeded strain-like transmission of beta-amyloid morphotypes in APP transgenic mice. *EMBO Rep*, 2013; 14: 1017-22.
- Heneka MT, O'Banion MK. Inflammatory processes in Alzheimer's disease. *J. Neuroimmunol.*, 2007; 184: 69-91.

- Hickman SE, Allison EK, El Khoury J. Microglial dysfunction and defective beta-amyloid clearance pathways in aging Alzheimer's disease mice. *J. Neurosci.*, 2008; 28: 8354-60.
- Holmes C, Cunningham C, Zotova E, Woolford J, Dean C, Kerr S, et al. Systemic inflammation and disease progression in Alzheimer disease. *Neurology*, 2009; 73: 768-74.
- Hsiao K, Chapman P, Nilsen S, Eckman C, Harigaya Y, Younkin S, et al. Correlative memory deficits, abeta elevation, and amyloid plaques in transgenic mice. *Science*, 1996; 274: 99-102.
- Hu X, Crick SL, Bu G, Frieden C, Pappu RV, Lee JM. Amyloid seeds formed by cellular uptake, concentration, and aggregation of the amyloid-beta peptide. *Proc. Natl. Acad. Sci. U. S. A.*, 2009; 106: 20324-9.
- Iqbal K, Grundke-Iqbal I, Zaidi T, Merz PA, Wen GY, Shaikh SS, et al. Defective brain microtubule assembly in Alzheimer's disease. *Lancet*, 1986; 2: 421-6.
- Itagaki S, Mcgeer PL, Akiyama H, Zhu S, Selkoe D. Relationship of Microglia and Astrocytes to Amyloid Deposits of Alzheimer-Disease. *J. Neuroimmunol.*, 1989; 24: 173-82.
- Jarrett JT, Lansbury PT, Jr. Seeding "one-dimensional crystallization" of amyloid: a pathogenic mechanism in Alzheimer's disease and scrapie? *Cell*, 1993; 73: 1055-8.
- Jaunmuktane Z, Mead S, Ellis M, Wadsworth JD, Nicoll AJ, Kenny J, et al. Evidence for human transmission of amyloid-beta pathology and cerebral amyloid angiopathy. *Nature*, 2015; 525: 247-50.
- Jellinger KA. Alzheimer disease and cerebrovascular pathology: an update. *J. Neural Transm.*, 2002; 109: 813-36.
- Jiang Q, Lee CY, Mandrekar S, Wilkinson B, Cramer P, Zelcer N, et al. ApoE promotes the proteolytic degradation of Abeta. *Neuron*, 2008; 58: 681-93.
- Jobst KA, Smith AD, Szatmari M, Esiri MM, Jaskowski A, Hindley N, et al. Rapidly progressing atrophy of medial temporal lobe in Alzheimer's disease. *Lancet*, 1994; 343: 829-30.
- Johansson S, Jamsa A, Vasange M, Winblad B, Luthman J, Cowburn RF. Increased tau phosphorylation at the Ser396 epitope after amyloid beta-exposure in organotypic cultures. *Neuroreport*, 2006a; 17: 907-11.
- Johansson S, Radesater AC, Cowburn RF, Thyberg J, Luthman J. Modelling of amyloid beta-peptide induced lesions using roller-drum incubation of hippocampal slice cultures from neonatal rats. *Exp. Brain Res.*, 2006b; 168: 11-24.
- Jonsson T, Stefansson H, Steinberg S, Jonsdottir I, Jonsson PV, Snaedal J, et al. Variant of TREM2 associated with the risk of Alzheimer's disease. *N. Engl. J. Med.*, 2013; 368: 107-16.
- Jucker M. The benefits and limitations of animal models for translational research in neurodegenerative diseases. *Nat. Med.*, 2010; 16: 1210-4.
- Jucker M, Walker LC. Self-propagation of pathogenic protein aggregates in neurodegenerative diseases. *Nature*, 2013; 501: 45-51.

- Kamino K, Orr HT, Payami H, Wijsman EM, Alonso ME, Pulst SM, et al. Linkage and mutational analysis of familial Alzheimer disease kindreds for the APP gene region. *Am. J. Hum. Genet.*, 1992; 51: 998-1014.
- Kane MD, Lipinski WJ, Callahan MJ, Bian F, Durham RA, Schwarz RD, et al. Evidence for seeding of beta - amyloid by intracerebral infusion of Alzheimer brain extracts in beta -amyloid precursor protein-transgenic mice. *J. Neurosci.*, 2000; 20: 3606-11.
- Kang J, Lemaire HG, Unterbeck A, Salbaum JM, Masters CL, Grzeschik KH, et al. The precursor of Alzheimer's disease amyloid A4 protein resembles a cell-surface receptor. *Nature*, 1987; 325: 733-6.
- Karch CM, Cruchaga C, Goate AM. Alzheimer's disease genetics: from the bench to the clinic. *Neuron*, 2014; 83: 11-26.
- Katzman R. Editorial: The prevalence and malignancy of Alzheimer disease. A major killer. *Arch. Neurol.*, 1976; 33: 217-8.
- Katzman R, Karasu TB. Differential diagnosis of dementia. Neurological and sensory disorders in the elderly. Stratton Intercontinental Medical Book corporation: WS Fields (Ed.), 1975: 103-34.
- Kawabori M, Kacimi R, Kauppinen T, Calosing C, Kim JY, Hsieh CL, et al. Triggering receptor expressed on myeloid cells 2 (TREM2) deficiency attenuates phagocytic activities of microglia and exacerbates ischemic damage in experimental stroke. *J. Neurosci.*, 2015; 35: 3384-96.
- Kidd M. Paired helical filaments in electron microscopy of Alzheimer's disease. *Nature*, 1963; 197: 192-3.
- Kimberlin RH, Walker CA. Pathogenesis of scrapie (strain 263K) in hamsters infected intracerebrally, intraperitoneally or intraocularly. *J. Gen. Virol.*, 1986; 67 (Pt 2): 255-63.
- Kitaguchi N, Takahashi Y, Tokushima Y, Shiojiri S, Ito H. Novel precursor of Alzheimer's disease amyloid protein shows protease inhibitory activity. *Nature*, 1988; 331: 530-2.
- Klingstedt T, Aslund A, Simon RA, Johansson LB, Mason JJ, Nystrom S, et al. Synthesis of a library of oligothiophenes and their utilization as fluorescent ligands for spectral assignment of protein aggregates. *Org. Biomol. Chem.*, 2011; 9: 8356-70.
- Knowles TP, Vendruscolo M, Dobson CM. The amyloid state and its association with protein misfolding diseases. *Nat. Rev. Mol. Cell Biol.*, 2014; 15: 384-96.
- Kordower JH, Chu Y, Hauser RA, Freeman TB, Olanow CW. Lewy body-like pathology in long-term embryonic nigral transplants in Parkinson's disease. *Nat. Med.*, 2008; 14: 504-6.
- Kosik KS, Joachim CL, Selkoe DJ. Microtubule-associated protein tau (tau) is a major antigenic component of paired helical filaments in Alzheimer disease. *Proc. Natl. Acad. Sci. U. S. A.*, 1986; 83: 4044-8.
- Kraepelin E. Ein Lehrbuch für Studierende und Ärzte. *Psychatrie II*, 1910; 8.
- Kreutzberg GW. Microglia: a sensor for pathological events in the CNS. *Trends Neurosci.*, 1996; 19: 312-8.
- Kumar S, Walter J. Phosphorylation of amyloid beta (A β) peptides - a trigger for formation of toxic aggregates in Alzheimer's disease. *Aging (Albany NY)*, 2011; 3: 803-12.

- Kurowska Z, Englund E, Widner H, Lindvall O, Li JY, Brundin P. Signs of degeneration in 12-22-year old grafts of mesencephalic dopamine neurons in patients with Parkinson's disease. *J. Parkinsons Dis.*, 2011; 1: 83-92.
- Lambert JC, Ibrahim-Verbaas CA, Harold D, Naj AC, Sims R, Bellenguez C, et al. Meta-analysis of 74,046 individuals identifies 11 new susceptibility loci for Alzheimer's disease. *Nat. Genet.*, 2013; 45: 1452-8.
- Lambert MP, Barlow AK, Chromy BA, Edwards C, Freed R, Liosatos M, et al. Diffusible, nonfibrillar ligands derived from A β 1-42 are potent central nervous system neurotoxins. *Proc. Natl. Acad. Sci. U. S. A.*, 1998; 95: 6448-53.
- Langer F, Eisele YS, Fritschi SK, Staufenbiel M, Walker LC, Jucker M. Soluble A β seeds are potent inducers of cerebral beta-amyloid deposition. *J. Neurosci.*, 2011; 31: 14488-95.
- Legname G, Nguyen HO, Peretz D, Cohen FE, DeArmond SJ, Prusiner SB. Continuum of prion protein structures enciphers a multitude of prion isolate-specified phenotypes. *Proc. Natl. Acad. Sci. U. S. A.*, 2006; 103: 19105-10.
- Levy E, Carman MD, Fernandez-Madrid IJ, Power MD, Lieberburg I, van Duinen SG, et al. Mutation of the Alzheimer's disease amyloid gene in hereditary cerebral hemorrhage, Dutch type. *Science*, 1990; 248: 1124-6.
- Li JY, Englund E, Holton JL, Soulet D, Hagell P, Lees AJ, et al. Lewy bodies in grafted neurons in subjects with Parkinson's disease suggest host-to-graft disease propagation. *Nat. Med.*, 2008; 14: 501-3.
- Lindvall O, Brundin P, Widner H, Rehncrona S, Gustavii B, Frackowiak R, et al. Grafts of fetal dopamine neurons survive and improve motor function in Parkinson's disease. *Science*, 1990; 247: 574-7.
- Lopez De La Paz M, Goldie K, Zurdo J, Lacroix E, Dobson CM, Hoenger A, et al. De novo designed peptide-based amyloid fibrils. *Proc. Natl. Acad. Sci. U. S. A.*, 2002; 99: 16052-7.
- Lossi L, Alasia S, Salio C, Merighi A. Cell death and proliferation in acute slices and organotypic cultures of mammalian CNS. *Prog. Neurobiol.*, 2009; 88: 221-45.
- Lu JX, Qiang W, Yau WM, Schwieters CD, Meredith SC, Tycko R. Molecular structure of beta-amyloid fibrils in Alzheimer's disease brain tissue. *Cell*, 2013; 154: 1257-68.
- Malouf AT. Effect of beta amyloid peptides on neurons in hippocampal slice cultures. *Neurobiol. Aging*, 1992; 13: 543-51.
- Mandrekar S, Jiang Q, Lee CY, Koenigsnecht-Talboo J, Holtzman DM, Landreth GE. Microglia mediate the clearance of soluble A β through fluid phase macropinocytosis. *J. Neurosci.*, 2009; 29: 4252-62.
- Masliah E, Mallory M, Alford M, DeTeresa R, Hansen LA, McKeel DW, Jr., et al. Altered expression of synaptic proteins occurs early during progression of Alzheimer's disease. *Neurology*, 2001; 56: 127-9.
- Masters CL, Multhaup G, Simms G, Pottgiesser J, Martins RN, Beyreuther K. Neuronal origin of a cerebral amyloid: neurofibrillary tangles of Alzheimer's disease contain the same protein as the amyloid of plaque cores and blood vessels. *EMBO J.*, 1985a; 4: 2757-63.

- Masters CL, Simms G, Weinman NA, Multhaup G, McDonald BL, Beyreuther K. Amyloid plaque core protein in Alzheimer disease and Down syndrome. *Proc. Natl. Acad. Sci. U. S. A.*, 1985b; 82: 4245-9.
- Mastrianni JA, Nixon R, Layzer R, Telling GC, Han D, DeArmond SJ, et al. Prion protein conformation in a patient with sporadic fatal insomnia. *N. Engl. J. Med.*, 1999; 340: 1630-8.
- Meinhardt J, Tartaglia GG, Pawar A, Christopeit T, Hortschansky P, Schroeckh V, et al. Similarities in the thermodynamics and kinetics of aggregation of disease-related A β (1-40) peptides. *Protein Sci.*, 2007; 16: 1214-22.
- Meyer-Luehmann M, Coomaraswamy J, Bolmont T, Kaeser S, Schaefer C, Kilger E, et al. Exogenous induction of cerebral beta-amyloidogenesis is governed by agent and host. *Science*, 2006; 313: 1781-4.
- Meyer-Luehmann M, Spires-Jones TL, Prada C, Garcia-Alloza M, de Calignon A, Rozkalne A, et al. Rapid appearance and local toxicity of amyloid-beta plaques in a mouse model of Alzheimer's disease. *Nature*, 2008; 451: 720-4.
- Mullan M, Crawford F, Axelman K, Houlden H, Lilius L, Winblad B, et al. A pathogenic mutation for probable Alzheimer's disease in the APP gene at the N-terminus of beta-amyloid. *Nat. Genet.*, 1992; 1: 345-7.
- Murrell J, Farlow M, Ghetti B, Benson MD. A mutation in the amyloid precursor protein associated with hereditary Alzheimer's disease. *Science*, 1991; 254: 97-9.
- Nassif M, Hoppe J, Santin K, Frozza R, Zamin LL, Simao F, et al. Beta-amyloid peptide toxicity in organotypic hippocampal slice culture involves Akt/PKB, GSK-3 β , and PTEN. *Neurochem. Int.*, 2007; 50: 229-35.
- Neumann H, Daly MJ. Variant TREM2 as risk factor for Alzheimer's disease. *N. Engl. J. Med.*, 2013; 368: 182-4.
- NIA-RI Consensus. Consensus recommendations for the postmortem diagnosis of Alzheimer's disease. The National Institute on Aging, and Reagan Institute Working Group on Diagnostic Criteria for the Neuropathological Assessment of Alzheimer's Disease. *Neurobiol. Aging*, 1997; 18: S1-2.
- Nilsson KP, Aslund A, Berg I, Nystrom S, Konradsson P, Herland A, et al. Imaging distinct conformational states of amyloid-beta fibrils in Alzheimer's disease using novel luminescent probes. *ACS Chem. Biol.*, 2007; 2: 553-60.
- Novotny R, Langer F, Mahler J, Skodras A, Vlachos A, Wegenast-Braun BM, et al. Conversion of synthetic A β to *in vivo* active seeds and amyloid plaque formation in a hippocampal slice culture model. *J. Neurosci* (in press), 2016.
- Oddo S, Caccamo A, Shepherd JD, Murphy MP, Golde TE, Kaye R, et al. Triple-transgenic model of Alzheimer's disease with plaques and tangles: intracellular A β and synaptic dysfunction. *Neuron*, 2003; 39: 409-21.
- Pan KM, Baldwin M, Nguyen J, Gasset M, Serban A, Groth D, et al. Conversion of alpha-helices into beta-sheets features in the formation of the scrapie prion proteins. *Proc. Natl. Acad. Sci. U. S. A.*, 1993; 90: 10962-6.

- Paresce DM, Ghosh RN, Maxfield FR. Microglial cells internalize aggregates of the Alzheimer's disease amyloid beta-protein via a scavenger receptor. *Neuron*, 1996; 17: 553-65.
- Pattison IH. Resistance of the Scrapie Agent to Formalin. *J. Comp. Pathol.*, 1965; 75: 159-64.
- Pensalfini A, Albay R, 3rd, Rasool S, Wu JW, Hatami A, Arai H, et al. Intracellular amyloid and the neuronal origin of Alzheimer neuritic plaques. *Neurobiol. Dis.*, 2014; 71: 53-61.
- Peretz D, Scott MR, Groth D, Williamson RA, Burton DR, Cohen FE, et al. Strain-specified relative conformational stability of the scrapie prion protein. *Protein Sci.*, 2001; 10: 854-63.
- Perlmutter LS, Barron E, Chui HC. Morphologic association between microglia and senile plaque amyloid in Alzheimer's disease. *Neurosci. Lett.*, 1990; 119: 32-6.
- Petkova AT, Ishii Y, Balbach JJ, Antzutkin ON, Leapman RD, Delaglio F, et al. A structural model for Alzheimer's beta -amyloid fibrils based on experimental constraints from solid state NMR. *Proc. Natl. Acad. Sci. U. S. A.*, 2002; 99: 16742-7.
- Petkova AT, Leapman RD, Guo Z, Yau WM, Mattson MP, Tycko R. Self-propagating, molecular-level polymorphism in Alzheimer's beta-amyloid fibrils. *Science*, 2005; 307: 262-5.
- Ponte P, DeWhitt PG, Schilling J, Miller J, Hsu D, Greenberg B, et al. A new A4 amyloid mRNA contains a domain homologous to serine proteinase inhibitors. *Nature*, 1988; 331: 525-7.
- Prinz M, Priller J. Microglia and brain macrophages in the molecular age: from origin to neuropsychiatric disease. *Nat. Rev. Neurosci.*, 2014; 15: 300-12.
- Prinz M, Priller J, Sisodia SS, Ransohoff RM. Heterogeneity of CNS myeloid cells and their roles in neurodegeneration. *Nat. Neurosci.*, 2011; 14: 1227-35.
- Prokop S, Miller KR, Heppner FL. Microglia actions in Alzheimer's disease. *Acta Neuropathol.*, 2013; 126: 461-77.
- Prusiner SB. Cell biology. A unifying role for prions in neurodegenerative diseases. *Science*, 2012; 336: 1511-3.
- Prusiner SB. Novel proteinaceous infectious particles cause scrapie. *Science*, 1982; 216: 136-44.
- Prusiner SB. Prions. *Proc. Natl. Acad. Sci. U. S. A.*, 1998; 95: 13363-83.
- Radde R, Bolmont T, Kaeser SA, Coomaraswamy J, Lindau D, Stoltze L, et al. Abeta42-driven cerebral amyloidosis in transgenic mice reveals early and robust pathology. *EMBO Rep*, 2006; 7: 940-6.
- Rajendran L, Knobloch M, Geiger KD, Dienel S, Nitsch R, Simons K, et al. Increased Abeta production leads to intracellular accumulation of Abeta in flotillin-1-positive endosomes. *Neurodegener. Dis.*, 2007; 4: 164-70.
- Reitz C, Brayne C, Mayeux R. Epidemiology of Alzheimer disease. *Nat. Rev. Neurol.*, 2011; 7: 137-52.
- Robakis NK, Ramakrishna N, Wolfe G, Wisniewski HM. Molecular cloning and characterization of a cDNA encoding the cerebrovascular and the neuritic plaque amyloid peptides. *Proc. Natl. Acad. Sci. U. S. A.*, 1987; 84: 4190-4.

- Rovelet-Lecrux A, Hannequin D, Raux G, Le Meur N, Laquerriere A, Vital A, et al. APP locus duplication causes autosomal dominant early-onset Alzheimer disease with cerebral amyloid angiopathy. *Nat. Genet.*, 2006; 38: 24-6.
- Rupp NJ, Wegenast-Braun BM, Radde R, Calhoun ME, Jucker M. Early onset amyloid lesions lead to severe neuritic abnormalities and local, but not global neuron loss in APPPS1 transgenic mice. *Neurobiol. Aging*, 2011; 32: 2324 e1-6.
- Saborio GP, Permanne B, Soto C. Sensitive detection of pathological prion protein by cyclic amplification of protein misfolding. *Nature*, 2001; 411: 810-3.
- Scheff SW, Price DA, Schmitt FA, DeKosky ST, Mufson EJ. Synaptic alterations in CA1 in mild Alzheimer disease and mild cognitive impairment. *Neurology*, 2007; 68: 1501-8.
- Schellenberg GD, Bird TD, Wijsman EM, Orr HT, Anderson L, Nemens E, et al. Genetic linkage evidence for a familial Alzheimer's disease locus on chromosome 14. *Science*, 1992; 258: 668-71.
- Schmechel DE, Saunders AM, Strittmatter WJ, Crain BJ, Hulette CM, Joo SH, et al. Increased amyloid beta-peptide deposition in cerebral cortex as a consequence of apolipoprotein E genotype in late-onset Alzheimer disease. *Proc. Natl. Acad. Sci. U. S. A.*, 1993; 90: 9649-53.
- Serpell LC, Berriman J, Jakes R, Goedert M, Crowther RA. Fiber diffraction of synthetic alpha-synuclein filaments shows amyloid-like cross-beta conformation. *Proc. Natl. Acad. Sci. U. S. A.*, 2000; 97: 4897-902.
- Shankar GM, Walsh DM. Alzheimer's disease: synaptic dysfunction and A β . *Mol. Neurodegener.*, 2009; 4: 48.
- Sigurdson CJ, Nilsson KP, Hornemann S, Manco G, Polymenidou M, Schwarz P, et al. Prion strain discrimination using luminescent conjugated polymers. *Nat Methods*, 2007; 4: 1023-30.
- Sipe JD, Benson MD, Buxbaum JN, Ikeda S, Merlini G, Saraiva MJ, et al. Nomenclature 2014: Amyloid fibril proteins and clinical classification of the amyloidosis. *Amyloid*, 2014; 21: 221-4.
- Sleegers K, Brouwers N, Gijssels I, Theuns J, Goossens D, Wauters J, et al. APP duplication is sufficient to cause early onset Alzheimer's dementia with cerebral amyloid angiopathy. *Brain*, 2006; 129: 2977-83.
- Spillantini MG, Crowther RA, Jakes R, Cairns NJ, Lantos PL, Goedert M. Filamentous alpha-synuclein inclusions link multiple system atrophy with Parkinson's disease and dementia with Lewy bodies. *Neurosci. Lett.*, 1998a; 251: 205-8.
- Spillantini MG, Crowther RA, Jakes R, Hasegawa M, Goedert M. alpha-Synuclein in filamentous inclusions of Lewy bodies from Parkinson's disease and dementia with Lewy bodies. *Proc. Natl. Acad. Sci. U. S. A.*, 1998b; 95: 6469-73.
- St George-Hyslop P, Haines J, Rogaev E, Mortilla M, Vaula G, Pericak-Vance M, et al. Genetic evidence for a novel familial Alzheimer's disease locus on chromosome 14. *Nat. Genet.*, 1992; 2: 330-4.
- St George-Hyslop PH, Tanzi RE, Polinsky RJ, Haines JL, Nee L, Watkins PC, et al. The genetic defect causing familial Alzheimer's disease maps on chromosome 21. *Science*, 1987; 235: 885-90.
- Stalder M, Phinney A, Probst A, Sommer B, Staufenbiel M, Jucker M. Association of microglia with amyloid plaques in brains of APP23 transgenic mice. *Am. J. Pathol.*, 1999; 154: 1673-84.

- Stewart CR, Stuart LM, Wilkinson K, van Gils JM, Deng J, Halle A, et al. CD36 ligands promote sterile inflammation through assembly of a Toll-like receptor 4 and 6 heterodimer. *Nat. Immunol.*, 2010; 11: 155-61.
- Stohr J, Condello C, Watts JC, Bloch L, Oehler A, Nick M, et al. Distinct synthetic Abeta prion strains producing different amyloid deposits in bigenic mice. *Proc. Natl. Acad. Sci. U. S. A.*, 2014; 111: 10329-34.
- Stohr J, Watts JC, Mensinger ZL, Oehler A, Grillo SK, DeArmond SJ, et al. Purified and synthetic Alzheimer's amyloid beta (Abeta) prions. *Proc. Natl. Acad. Sci. U. S. A.*, 2012; 109: 11025-30.
- Stoppini L, Buchs PA, Muller D. Lesion-induced neurite sprouting and synapse formation in hippocampal organotypic cultures. *Neuroscience*, 1993; 57: 985-94.
- Stoppini L, Buchs PA, Muller D. A simple method for organotypic cultures of nervous tissue. *J. Neurosci. Methods*, 1991; 37: 173-82.
- Strittmatter WJ, Saunders AM, Schmechel D, Pericak-Vance M, Enghild J, Salvesen GS, et al. Apolipoprotein E: high-avidity binding to beta-amyloid and increased frequency of type 4 allele in late-onset familial Alzheimer disease. *Proc. Natl. Acad. Sci. U. S. A.*, 1993; 90: 1977-81.
- Sturchler-Pierrat C, Abramowski D, Duke M, Wiederhold KH, Mistl C, Rothacher S, et al. Two amyloid precursor protein transgenic mouse models with Alzheimer disease-like pathology. *Proc. Natl. Acad. Sci. U. S. A.*, 1997; 94: 13287-92.
- Sze CI, Troncoso JC, Kawas C, Mouton P, Price DL, Martin LJ. Loss of the presynaptic vesicle protein synaptophysin in hippocampus correlates with cognitive decline in Alzheimer disease. *J. Neuropathol. Exp. Neurol.*, 1997; 56: 933-44.
- Takahashi RH, Milner TA, Li F, Nam EE, Edgar MA, Yamaguchi H, et al. Intraneuronal Alzheimer abeta42 accumulates in multivesicular bodies and is associated with synaptic pathology. *Am. J. Pathol.*, 2002; 161: 1869-79.
- Takami M, Nagashima Y, Sano Y, Ishihara S, Morishima-Kawashima M, Funamoto S, et al. gamma-Secretase: successive tripeptide and tetrapeptide release from the transmembrane domain of beta-carboxyl terminal fragment. *J. Neurosci.*, 2009; 29: 13042-52.
- Tanaka S, Nakamura S, Ueda K, Kameyama M, Shiojiri S, Takahashi Y, et al. Three types of amyloid protein precursor mRNA in human brain: their differential expression in Alzheimer's disease. *Biochem. Biophys. Res. Commun.*, 1988; 157: 472-9.
- Tanzi RE, McClatchey AI, Lamperti ED, Villa-Komaroff L, Gusella JF, Neve RL. Protease inhibitor domain encoded by an amyloid protein precursor mRNA associated with Alzheimer's disease. *Nature*, 1988; 331: 528-30.
- Terry RD, Gonatas NK, Weiss M. Ultrastructural studies in Alzheimer's presenile dementia. *Am. J. Pathol.*, 1963; 44: 269-97.
- Terry RD, Masliah E, Salmon DP, Butters N, DeTeresa R, Hill R, et al. Physical basis of cognitive alterations in Alzheimer's disease: synapse loss is the major correlate of cognitive impairment. *Ann. Neurol.*, 1991; 30: 572-80.

- Thinakaran G, Koo EH. Amyloid precursor protein trafficking, processing, and function. *J. Biol. Chem.*, 2008; 283: 29615-9.
- Van Broeckhoven C, Haan J, Bakker E, Hardy JA, Van Hul W, Wehnert A, et al. Amyloid beta protein precursor gene and hereditary cerebral hemorrhage with amyloidosis (Dutch). *Science*, 1990; 248: 1120-2.
- Walker LC, Callahan MJ, Bian F, Durham RA, Roher AE, Lipinski WJ. Exogenous induction of cerebral beta-amyloidosis in betaAPP-transgenic mice. *Peptides*, 2002; 23: 1241-7.
- Walker LC, Jucker M. Neurodegenerative diseases: expanding the prion concept. *Annu. Rev. Neurosci.*, 2015; 38: 87-103.
- Walsh DM, Klyubin I, Fadeeva JV, Cullen WK, Anwyl R, Wolfe MS, et al. Naturally secreted oligomers of amyloid beta protein potently inhibit hippocampal long-term potentiation in vivo. *Nature*, 2002; 416: 535-9.
- Wang Q, Walsh DM, Rowan MJ, Selkoe DJ, Anwyl R. Block of long-term potentiation by naturally secreted and synthetic amyloid beta-peptide in hippocampal slices is mediated via activation of the kinases c-Jun N-terminal kinase, cyclin-dependent kinase 5, and p38 mitogen-activated protein kinase as well as metabotropic glutamate receptor type 5. *J. Neurosci.*, 2004; 24: 3370-8.
- Wang Y, Cella M, Mallinson K, Ulrich JD, Young KL, Robinette ML, et al. TREM2 lipid sensing sustains the microglial response in an Alzheimer's disease model. *Cell*, 2015; 160: 1061-71.
- Watts JC, Condello C, Stohr J, Oehler A, Lee J, DeArmond SJ, et al. Serial propagation of distinct strains of Abeta prions from Alzheimer's disease patients. *Proc. Natl. Acad. Sci. U. S. A.*, 2014; 111: 10323-8.
- Weingarten MD, Lockwood AH, Hwo SY, Kirschner MW. A protein factor essential for microtubule assembly. *Proc. Natl. Acad. Sci. U. S. A.*, 1975; 72: 1858-62.
- West MJ, Coleman PD, Flood DG, Troncoso JC. Differences in the pattern of hippocampal neuronal loss in normal ageing and Alzheimer's disease. *Lancet*, 1994; 344: 769-72.
- Westermarck P, Benson MD, Buxbaum JN, Cohen AS, Frangione B, Ikeda S, et al. A primer of amyloid nomenclature. *Amyloid*, 2007; 14: 179-83.
- Wisniewski H, Narang H, Terry R. Neurofibrillary tangles of paired helical filaments. *J. Neurol. Sci.*, 1976; 27: 173-81.
- Xiao X, Cali I, Yuan J, Cracco L, Curtiss P, Zeng L, et al. Synthetic Abeta peptides acquire prion-like properties in the brain. *Oncotarget*, 2015; 6: 642-50.
- Xu Q, Bernardo A, Walker D, Kanegawa T, Mahley RW, Huang Y. Profile and regulation of apolipoprotein E (ApoE) expression in the CNS in mice with targeting of green fluorescent protein gene to the ApoE locus. *J. Neurosci.*, 2006; 26: 4985-94.
- Xu Q, Li Y, Cyras C, Sanan DA, Cordell B. Isolation and characterization of apolipoproteins from murine microglia. Identification of a low density lipoprotein-like apolipoprotein J-rich but E-poor spherical particle. *J. Biol. Chem.*, 2000; 275: 31770-7.
- Yan SD, Chen X, Fu J, Chen M, Zhu H, Roher A, et al. RAGE and amyloid-beta peptide neurotoxicity in Alzheimer's disease. *Nature*, 1996; 382: 685-91.

Yan Y, Wang C. Abeta42 is more rigid than Abeta40 at the C terminus: implications for Abeta aggregation and toxicity. *J. Mol. Biol.*, 2006; 364: 853-62.

Zhang B, Gaiteri C, Bodea LG, Wang Z, McElwee J, Podtelezhnikov AA, et al. Integrated systems approach identifies genetic nodes and networks in late-onset Alzheimer's disease. *Cell*, 2013a; 153: 707-20.

Zhang Z, Zhang Y, Wang F, Wang X, Xu Y, Yang H, et al. De novo generation of infectious prions with bacterially expressed recombinant prion protein. *FASEB J.*, 2013b; 27: 4768-75.

3. Publications

3.1 Description of personal contribution

- | Götz Heilbronner, Yvonne S. Eisele, Franziska Langer, Stephan A. Kaeser, **Renata Novotny**, Amudha Nagarathinam, Andreas Åslund, Per Hammarström, K. Peter R. Nilsson & Mathias Jucker

Seeded strain-like transmission of β -amyloid morphotypes in APP transgenic mice

Personal contribution: Assistance in immunoblotting and analysis of laser-dissected tissue; correcting/editing of the final manuscript.

- || **Renata Novotny***, Franziska Langer*, Jasmin Mahler, Angelos Skodras, Andreas Vlachos, Bettina M. Wegenast-Braun, Stephan A. Kaeser, Jonas J. Neher, Yvonne S. Eisele, Marie J. Pietrowski, K. Peter R. Nilsson, Thomas Deller, Matthias Staufenbiel, Bernd Heimrich# and Mathias Jucker#

Conversion of synthetic A β to *in vivo* active seeds and amyloid plaque formation in a hippocampal slice culture model

Personal contribution: Experimental design of the study (together with F.L., B.H. and M.J.); performance of culture preparation (together with B.H.); intracerebral injections of brain extracts from APP tg mice and slice culture homogenate; immunohistochemistry of seeded brain sections and analysis of the resultant data; design and figure preparation (together with M.J.); writing the manuscript with the help of F.L., M.J. and M.S.

*equal contribution, #corresponding authors

- ||| **Renata Novotny***, Mehtap Bacioglu*, Manuel Schweighauser, Jasmin Mahler, K. Peter R. Nilsson, Bernd Heimrich and Mathias Jucker

Organotypic hippocampal slice cultures as a new tool to study α -synuclein lesions

Personal contribution: Experimental design of the study (together with M.B. and M.J.); performance of culture preparation (together with B.H.); immunohistochemistry of seeded brain sections and analysis of the resultant data (together with M.B.); design and figure preparation (together with M.B.); writing the manuscript (with the help of M.B. and M.S).

*equal contribution

3.2 Seeded strain-like transmission of β -amyloid morphotypes in APP transgenic mice

Götz Heilbronner, Yvonne S. Eisele, Franziska Langer, Stephan A. Kaeser, **Renata Novotny**,
Amudha Nagarathinam, Andreas Åslund, PerHammarström, K. Peter R. Nilsson and Mathias
Jucker

Published in:

EMBO Reports (2013)

scientific report

Seeded strain-like transmission of β -amyloid morphotypes in APP transgenic mice

Götz Heilbronner^{1,2}, Yvonne S. Eisele^{1,2}, Franziska Langer^{1,2}, Stephan A. Kaeser^{1,2}, Renata Novotny^{1,2,3}, Amudha Nagarathinam^{1,2}, Andreas Åslund⁴, Per Hammarström⁴, K. Peter R. Nilsson⁴ & Mathias Jucker^{1,2+}

¹Department of Cellular Neurology, Hertie Institute for Clinical Brain Research, University of Tübingen, Tübingen, Germany, ²DZNE, German Center for Neurodegenerative Diseases, Tübingen, Germany, ³Graduate School of Cellular and Molecular Neuroscience, University of Tübingen, Tübingen, Germany, and ⁴Department of Chemistry, IFM, Linköping University, Linköping, Sweden

The polymorphic β -amyloid lesions present in individuals with Alzheimer's disease are collectively known as cerebral β -amyloidosis. Amyloid precursor protein (APP) transgenic mouse models similarly develop β -amyloid depositions that differ in morphology, binding of amyloid conformation-sensitive dyes, and A β 40/A β 42 peptide ratio. To determine the nature of such β -amyloid morphotypes, β -amyloid-containing brain extracts from either aged APP23 brains or aged APPS1 brains were intracerebrally injected into the hippocampus of young APP23 or APPS1 transgenic mice. APPS1 brain extract injected into young APP23 mice induced β -amyloid deposition with the morphological, conformational, and A β 40/A β 42 ratio characteristics of β -amyloid depositions in aged APPS1 mice, whereas APP23 brain extract injected into young APP23 mice induced β -amyloid deposits with the characteristics of β -amyloid depositions in aged APP23 mice. Injecting the two extracts into the APPS1 host revealed a similar difference between the induced β -amyloid deposits, although less prominent, and the induced deposits were similar to the β -amyloid depositions found in aged APPS1 hosts. These results indicate that the molecular composition and conformation of aggregated A β in APP transgenic mice can be maintained by seeded conversion.

Keywords: Alzheimer; amyloid; protein aggregation; prion strain

EMBO reports (2013) 14, 1017–1022. doi:10.1038/embor.2013.137

¹Department of Cellular Neurology, Hertie Institute for Clinical Brain Research, University of Tübingen, D-72076 Tübingen, Germany

²DZNE, German Center for Neurodegenerative Diseases, D-72076 Tübingen, Germany

³Graduate School of Cellular and Molecular Neuroscience, University of Tübingen, D-72074 Tübingen, Germany

⁴Department of Chemistry, IFM, Linköping University, SE-581 83 Linköping, Sweden

+Corresponding author. Tel: +49 7071 29 86863; Fax: +49 7071 29 4521;

E-mail: mathias.jucker@uni-tuebingen.de

Received 26 March 2013; revised 12 August 2013; accepted 12 August 2013; published online 3 September 2013

INTRODUCTION

The aggregation and deposition of the β -amyloid peptide (A β) in brain is considered an early and predictive lesion of Alzheimer's disease (AD) [1–3]. A β of various lengths are generated by cleavage of amyloid precursor protein (APP) by β -secretase and γ -secretase [4,5]. The most prominent A β species are full-length or N-truncated A β _x-40 (A β 40) and A β _x-42 (A β 42) with A β 42 being much more prone to aggregation and more neurotoxic compared with A β 40 [4,5].

There are multiple lines of evidence for polymorphic A β aggregation [6,7]. A β deposits in brain can differ in morphology and in biochemical composition within and among individuals with AD, between normal aging and AD, and among APP transgenic mouse models [6–13]. Such A β morphotypes might be governed by host factors, such as A β posttranslational modifications, A β length variant generation or A β amino-acid substitutions as found in familial AD. However, we have previously shown the induction of different A β morphotypes in a given transgenic mouse line after intracerebral application of aggregated A β -containing brain extracts from two different sources [14]. Similarly, *in vitro*, distinct structural variants of synthetic A β fibrils can be grown and are self-propagating under seeded growth conditions [15,16].

The aim of the present study was to determine whether the induction of different A β morphotypes in genetically defined recipient mice reflect variations in the molecular composition and/or conformation of the aggregated A β in the donor brain extracts. This would suggest that the prion conformation strain concept [17–20] might also apply to cerebral β -amyloidosis and further supports the concept of prion-like templated misfolding of A β .

RESULTS AND DISCUSSION

A β morphotypes in APP23 and APPS1 mice

APP23 and APPS1 transgenic mice develop age-dependent depositions of A β in the brain [21,22]. While amyloid depositions in APP23 mice are characterized by fairly large A β deposits consisting of congophilic amyloid cores with diffuse penumbras, as well as diffuse A β deposition, APPS1 mice develop small,

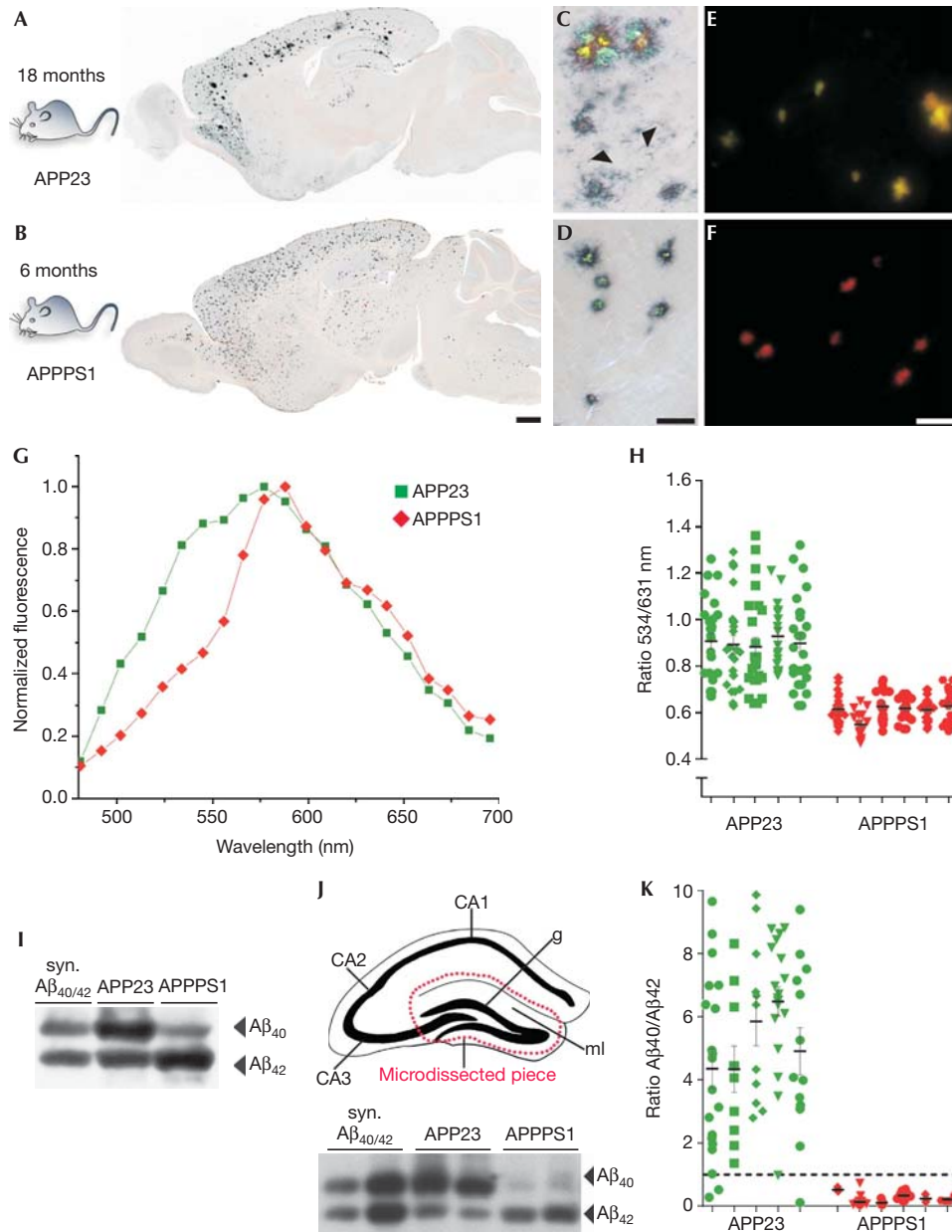


Fig 1 | A β deposits in APP23 and APPPS1 mice differ in morphology, spectral properties and A β 40/42 ratio. (A,B) A β -immunostaining and Congo red staining of an 18-month-old APP23 and 6-month-old APPPS1 mouse. (C,D) Higher magnification of the hippocampal plaques. Note the rather large congophilic (yellow–green birefringence) plaques and diffuse (arrowheads) A β deposits in APP23 mice (C) in comparison with the smaller, compact and congophilic plaques in APPPS1 mice (D). (E,F) tPTAA staining of the hippocampal plaques. Note the shift to yellow–green colours of the A β deposits in the 18-month-old APP23 mice (E) and the reddish colour of the deposits in the 6-month-old APPPS1 mice (F). Scale bars, 500 μ m (B), 100 μ m (D), 50 μ m (F). (G) Emission spectra of tPTAA bound to the hippocampal A β deposits. (H) For quantitative analysis, the ratio of the intensity of the emitted light at 534 and 631 nm was calculated. Each dot represents one A β plaque. Mean and s.e.m. are indicated for each animal. *t*-Test revealed a significant difference between the two groups (APP23: 5 mice, 18–22 months old; APPPS1: 6 mice, 4–6 months old; $t(9) = 19.4$; $P < 0.001$). Note the greater variation between individual plaques within the APP23 mice compared with APPPS1 mice. (I–K) Urea-based immunoblot of amyloid-depositing APP23 and APPPS1 mouse brain (I; lane 1: synthetic A β 40 + A β 42 (400 pg each), lane 2: APP23 brain extract, lane 3: APPPS1 brain extract). Note the dominance of A β 40 over A β 42 in APP23 mice and of A β 42 over A β 40 in APPPS1 mice. Similar results were obtained with laser-dissected tissue pieces from the dentate gyrus (J) top; schematic drawing; CA1–3 = cornu ammonis area; g = granular cell layer; ml = molecular layer; J bottom: immunoblot of two laser-dissected tissue pieces from APP23 and APPPS1; synthetic A β 40 + A β 42 were 400 and 800 pg each). Quantitative densitometric A β 40/A β 42 ratio in immunoblots for each laser-dissected tissue piece (K, for each animal between 3 and 28 sections were analysed and are represented by dots). The dotted line indicates a ratio of 1. The same 5–6 mice/group were used as in (H). Mean and s.e.m. are indicated. *t*-Test revealed a significant difference between the two groups ($t(9) = 11.5$; $P < 0.001$). A β , β -amyloid peptide; tPTAA, trimeric polythiophene acetic acid.

compact and highly congophilic A β deposits [21,22]. These mouse strain-specific plaque morphotypes can be found throughout the neocortex and hippocampus (Fig 1A–D).

Conformational differences of variant A β morphotypes can be studied by anionic luminescent conjugated polythiophene (LCP) including trimeric polythiophene acetic acid (tPTAA) [23]. LCPs are flexible amyloid-binding dyes whose spectral properties depend on the amyloid conformation. An LCP-based histo-optical imaging technique has previously been used to discriminate various prion strains, types of systemic amyloids and heterogeneous A β deposits [12,24,25]. When tPTAA was applied to tissue sections of amyloid-bearing APP23 and APPPS1 mice, fluorescence images revealed a shift towards bright yellow–greenish colours for the amyloid plaques in APP23 mice, whereas the amyloid plaques in APPPS1 mice showed a reddish appearance (Fig 1E,F). Subsequent spectral analysis revealed tPTAA emission spectra in APP23 mice with a maximum intensity at \sim 575 nm and a shoulder at shorter wavelengths (around 535 nm), with more red-shifted spectra also present (Fig 1G). In contrast, plaques in the APPPS1 mice showed a narrower tPTAA spectral distribution with a maximum intensity at \sim 590 nm and a shoulder at longer wavelengths (around 630 nm) (Fig 1G). Quantitative results revealed a significant difference in the 534/631 nm emission ratio between the amyloid deposits in APP23 and APPPS1 mice (Fig 1H; see also supplementary Fig S1 online). The spectral difference was also present, albeit less distinct, when amyloid fibrils were isolated from whole brains of APP23 and APPPS1 mice (supplementary Fig S2 online).

APP23 mice express Swedish-mutated human APP, with A β 40 generation exceeding that of A β 42. In contrast, APPPS1 mice harbour mutated presenilin (PS) 1 in addition to Swedish-mutated APP, and thus generate more A β 42 than A β 40 albeit lower total amounts of total A β compared with APP23 mice [21,22]. To test whether this difference in A β length variant generation is also reflected in the amyloid plaques, laser dissection of amyloid plaques with subsequent A β -immunoblotting was performed. Results revealed an A β 40/42 ratio of 4.7/1 for aged APP23 mice, and a ratio of 0.3/1 for APPPS1 mice (Fig 1I–K) consistent with enzyme-linked immunosorbent assays from brain homogenates [14,21,22].

Propagation of A β morphotypes by seeding

Intracerebral injection of minute amounts of brain extract from β -amyloid-laden aged APP23 or APPPS1 mice induces β -amyloidosis in young pre-depositing APP23 and APPPS1 mice [14]. Here we have replicated these findings and show that β -amyloid-containing APP23 extract injected into the hippocampus (dentate gyrus) of young, pre-depositing, 4–6-month-old APP23 mice induces β -amyloid deposits surrounded by diffuse, filamentous A β immunoreactivity 3 months after injections. In contrast, β -amyloid-containing APPPS1 extract injected in the same host induces punctate, coarse and compact A β -plaques 3 months after injections (Fig 2A–C). While the APP23 extract induced A β deposits throughout the subgranular and molecular layers of the dentate gyrus, the induced A β deposits by the APPPS1 extract were largely confined to the subgranular layer and polymorphic region of the dentate gyrus (Fig 2B,C). Quantification revealed that total A β deposition induced by the APP23 extract was more than double compared with the

APPPS1 extract (Fig 2B,C). In contrast, when only the compact A β deposition was quantified, there was no clear difference between the two extracts (Fig 2B,C).

The reverse experiment, that is, APP23 and APPPS1 extracts injected into young, pre-depositing 1.5–3-month-old APPPS1 mice and analysed 1.5–3 months later, revealed again a more diffuse and filamentous pattern of A β -deposition for the APP23 extract and prominent A β -deposition in the subgranular cell layer for the APPPS1 extract. However, this morphological difference between the extracts was not as obvious as in the APP23 host and also the induced amount and pattern of total or compact A β immunoreactivity appeared similar between the two extracts (Fig 2D,E).

APP23 and APPPS1 mice analysed 1 week after the injection of the β -amyloid-containing brain extracts did not show amyloid deposition demonstrating that the A β deposits did not simply represent the injected A β -containing material ($n=8$; 2 mice/group; results not shown) [14,26].

tPTAA spectral emission of seeded A β deposits

To study conformational differences of the induced A β morphotypes, tPTAA staining with spectral analysis was applied (Fig 2F–I). Strikingly, while the APP23 extract injected in APP23 mice induced A β deposits with a yellow–greenish appearance, the APPPS1 extract injected in APP23 mice induced A β deposits with a reddish shifted appearance (Fig 2F,G). Vice versa, while the A β deposits in APP23 extract-seeded APPPS1 mice revealed a spectral shift towards a yellow–greenish colour, the APPPS1 extract-seeded APPPS1 mice revealed a more reddish pattern, although this difference appeared again less striking compared with the APP23 host (Fig 2H,I). Quantitative spectral analysis of the 534/631 nm emission ratio confirmed this qualitative histological impression (Fig 3A). When compared with the endogenous A β deposits of the hosts (Fig 1H), the 534/631 nm emission ratios in APP23-seeded APP23 mice and APPPS1-seeded APPPS1 mice were reminiscent of the emission ratios in APP23 and APPPS1 mice, respectively.

A β 40/42 ratio of seeded A β deposits

To test whether the ratio of A β 40/42 might underlie the different morphology and LCP spectral analysis of the induced A β deposits, laser dissection of induced A β deposition with subsequent A β -immunoblotting was performed (Fig 3B). Intriguingly, there was a significant difference between APP23-seeded and APPPS1-seeded A β deposits in the APP23 host. While APP23-seeded A β deposits showed a mean A β 40/42 ratio of 3.7/1, APPPS1-seeded APP23 mice revealed a mean A β 40/42 ratio of 1.5/1. (Note that in ‘unseeded’ APP23 mice, the ratio was 4.7/1 and in APPPS1 mice 0.3/1, see Fig 1K). This finding implies the existence of a selection mechanism, whereby the seeded A β deposits incorporate mainly the host-generated A β isoform that resembles the composition of the seed. This seeded imprinting of the A β 40/42 ratio in the APP23 host paralleled the morphological characteristics of the induced A β deposits and LCP staining.

In the APPPS1 host and in contrast to the LCP staining, immunoblot analysis of the induced A β deposition failed to reach significance between the two extracts (A β 40/42 ratio of 0.35/1 for APP23 extract versus 0.25/1 for APPPS1 extract; Fig 3B) and the ratios of both APP23- and APPPS1-seeded A β deposits were

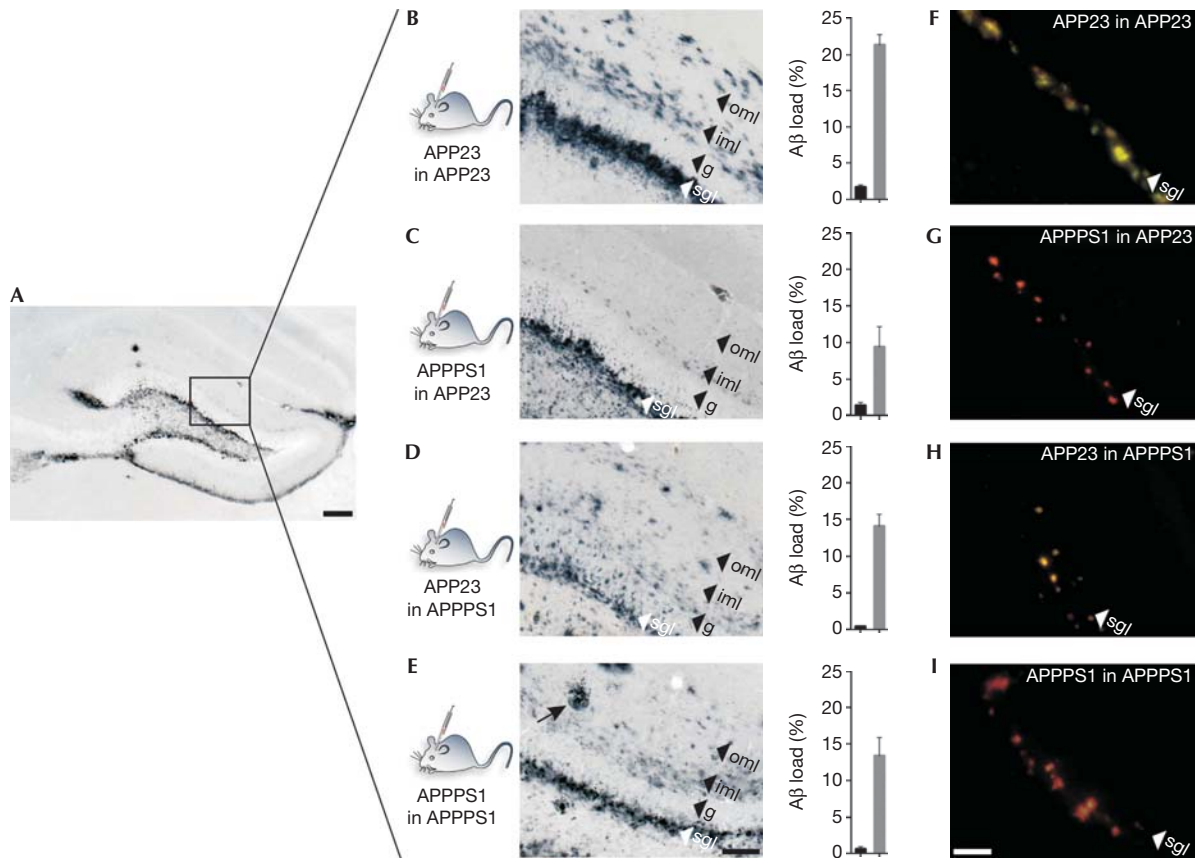


Fig 2 | Propagation of A β morphotypes by seeding. Brain extracts from aged amyloid-depositing APP23 or APPPS1 mice were injected into the hippocampus (dentate gyrus) of APP23 or APPPS1 mice. APP23 mice were 4–6 months old when they were injected. They were analysed 3 months later ($n = 5$ /extract). APPPS1 mice were either 1.5–2 months or 3 months old when they were injected. The 1.5–2-month-old group was analysed 1.5–2 months later ($n = 6$ /extract). The 3-month-old group was analysed 3 months later ($n = 2$ /extract). (A) Pattern of induced A β -deposition (A β immunostaining) in the dentate gyrus. Shown is an APPPS1 extract-inoculated APPPS1 host. (B–E) Higher magnifications of A β -immunostained layers of the dentate gyrus for the four experimental groups. The APP23 extract-induced A β deposits in APP23 hosts are more diffuse and filamentous compared with the highly coarse, punctate and compact A β deposits in APPPS1 extract-induced APP23 hosts (B,C). The distribution of the induced A β deposits throughout the different layers was also different between the two extracts in the APP23 host (sgl = subgranular cell layer; g = granular cell layer; iml, oml = inner and outer molecular layer). In the APPPS1 host, the APP23 extract-induced A β -deposits also appeared somewhat more diffuse and filamentous compared with the APPPS1 extract-induced A β -deposits, whereas the APPPS1 extract induced again more prominent A β -deposition in the sgl compared with the APP23 extract (D,E). Overall, the morphological differences between the two extracts in the APPPS1 host were less obvious than in the APP23 host and this appeared true independent of the age of the host at the time of inoculation and of the inoculation period. Note that untreated APP23 mice at 7–9 months of age do not yet show endogenous A β plaques in the hippocampus whereas APPPS1 mice at 4–6 months of age occasionally have some endogenous hippocampal plaques, which however can easily be identified (arrowhead in E). Total A β load (grey bars) and compact A β load (black bars) in dentate gyrus is shown in the panels next to the histological panels. Mean and s.e.m. are indicated (for the APP23 host $n = 5$ /extract, for the APPPS1 host $n = 8$ /extract). ANOVA (extract \times host) for the A β load revealed a significant interaction $F(1,22) = 6.19$; $P < 0.05$ and a significant main effect for extract ($F(1,22) = 7.78$; $P < 0.05$) but not for host ($P > 0.05$). ANOVA for the compact A β revealed a significant main effect for host ($F(1,22) = 10.12$; $P < 0.01$) but not for extract or interaction ($P > 0.05$). (F–I) tPTAA stained dentate gyrus for the four experimental groups. Note the difference in colour between the APP23 extract-induced A β deposits (yellow–greenish, F) and the APPPS1 extract-induced A β deposits (yellow–reddish, G) in APP23 hosts. The difference between the two extract in the APPPS1 host was again somewhat less prominent (H, I). Scale bars, 200 μ m (A), 100 μ m (E) and 50 μ m (I). A β , β -amyloid peptide; ANOVA, analysis of variance; tPTAA, trimeric polythiophene acetic acid.

similar to ratio in the ‘unseeded’ APPPS1 host. This observation might reflect that seeded nucleation in the APPPS1 host was obscured by endogenous spontaneous nucleation events and/or cross-seeding of the abundant and highly aggregate-prone A β 42 generated by the APPPS1 host [6,22].

‘Strain-like’ A β morphotypes

Prion strains might differ in amino-acid sequence of the prion protein or are based on polymorphic assembled states of the same prion protein molecule [17–20]. While the latter has at least been shown for A β *in vitro* [15,16], the results of the present study

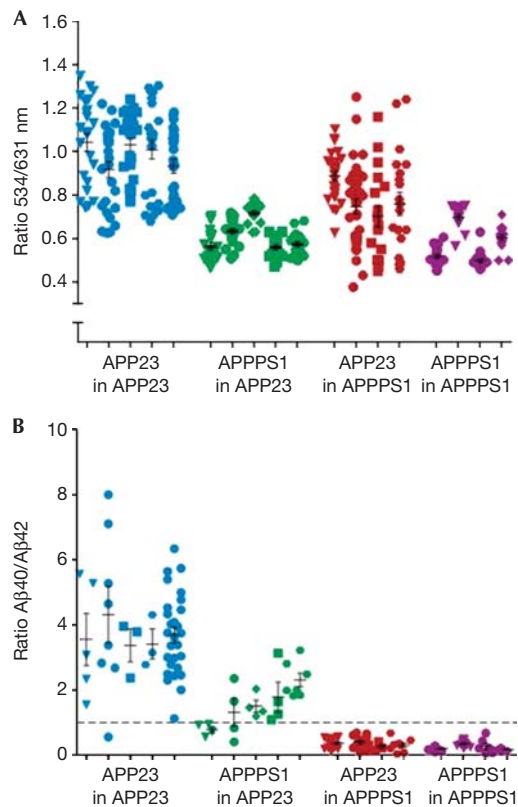


Fig 3 | Quantitative tPTAA spectral emission and A β 40/42 ratio of induced A β deposits. The analysis is from the same mice as in Fig 2. For the APP23 host, all mice ($n=5$ /extract) were included in the analysis; for the APPPS1 host, the two extremes were selected for analysis, that is, the 1.5-month-old mice that were analysed 1.5 months later, and the 3-month-old mice that were analysed 3 months later (total $n=4$ /extract). **(A)** Quantitative emission spectra of the ratio of the emitted light at 534 nm and 631 nm. For methodological details see Fig 1. Mean and s.e.m. are indicated. ANOVA (host \times extract) revealed significant main effects (host $F(1,14)=12.0$; $P<0.01$; Extract $F(1,14)=67.1$; $P<0.001$) and interaction ($F(1,14)=6.8$; $P<0.05$). *Post hoc* analysis revealed significant differences between APP23- and APPPS1-induced A β deposits in the APP23 host ($P<0.001$) and APPPS1 host ($P<0.01$). **(B)** Densitometric analysis of the A β 40/A β 42 ratio plotted for each laser-dissected tissue piece. For methodological details see Fig 1. Mean and s.e.m. are indicated. The dotted line indicates a ratio of 1. ANOVA (host \times extract) revealed significant main effects (Host $F(1,14)=175.9$; $P<0.001$; extract $F(1,14)=40.5$; $P<0.001$) and interaction ($F(1,14)=34.41$; $P<0.001$). *Post hoc* analysis revealed a difference between the APP23- and APPPS1-induced A β deposits in the APP23 host ($P<0.001$) but failed to reach significance in the APPPS1 host ($P>0.05$). A β , β -amyloid peptide; ANOVA, analysis of variance; tPTAA, trimeric polythiophene acetic acid.

suggest that, for β -amyloidosis in brain, C-terminal chain-length variants might contribute to the nature of the A β conformers and can be sustained by seeded induction ('strains'). In apparent contrast, previous *in vitro* studies have reported that assemblies of A β protofibrils with different A β 40/42 ratios have similar molecular structures [27,28]. However, *in vivo* and within

a cellular environment A β aggregation is likely different [10]. While the present study only focused on A β 40 and A β 42, it should be noted that there are many additional A β isoforms with various amino- and carboxy terminal lengths. In addition, there are A β amino-acid sequence differences associated with familial forms of cerebral β -amyloidosis [5,29].

The physiological relevance of A β 'strains' and whether they can be linked to phenotypic variability of AD and/or cerebral β -amyloidosis, as reported for prion strains in prionoses [18–20], remains to be shown. However, *in vitro*, the neurotoxicity of A β fibrils is dependent on their molecular and structural composition, including their A β 40/42 ratio [15,30–32]. *In vivo*, it has been shown that subtle changes in the A β 40/42 ratio have profound effects on neurotoxicity [33]. Finally, the A β 40/42 ratio correlates with disease onset in familial AD [34,35].

Cerebral β -amyloidosis is likely initiated by stochastic A β seed formation, with subsequent propagation and spreading [6,36]. The finding that variants of A β seeds might govern the type (and possibly toxicity) of A β aggregates might at least partly explain the heterogeneous morphology, pathogenicity and progression of A β lesions and associated pathologies in AD. The identification of factors that influence the conformational characteristics of the initial seed might thus have therapeutic implications.

METHODS

Detailed methods can be found in the Supplementary Information Online.

Mice and brain extracts. APP23 and APPPS1 transgenic mice develop first amyloid deposits at 6–8 months (APP23) and 2–4 months (APPPS1) of age. In both strains, A β deposits develop first in neocortex and later in the hippocampus [21,22]. Brain extracts were prepared from 27–28-month-old APP23 and 16–22-month-old APPPS1 mice (10–20 ng A β / μ l for both extracts). Injections were done into the hippocampus/dentate gyrus (AP -2.5 mm, L $+/-2.0$ mm, DV -1.8 mm) [26].

Immunohistochemistry and stereology. Sections were stained with Congo red and polyclonal antibody to A β [37]. Induced A β deposition was quantified on a set of every 12th systematically sampled coronal section throughout the dentate gyrus [14]. Total A β -load was determined by calculating the areal fraction (percentage) occupied by A β -staining; the compact plaque load by calculating the areal fraction occupied by Congo red.

tPTAA staining and emission spectra. Spectra were collected from tPTAA-stained sections [23] with a LSM 780 or 510 META (Carl Zeiss, Jena, Germany) with an argon 488 nm laser, and a Leica DM6000 B fluorescence microscope (Leica, Wetzlar, Germany) equipped with a SpectraCube (optical head) module (Applied Spectral Imaging, Migdal Ha-Emek, Israel). SpectraView 3.0 EXPO software (Applied Spectral Imaging) was used for images and selection of spectral regions. Spectra were collected from eight spots within 15–20 plaques/animal. Twisted separated LCP molecules emit light at 530–540 nm, whereas planar, stacked (aggregated) LCP multimers emit light at 630–650 nm. The ratio of the intensity of the emitted light at 534 and 631 nm was used as a parameter for spectral distinction of different plaques [12].

Immunoblotting of Laser-Dissected Tissue. Laser-microdissected (MicroBeam, P.A.L.M., Bernried, Germany) patches of the dentate gyrus (see Fig 1) were cut from sections adjacent to

A β -immunostained sections in which the location of the A β induction was confirmed. Bicine-Tris urea SDS-PAGE immunoblotting was used to separate A β 40 and A β 42 using antibody 6E10 specific to human A β [14]. Densitometric values of band intensities were analysed to calculate the A β 40:A β 42 ratio using ImageJ, version 1.42q (<http://rsb.info.nih.gov/ij>).

Supplementary information is available at EMBO reports online (<http://www.emboreports.org>).

ACKNOWLEDGEMENTS

We thank Matthias Staufenbiel (Basel) and Lary Walker (Atlanta) for comments to this manuscript; Ulla Welzel, Sarah Fritschi, Uli Obermüller, Claudia Schäfer (Tübingen), and Sofie Nyström (Linköping) for experimental help; Monika Schütz and Ingo Autenrieth (Tübingen) for help with the laser-microdissection. Supported by BMBF (ERA-Net NEURON—MIPROTRAN), European Union FP7 HEALTH (LUPAS), the Swedish Foundation for Strategic Research (SSF), and an ERC starting independent researcher grant (K.P.R.N.).

Author contributions: Y.S.E. and M.J. designed the research; G.H., Y.S.E., F.L. S.A.K., R.N., A.Ä., P.H. and K.P.R.N. performed the research; G.H., Y.S.E., A.N., K.P.R.N., P.H. and M.J. analysed data and prepared figures; M.J., K.P.R.N., P.H. wrote manuscript.

CONFLICT OF INTEREST

The authors declare that they have no conflict of interest.

REFERENCES

- Morris JC, Roe CM, Grant EA, Head D, Storandt M, Goate AM, Fagan AM, Holtzman DM, Mintun MA (2009) Pittsburgh compound B imaging and prediction of progression from cognitive normality to symptomatic Alzheimer disease. *Arch Neurol* **66**: 1469–1475
- Weiner MW et al (2010) The Alzheimer's disease neuroimaging initiative: progress report and future plans. *Alzheimers Dement* **6**: 202–211; e207
- Bateman RJ et al (2012) Clinical and biomarker changes in dominantly inherited Alzheimer's disease. *N Engl J Med* **367**: 795–804
- Haass C, Selkoe DJ (2007) Soluble protein oligomers in neurodegeneration: lessons from the Alzheimer's amyloid beta-peptide. *Nat Rev Mol Cell Biol* **8**: 101–112
- De Strooper B (2010) Proteases and proteolysis in Alzheimer disease: a multifactorial view on the disease process. *Physiol Rev* **90**: 465–494
- Eisenberg D, Jucker M (2012) The amyloid state of proteins in human diseases. *Cell* **148**: 1188–1203
- Levine H 3rd, Walker LC (2010) Molecular polymorphism of Abeta in Alzheimer's disease. *Neurobiol Aging* **31**: 542–548
- Piccini A et al (2005) beta-amyloid is different in normal aging and in Alzheimer disease. *J Biol Chem* **280**: 34186–34192
- Maarouf CL et al (2008) Histopathological and molecular heterogeneity among individuals with dementia associated with Presenilin mutations. *Mol Neurodegener* **3**: 20
- Paravastu AK, Qahwash I, Leapman RD, Meredith SC, Tycko R (2009) Seeded growth of beta-amyloid fibrils from Alzheimer's brain-derived fibrils produces a distinct fibril structure. *Proc Natl Acad Sci USA* **106**: 7443–7448
- Rosen RF, Ciliax BJ, Wingo TS, Gearing M, Dooyema J, Lah JJ, Ghiso JA, LeVine H 3rd, Walker LC (2010) Deficient high-affinity binding of Pittsburgh compound B in a case of Alzheimer's disease. *Acta Neuropathol* **119**: 221–233
- Nilsson KP et al (2007) Imaging distinct conformational states of amyloid-beta fibrils in Alzheimer's disease using novel luminescent probes. *ACS Chem Biol* **2**: 553–560
- Herzig MC, Eisele YS, Staufenbiel M, Jucker M (2009) E22Q-mutant Abeta peptide (AbetaDutch) increases vascular but reduces parenchymal Abeta deposition. *Am J Pathol* **174**: 722–726
- Meyer-Luehmann M et al (2006) Exogenous induction of cerebral beta-amyloidogenesis is governed by agent and host. *Science* **313**: 1781–1784
- Petkova AT, Leapman RD, Guo Z, Yau WM, Mattson MP, Tycko R (2005) Self-propagating, molecular-level polymorphism in Alzheimer's beta-amyloid fibrils. *Science* **307**: 262–265
- Meinhardt J, Sachse C, Hortschansky P, Grigorieff N, Fandrich M (2009) Abeta(1-40) fibril polymorphism implies diverse interaction patterns in amyloid fibrils. *J Mol Biol* **386**: 869–877
- Jones EM, Surewicz WK (2005) Fibril conformation as the basis of species- and strain-dependent seeding specificity of mammalian prion amyloids. *Cell* **121**: 63–72
- Collinge J, Clarke AR (2007) A general model of prion strains and their pathogenicity. *Science* **318**: 930–936
- Aguzzi A, Heikenwalder M, Polymenidou M (2007) Insights into prion strains and neurotoxicity. *Nat Rev Mol Cell Biol* **8**: 552–561
- Colby DW, Prusiner SB (2011) Prions. *Cold Spring Harb Perspect Biol* **3**: a006833
- Sturchler-Pierrat C et al (1997) Two amyloid precursor protein transgenic mouse models with Alzheimer disease-like pathology. *Proc Natl Acad Sci USA* **94**: 13287–13292
- Radde R et al (2006) Abeta42-driven cerebral amyloidosis in transgenic mice reveals early and robust pathology. *EMBO Rep* **7**: 940–946
- Aslund A, Herland A, Hammarstrom P, Nilsson KP, Jonsson BH, Inganäs O, Konradsson P (2007) Studies of luminescent conjugated polythiophene derivatives: enhanced spectral discrimination of protein conformational states. *Bioconjug Chem* **18**: 1860–1868
- Sigurdson CJ et al (2007) Prion strain discrimination using luminescent conjugated polymers. *Nat Methods* **4**: 1023–1030
- Nilsson KP, Ikenberg K, Aslund A, Fransson S, Konradsson P, Rocken C, Moch H, Aguzzi A (2010) Structural typing of systemic amyloidoses by luminescent-conjugated polymer spectroscopy. *Am J Pathol* **176**: 563–574
- Eisele YS et al (2009) Induction of cerebral beta-amyloidosis: intracerebral versus systemic Abeta inoculation. *Proc Natl Acad Sci USA* **106**: 12926–12931
- Schmidt M, Sachse C, Richter W, Xu C, Fandrich M, Grigorieff N (2009) Comparison of Alzheimer Abeta(1–40) and Abeta(1–42) amyloid fibrils reveals similar protofilament structures. *Proc Natl Acad Sci USA* **106**: 19813–19818
- Pauwels K et al (2012) Structural basis for increased toxicity of pathological abeta42:abeta40 ratios in Alzheimer disease. *J Biol Chem* **287**: 5650–5660
- Hardy J (1997) The Alzheimer family of diseases: many etiologies, one pathogenesis? *Proc Natl Acad Sci USA* **94**: 2095–2097
- Seilheimer B, Bohrmann B, Bondolfi L, Muller F, Stuber D, Dobeli H (1997) The toxicity of the Alzheimer's beta-amyloid peptide correlates with a distinct fiber morphology. *J Struct Biol* **119**: 59–71
- Yoshiike Y, Chui DH, Akagi T, Tanaka N, Takashima A (2003) Specific compositions of amyloid-beta peptides as the determinant of toxic beta-aggregation. *J Biol Chem* **278**: 23648–23655
- Hameier A et al (2009) Role of amyloid-beta glycine 33 in oligomerization, toxicity, and neuronal plasticity. *J Neurosci* **29**: 7582–7590
- Kuperstein I et al (2010) Neurotoxicity of Alzheimer's disease Abeta peptides is induced by small changes in the Abeta42 to Abeta40 ratio. *EMBO J* **29**: 3408–3420
- Duering M, Grimm MO, Grimm HS, Schroder J, Hartmann T (2005) Mean age of onset in familial Alzheimer's disease is determined by amyloid beta 42. *Neurobiol Aging* **26**: 785–788
- Kumar-Singh S et al (2006) Mean age-of-onset of familial Alzheimer disease caused by presenilin mutations correlates with both increased Abeta42 and decreased Abeta40. *Hum Mutat* **27**: 686–695
- Jarrett JT, Lansbury PT Jr (1993) Seeding 'one-dimensional crystallization' of amyloid: a pathogenic mechanism in Alzheimer's disease and scrapie? *Cell* **73**: 1055–1058
- Eisele YS et al (2010) Peripherally applied Abeta-containing inoculates induce cerebral beta-amyloidosis. *Science* **330**: 980–982

SUPPLEMENTARY INFORMATION

Seeded strain-like transmission of β -amyloid morphotypes in APP transgenic mice

Götz Heilbronner^{1,2}, Yvonne S. Eisele^{1,2}, Franziska Langer^{1,2}, Stephan A. Kaeser^{1,2}, Renata Novotny^{1,2,3}, Amudha Nagarathinam^{1,2}, Andreas Åslund⁴, Per Hammarström⁴, K. Peter R. Nilsson⁴, Mathias Jucker^{1,2}

SUPPLEMENTARY METHODS

Transgenic mice

Male and female hemizygous APP23 and APPPS1 mice were used with gender balanced between groups. APP23 mice carry the cDNA encoding human APP with the Swedish double mutation at positions 670/671 (KM→NL), driven by a murine Thy1 promoter element [1]. APP23 mice have been backcrossed with B6 mice for more than 20 generations (C57BL/6J-Tg (Thy1-APP_{K670N;M671L})23). APPPS1 mice express the same Swedish mutated APP cDNA construct together with human L166P mutated PS1 both driven by the murine Thy-1-promoter on a C57BL/6 background [2]. Amyloid deposits in APP23 mice occur at the age of 6-8 months while APPPS1 mice develop amyloidosis at 2-4 months. In both strains A β deposits develop first in the neocortex and later in the hippocampus [1,2].

Preparation of tissue extracts for intracerebral infusion

APP23 mouse brain extracts were prepared from brain without cerebellum of aged, β -amyloid-laden 27-28 month-old APP23 transgenic mice. Amyloid-laden APPPS1 brain extract was prepared from 16-22 month-old APPPS1 mice. Brains were removed, frozen, and stored at -80°C until use. Tissue was then homogenized at 10% (w/v) in sterile, phosphate-buffered saline (PBS), vortexed, sonicated 3 x 5 seconds and centrifuged at 3000 x g at 4°C for 5 minutes. The supernatant was aliquoted and immediately frozen. A β in the extract was measured by immunoblots and/or MSD (Meso Scale Discovery, Gaithersburg, MD) as previously described [3] and revealed a concentration of 10-20 ng/ μ l for both extracts.

Isolation of amyloid fibrils from brain

A β fibrils were isolated from brain homogenates of APP23 or APPPS1 transgenic mice using multiple steps of iodixanol (Sigma-Aldrich) density gradient centrifugation. Residual nucleic acid and protein contaminants were removed by incubation with benzonase (Novagen) and proteinase K (Roche). Aggregates were finally concentrated by centrifugation over a sucrose

cushion, resuspended in dH₂O, and snap frozen in liquid nitrogen, overall similar to previously described [4].

Intracerebral injection of brain extract

APP23 mice (4 - 6 months old) and APPPS1 (1.5 - 3 month-old) were anaesthetized with a mixture of ketamine (100mg/kg body weight) and xylazine (10mg/kg body weight) in saline. Bilateral stereotaxic injections of 2.5 μ l brain extract were placed with a Hamilton syringe into the hippocampus (AP -2.5mm, L +/-2.0mm, DV -1.8mm). Injection speed was 1 μ l/minute and the needle was kept in place for additional 2 minutes before it was slowly withdrawn. The surgical area was cleaned with sterile saline, the incision was sutured, and the mice were monitored until recovery from anesthesia. After stereotaxic surgery mice were housed individually in standard lab cages (1284L-116, Tecniplast, Milan, Italy) on a 12:12h light cycle (lights on at 06.00 am) with ad libitum access to food and water. Mice were sacrificed for analysis 1.5 - 3 months after surgery. Some mice/tissue was taken from a previous study [5]. All the experimental procedures were in accordance with the veterinary office regulations of Baden-Württemberg (Germany) and approved by the local Animal Care and Use Committees.

Preparation of brain sections

Under deep inhalation anesthesia, mice were sacrificed by decapitation. Brains were removed, fixed in 4% paraformaldehyde, cryoprotected in 30% sucrose, and sectioned (25 μ m-thick) on a Microtome (SM200R, Leica Microsystems, Wetzlar, Germany) in ice-cold PBS. Until use, sections were stored in cryoprotectant solution (25% (v/v) glycerine; 30% (v/v) ethylene glycol in PBS) at -20°C.

A β -immunohistochemistry of brain sections

For immunohistochemical staining sections were washed in TBS and incubated with 0.3% H₂O₂ in TBS for 30 minutes. Subsequently sections were washed in TBS, incubated 10 minutes with 0.3% Triton X-100 (Sigma, St. Louis, MO, USA) in TBS and blocked for 30

minutes with 5% goat serum. Sections were then probed overnight with polyclonal antibody NT12 (or its succeeding antibody CN3) raised against synthetic fibrillary human A β 40 (dilution 1:2000 in TBS). Both antibodies recognize A β 40 and A β 42 in tissue sections and are virtually identical [5,6]. Sections were washed in TBS and incubated with biotinylated goat anti-rabbit IgG (Vectastain Elite ABC kit, Vector Laboratories, Burlingame, CA, USA) for 90 minutes. Sections were again washed in TBS and incubated in 0.8% avidin and 0.8% biotin (Vectastain Elite ABC kit, Vector Laboratories, Burlingame, CA, USA) in TBS for 90 minutes. Sections were again washed and reacted with 3% peroxidase substrate (SG Blue, Vector Laboratories, Burlingame, CA, USA) and 3% H₂O₂ in 0.1M PBS for approx. 2 minutes until desired intensity of staining was achieved. Sections were washed in TBS and mounted on gelatin coated glass slides (Super Frost+, R. Langenbrinck, Emmending, Germany) and dried for 2 hours at room temperature. Through a series of graded ethanols, sections were dehydrated and coverslipped with xylene-based mounting medium (Pertex, Cellpath, Newtown, UK)

Quantitative analysis of the induced A β -deposition

The induced A β deposition was quantified on a set of every 12th systematically sampled, coronal, double stained for A β (immunohistochemistry) and Congo red section throughout the dentate gyrus. Stereological analysis was performed using a microscope equipped with a motorized x-y-z stage coupled to a video-microscopy system and the Stereo Investigator software (MicroBrightField, Inc., Williston, VT) as previously described [5]. The A β -load (percentage) was determined in the dentate gyrus by calculating the areal fraction occupied by A β -positive immunostaining using a 20x objective and a Zeiss Axioskop 2 microscope (Zeiss, Oberkochen, Germany). The compact plaque load was determined by calculating the areal fraction occupied by Congo red staining. However, the Congo red staining was often masked by very dense A β positive immunostaining that in turn was also added to the congophilic amyloid and termed “compact amyloid load”. Note that for the total A β load and compact A β load the areal fraction was not determined at a single focal plane but was calculated from the 25 μ m-thick sections through the dentate gyrus and thus overestimates the true A β plaque load.

Staining of brain sections with t-PTAA and collection of emission spectra

t-PTAA [7] was dissolved in deionized water to a final concentration of 1.0 mg/ml. This stock solution was further diluted to a final concentration of 20 µg/ml with 100 mM Na-Carbonate pH 10 and added to the brain sections, which were then incubated for 30 min at RT and washed with 100 mM Na-Carbonate pH 10. The sections were mounted with Dakocytocrom fluorescent mounting medium (Dako, Denmark). The medium was allowed to solidify for 3 h. Spectra were collected with a LSM 780 or a 510 META (Carl Zeiss, Jena, Germany) with an argon 488 nm laser and a Leica DM6000 B fluorescence microscope (Leica, Wetzlar, Germany) equipped with a SpectraCube (optical head) module (Applied Spectral Imaging, Migdal Ha-Emek, Israel) using bandpass filters 470/40 (LP515) and 546/12 (LP590). SpectraView 3.0 EXPO software (Applied Spectral Imaging) was used for the presentation of images and selection of spectral regions. Spectra were collected from 8 individual spots within 15–20 plaques for each animal. As previously shown, twisted separated LCP molecules emit light at 530-540 nm, whereas planar, stacked (aggregated) LCP multimers emit light at 630-650 nm. Thus the ratio of the intensity of the emitted light at 534 nm and 631 nm was used as a parameter for spectral distinction of different plaques [8].

Staining of isolated amyloid fibrils from brain with t-PTAA and collection of emission spectra

Amyloid fibril preparations from the whole brain were diluted 1:5 with the tPTAA staining solution (20 µg/ml dissolved in 100 mM Na-Carbonate pH 10) and were left to incubate for 2 h at room temperature in the dark. Sample aliquots (3 µl) were applied to glass slides, air dried and coated with Dakocytocrom fluorescent mounting medium (DAKO, Denmark), and a cover slip. Non-transgenic age matched control samples prepared side-by-side, were used as references. Samples were imaged as described above for brain sections. Spectra were collected from 10 individual regions (2 pixel circle) within each of 4 images for each preparation.

Western blot analysis of A β in laser-dissected tissue pieces

Hippocampal sections were A β immunostained using antibody NT12 or CN3 (see above). With the aid of a laser microdissection microscope (MicroBeam, P.A.L.M., Bernried, Germany) patches of the dentate gyrus including polymorphic, granular and molecular layers and part of the CA3 region (see Fig. 1J) were cut from the hippocampus of unstained 25 μ m thick coronal sections adjacent to sections in which the location of the A β induction was confirmed. Patches were picked up and transferred with the aid of a cannula to a test tube. To separate A β 40 and A β 42 [40], samples were sonicated 3x5s in 0.718 M Bis-Tris; 0.318 M Bicine; 2% (w/v) SDS; 30% (w/v) sucrose; 5% (v/v) 2-mercaptoethanol; 0.008% (w/v) bromophenol blue, and then boiled for 5 minutes and subjected to 10% Bicine-Tris 8M Urea SDS-PAGE as previously described [5,9]. Synthetic A β 1-40 and A β 1-42 (American Peptide Company, Sunnyvale, CA, USA) were used as controls. Proteins were transferred onto a nitrocellulose membrane and probed with monoclonal antibody 6E10 specific to human A β (dilution 1:5000; Covance, NJ, USA). The secondary antibody was horseradish peroxidase-conjugated goat anti-mouse IgG (Santa Cruz Biotechnologies, Santa Cruz, CA, USA). Bands were visualized using Amersham ECL Plus (GE Healthcare, Little Chalfont, United Kingdom) and developed onto Kodak X-OMAT AR film (Kodak, Rochester, NY, USA). The mean densitometric values of band intensities in multiple exposures were analyzed to calculate the ratio of A β 40 to A β 42 using the public domain software ImageJ, version 1.42q (<http://rsb.info.nih.gov/ij>). In total 266 sections were analyzed.

SUPPLEMENTARY FIGURES

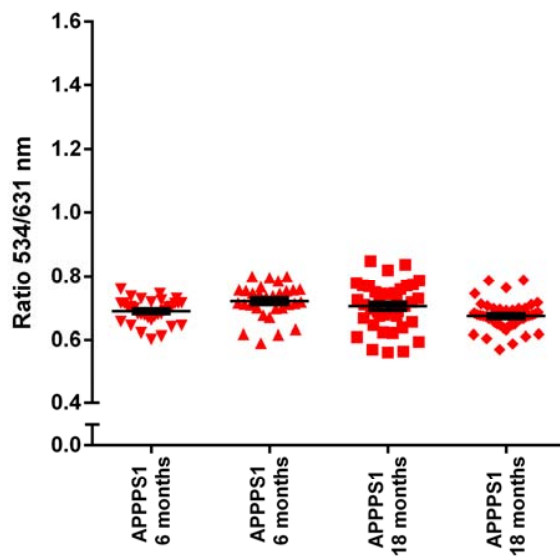


Figure S1. Because the APPS1 mice used for the analysis in Figure 1 were younger (6 months of age) compared to the APP23 mice (18 months of age) and an age-dependent difference in staining was reported when a combination of two distinct LCPs were used [10], the spectral profile of tPTAA was additionally assessed in 6 versus 18 months old APPS1 brain sections. However, no age-related difference was found. Experiments and analysis were performed as described in the main paper.

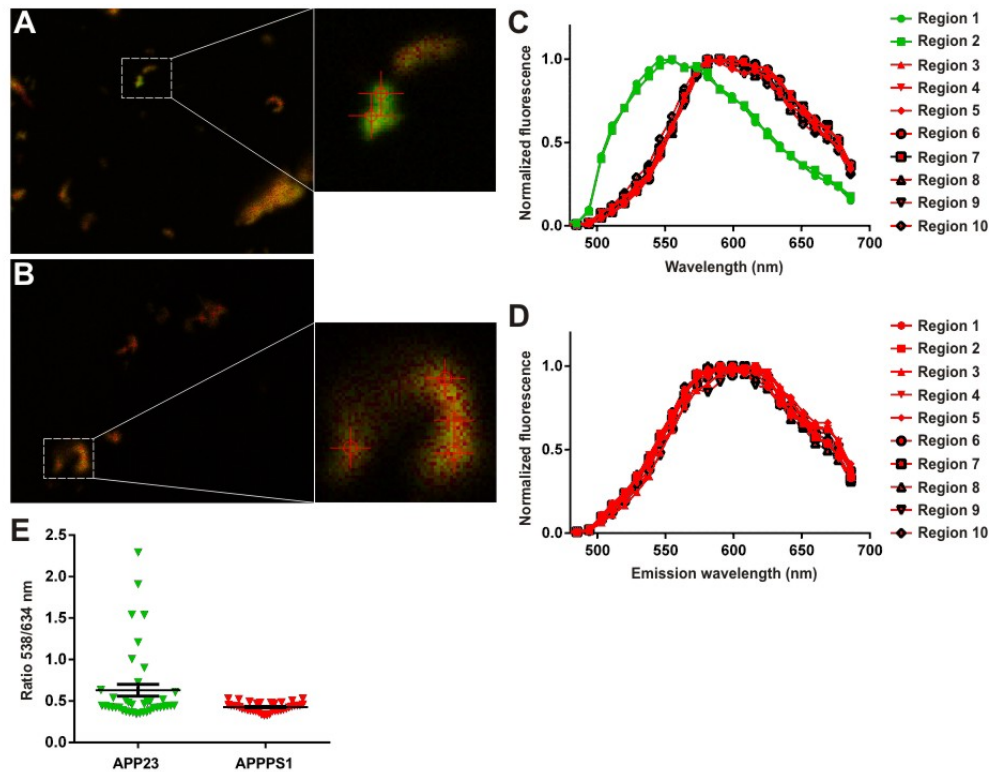


Figure S2. Fluorescence ratios of t-PTAA stained isolated amyloid fibrils from the brain of APP23 and APPPS1 mice. **(A,B)** t-PTAA staining of isolated amyloid fibrils from a 28 month-old APP23 mouse (A) and 20 month-old APPPS1 mouse (B). Note the shift to green colors of the A β fibrils of the APP23 mouse compared to the reddish color of the A β fibrils of the APPPS1 mouse. **(C,D)** Representative emission spectra of t-PTAA bound to the isolated A β fibrils of APP23 mice (C) and APPPS1 mice (D). Spectra were collected from 10 individual regions (2 pixel circle) within each of 4 images for each preparation. **(E)** For quantitative analysis the ratio of the intensity of the emitted light at 534 nm and 631 nm was calculated (see also method section). Each dot/triangle represents one spectrum from a 2 pixel circle region within the image (40 in total for each mouse preparation). Mean and SEM are indicated. A two-tailed t-test revealed a significant difference between the groups ($t(78)=2,84$; $p<0.01$). Note that the greater variation in the ratio of APP23 fibrils compared to APPPS1 fibrils is in accordance with the spectral analysis done in brain sections (see Figure 1).

SUPPLEMENTARY REFERENCES

1. Sturchler-Pierrat C *et al* (1997) Two amyloid precursor protein transgenic mouse models with Alzheimer disease-like pathology. *Proc Natl Acad Sci U S A* **94**: 13287-13292
2. Radde R *et al* (2006) Abeta42-driven cerebral amyloidosis in transgenic mice reveals early and robust pathology. *EMBO Rep* **7**: 940-946
3. Eisele YS *et al* (2009) Induction of cerebral beta-amyloidosis: intracerebral versus systemic Abeta inoculation. *Proc Natl Acad Sci U S A* **106**: 12926-12931
4. Sim VL, Caughey B (2009) Ultrastructures and strain comparison of under-glycosylated scrapie prion fibrils. *Neurobiol Aging* **30**: 2031-2042
5. Meyer-Luehmann M *et al* (2006) Exogenous induction of cerebral beta-amyloidogenesis is governed by agent and host. *Science* **313**: 1781-1784
6. Eisele YS *et al* (2010) Peripherally applied Abeta-containing inoculates induce cerebral beta-amyloidosis. *Science* **330**: 980-982
7. Aslund A, Herland A, Hammarstrom P, Nilsson KP, Jonsson BH, Inganas O, Konradsson P (2007) Studies of luminescent conjugated polythiophene derivatives: enhanced spectral discrimination of protein conformational states. *Bioconjug Chem* **18**: 1860-1868
8. Nilsson KP *et al* (2007) Imaging distinct conformational states of amyloid-beta fibrils in Alzheimer's disease using novel luminescent probes. *ACS Chem Biol* **2**: 553-560
9. Wiltfang J *et al* (1997) Improved electrophoretic separation and immunoblotting of beta-amyloid (A beta) peptides 1-40, 1-42, and 1-43. *Electrophoresis* **18**: 527-532
10. Nystrom S *et al* (2013) Evidence for Age-Dependent in Vivo Conformational Rearrangement within Abeta Amyloid Deposits. *ACS Chem Biol*, 10.1021/cb4000376

3.3 Conversion of synthetic A β to *in vivo* active seeds and amyloid plaque formation in a hippocampal slice culture model

Renata Novotny*, Franziska Langer*, Jasmin Mahler, Angelos Skodras, Andreas Vlachos, Bettina M. Wegenast-Braun, Stephan A. Kaeser, Jonas J. Neher, Yvonne S. Eisele, Marie J. Pietrowski, K. Peter R. Nilsson, Thomas Deller, Matthias Staufenbiel, Bernd Heimrich and Mathias Jucker

in press

The Journal of Neuroscience (2016)

Conversion of synthetic A β to *in vivo* active seeds and amyloid plaque formation in a hippocampal slice culture model

Renata Novotny^{1,2,3,*}, Franziska Langer^{1,2,*}, Jasmin Mahler^{1,2,3}, Angelos Skodras^{1,2}, Andreas Vlachos⁴, Bettina M. Wegenast-Braun^{1,2}, Stephan A. Kaeser^{1,2}, Jonas J. Neher^{1,2}, Yvonne S. Eisele^{1,2}, Marie J. Pietrowski⁵, K. Peter R. Nilsson⁶, Thomas Deller⁴, Matthias Staufenbiel^{1,2}, Bernd Heimrich⁵ and Mathias Jucker^{1,2}

¹Department of Cellular Neurology, Hertie Institute for Clinical Brain Research, University of Tübingen, D-72076 Tübingen, Germany; ²DZNE, German Center for Neurodegenerative Diseases, D-72076 Tübingen, Germany; ³Graduate School for Cellular and Molecular Neuroscience, University of Tübingen, D-72076 Tübingen, Germany; ⁴Institute of Clinical Neuroanatomy, Neuroscience Center, Goethe-University Frankfurt, D-60590 Frankfurt/Main, Germany; ⁵Institute of Anatomy and Cell Biology, University of Freiburg, D-79104 Freiburg, Germany; ⁶Department of Chemistry, IFM, Linköping University, SE-581 83 Linköping, Sweden

* contributed equally

Abbreviated title: *In vivo* active synthetic A β seeds in slice cultures

Figures: 6

Number of pages: 32

Number of words: 203 (abstract), 264 (introduction), 1072 (discussion)

Conflict of interest: none.

Author contribution: R.N., F.L., J.M., A.S., A.V., B.M.W-B., S.A.K., J.J.N., M.J.P. and B.H. performed the experimental work. R.N., F.L., J.M., A.S., B.H. and M.J. carried out the analysis. Experimental design and preparation of the manuscript was done by R.N., F.L., K.P.R.N., T.D., M.S., B.H. and M.J.

Acknowledgment: We would like to thank Ulrike Obermüller, Jay Rasmussen, Simone Zenker, Aileen Koch, Sigrun Nestel, Melanie Barth, Anke Biczysko and the other members of our laboratories for help and discussions. The antibody donation of Paul Mathews (NKI, Orangeburg, NJ) is greatly appreciated. This work was supported by grants to BH and MJ from the German Federal Ministry of Education and Research (BMBF-ALZKULT 031A198), to MJ from the EC Joint Programme on Neurodegenerative Diseases (JPND-NeuTARGETs), and to TD and AV from the German Research Council (DFG DE 551/11-2 and VL 72/1-2).

Correspondence to: Bernd Heimrich: bernd.heimrich@zfn.uni-freiburg.de, or Mathias Jucker: mathias.jucker@uni-tuebingen.de.

SUMMARY

The aggregation of amyloid-beta peptide (A β) in brain is an early event and hallmark of Alzheimer's disease (AD). We combined the advantages of *in vitro* and *in vivo* approaches to study cerebral β -amyloidosis by establishing a long-term hippocampal slice culture (HSC) model. While no A β deposition was noted in untreated HSC of postnatal A β precursor protein transgenic (APP tg) mice, A β deposition emerged in HSC when cultures were treated once with brain extract from aged APP tg mice and the culture medium was continuously supplemented with synthetic A β . Seeded A β deposition was also observed under the same conditions in HSC derived from wildtype or *App*-null mice but in no comparable way when HSC were fixed prior to cultivation. Both the nature of the brain extract and the synthetic A β species determined the conformational characteristics of HSC A β deposition. HSC A β deposits induced a microglia response, spine loss, and neuritic dystrophy but no obvious neuron loss. Remarkably, in contrast to *in vitro* aggregated synthetic A β , homogenates of A β deposits-containing HSC induced cerebral β -amyloidosis upon intracerebral inoculation into young APP tg mice. Our results demonstrate that a living cellular environment is necessary for the seeded conversion of synthetic A β into an *in vivo* seeding-active form.

Significance Statement

In this study, we report the seeded induction of A β aggregation and deposition in long-term hippocampal slice cultures. Remarkably, we find that the biological activities of the largely synthetic A β aggregates in the culture are very similar to those observed *in vivo*. This observation is first to show that biologically active A β aggregates can be obtained by seeded conversion of synthetic A β in a living (wildtype) cellular environment.

INTRODUCTION

A hallmark and early trigger of Alzheimer's Disease (AD) pathogenesis is the aggregation of amyloid-beta peptides (A β) in brain (Hardy and Selkoe, 2002; Holtzman et al., 2011). Although A β aggregation studies in cell-free systems have provided important insights into the dynamics and kinetics of amyloid formation (Harper and Lansbury, 1997; DaSilva et al., 2010; Du et al., 2011), it was the development of A β precursor protein transgenic (APP tg) mouse models that has revolutionized the research of cerebral β -amyloidosis (Games et al., 1995; Hsiao et al., 1996; Sturchler-Pierrat et al., 1997; Duyckaerts et al., 2008; Jucker, 2010). The need of *in vivo* approaches to study cerebral β -amyloidosis was further bolstered by the observation that *in vitro* aggregated synthetic A β is a poor *in vivo* seed for cerebral β -amyloidosis (Meyer-Luehmann et al., 2006; Stohr et al., 2012) likely due to conformational differences and/or cofactors compared to *in vivo* generated A β aggregates (Paravastu et al., 2009).

We and others (Harris-White et al., 1998; Johansson et al., 2006) have tried to model β -amyloidosis in hippocampal slice cultures (HSC) from APP tg mice for more than a decade, however with poor success. Now we report that seeding such cultures once with brain homogenates from aged APP tg mice while supplementing the medium continuously with synthetic A β induces robust A β aggregation and associated pathologies with biological activities remarkably similar to those observed *in vivo* in APP tg mice and AD brains. Our results demonstrate that *in vitro* formation of *in vivo* seeding-active A β aggregation can be achieved by seeded conversion of synthetic A β in a living cellular environment.

MATERIALS AND METHODS

Mice for Hippocampal Slice Cultures

Hippocampal slice cultures (HSC) were prepared from pups of the following mice: Male and female C57BL/6J mice, APP23 and APPPS1 tg mice, and crosses of APP23 x APPPS1 mice. APP23 tg mice overexpress human APP 7-fold and harbor the Swedish double mutation (Sturchler-Pierrat et al., 1997). APPPS1 tg mice overexpress human APP 3-fold and harbor Swedish double mutation and mutated human presenilin 1 (PS1) (Radde et al., 2006). We furthermore used *App*-null mice (Eisele et al., 2014) and mice expressing enhanced green fluorescence protein (GFP) under the control of the neuron-specific Thy-1 promoter (Thy1-GFP) (Feng et al., 2000; Vlachos et al., 2012).

Preparation of Hippocampal Slice Cultures

HSC were prepared from pups at postnatal day 2–3 according to previously published protocols (Brinks et al., 2004; Mayer et al., 2005). Postnatal pups were sacrificed by decapitation and brains were aseptically removed. Hippocampi were dissected and cut perpendicular to the longitudinal axis into 400 μm sections with a tissue chopper. Intact hippocampal sections were transferred into petri dishes, containing cold buffer solution of minimum essential medium (MEM) supplemented with 2 mM GlutaMAXTM (Life Technologies, Thermo Fisher Scientific Inc., Waltham) at pH 7.3. Four sections were placed onto one humidified porous membrane (Millicell Cell Culture Inserts CM30; Merck KGaA, Darmstadt, Germany) per well in six well plates filled with 1.2 ml culture medium/well. The culture medium consisted of heat-inactivated horse serum (25%), Hanks' balanced salt solution (25%) and MEM (50%), complemented with GlutaMAXTM (2 mM) adjusted to pH 7.2. HSCs were kept at 37°C in humidified CO₂-enriched atmosphere. The medium was changed three times per week. HSC of Thy1-GFP mice also contained entorhinal cortex and were prepared according to a similar and previously described protocol (Del Turco and Deller, 2007).

Treatment of Hippocampal Slice Cultures

HSC were kept for 10 days without any experimental treatment to obtain stable culturing conditions. At day 10 after the medium change synthetic A β 1–40 or A β 1–42 (from 100 μM frozen stock solution; initially prepared by adding PBS to lyophilized A β , followed by 3 x 1 min vortexing on wet ice) was added to the medium to reach a final concentration of 1.5 μM (American Peptide Company Inc., Sunnyvale, USA). Subsequently, 1 μl of brain extract of APP23 or APPPS1 tg mice or of non-

tg wildtype mice (for a description of the extracts, see below) was pipetted once on the surface of each culture. Over the following 9-week cultivation period all subsequent medium changes were done with culture medium containing 1.5 μ M synthetic A β . (note: no more extract was added). Some HSC were pre-fixed after one week with 4% paraformaldehyde (PFA) in 0.1 M phosphate buffer (PB) at room temperature for 2 hours, rinsed 3 times with PB for 10 min followed by the combined treatment as described above.

Histology and Immunohistochemistry of Hippocampal Slice Cultures

HSC were fixed with 4% PFA in 0.1 M PB, pH 7.4 for 2 hours. Cultures were rinsed 3 times with 0.1 M PB for 10 min. The Millipore membrane with the fixed cultures was cut off and cultures were mounted on a planar agar block and sliced into 50 μ m sections on a vibratome (Leica VT 1000S Vibratome, Leica Biosystems Nussloch GmbH, Nussloch, Germany). Typically 2–4 intact sections were obtained per culture and were collected in PBS. Immunohistochemistry was performed according to standard protocols on free-floating sections either using the Vectastain Elite ABC Kit (Vector laboratories Inc. Burlingame, USA) or standard immunofluorescence with appropriate secondary antibodies (goat anti-rabbit or goat anti-mouse Cy3- or Alexa 488-, 546-, 568-, or 647-conjugated antibodies (Life Technologies, Thermo Fisher Scientific Ink., Waltham) (Mayer et al., 2005; Eisele et al., 2010). As primary antibodies were used: polyclonal rabbit CN3 antibody to human A β (Eisele et al., 2010); rabbit polyclonal antibody against ionized calcium binding adapter molecule 1 (Iba-1, Wako Chemicals USA Ink., Richmond); mouse monoclonal antibody against neurofilament light polypeptide (NF-L; MAB1615; Millipore, Temecula, CA); mouse monoclonal antibody AT8 (Thermo Scientific, Waltham, MA) directed against p-Tau position 191/194 (murine). Some of the sections were counterstained with Congo red and examined for birefringence under polarized light. Immunofluorescence stained sections were routinely counterstained with DAPI nuclear stain (300 nM, Life Technologies, Thermo Fisher Scientific, Waltham, USA).

Extract Preparation from Brain and Hippocampal Slice Culture

Brain extracts were prepared from aged (24-month-old) male or female APP23 tg mice, aged (21-month-old) APPPS1 tg mice, and age-matched non-tg control mice as described previously (Meyer-Luehmann et al., 2006). In brief, after removal of the cerebellum and lower brainstem, the forebrain was immediately fresh-frozen on dry ice and stored at -80°C until use. Tissue was homogenized (Ultra Turrax T8, IKA®-Werke Staufen, Germany) at 10% (w/v) in sterile PBS (Lonza Group Ltd., Valais, Switzerland), vortexed, sonicated three times for 5 seconds each (LabSonic, B. Braun

Biotech International GmbH, Melsungen, Germany; 0.5 mm diameter sonotrode, cycle 1, amplitude 80%) and centrifuged at $3000 \times g$ for 5 min. The extract is referred to the supernatant and typically contained 1-10 ng/ μ l total A β (A β 40 and A β 42 combined). Extracts were aliquoted and immediately frozen at -80°C until use. Slice culture homogenates were prepared from 15 identically treated HSCs. Cultures were removed from the membrane, pooled and immediately frozen on dry ice and stored at -80°C until use. Frozen slice cultures were homogenized with EPPI-pestles (Schuett biotec, Göttingen, Germany) in 150 μ l sterile PBS, vortexed and sonicated three times for 5 seconds each. HSC homogenates were aliquoted and immediately frozen at -80°C until use.

SDS-Page and Immunoblot Analysis

HSC homogenates/extracts were analyzed on NuPAGE Bis-Tris mini gels using LDS sample buffer and MES running buffer (Life Technologies, Thermo Fisher Scientific Ink., Waltham). Proteins were transferred onto a nitrocellulose membrane, probed with monoclonal antibody m3.2 against murine A β (Morales-Corraliza et al., 2009) and visualized using SuperSignal West Dura chemiluminescent substrate (Life Technologies, Thermo Fisher Scientific Ink., Waltham).

Staining with Luminescent Conjugated Oligothiophenes

Luminescent conjugated oligothiophene (LCO) amyloid-binding dyes were used in order to distinguish between different A β morphotypes, by detecting fluorescence emission spectral differences. Specifically, the pentamer formyl acetic acid (pFTAA) LCO was used, as described previously (Fritschi et al., 2014). For visualizing A β deposition in HSCs from Thy1-GFP mice, an LCO with red-shifted fluorescence emission was chosen (the heptamer formyl acetic acid – hFTAA (Klingstedt et al., 2011)), in order to avoid fluorescence cross-talk between the eGFP signal and the LCO. A β deposition in microglia depleted HSCs was visualized with the blue-shifted LCO qFTAA (quadro-formylthiophene acetic acid (Klingstedt et al., 2011)) to avoid bleed-through into the CN3 (secondary antibody conjugated to Alexa 546) and Iba-1 (secondary antibody conjugated to Alexa 647) channels. For the staining of either LCO, HSC sections were washed in PBS (3 x 10 min) and subsequently mounted on Superfrost slides. Staining with the LCOs (1.5 mM in deionized water, diluted 1:1000 in PBS) was performed similar to a previous description (Klingstedt et al., 2011). Sections were allowed to dry for 2 h at RT and then coverslipped with Dako Fluorescence Mounting Medium.

Quantification of Total A β Load

The total A β load (%) of HSC was determined on each section (50 μ m thick) from the re-sliced cultures by calculating the areal fraction occupied by CN3-positive (peroxidase-based) immunostaining in two-dimensional sectors over the whole section volume (20x/0.45 NA objective). The mean A β load of all the sections from each culture (typically 2–4 sections) was regarded as the total A β load of the corresponding culture.

The total A β load (%) induced by the injection of HSC extract into the dentate gyrus of young APP23 tg mice was determined on a set of every 12th systematically sampled, serial (25 μ m thick) sections throughout the entire dentate gyrus by calculating the areal fraction occupied by CN3- and Congo red-positive immunostaining in two-dimensional sectors at a single focal plane (20x/0.45 NA objective). All the stereological quantification was done with a microscope equipped with a motorized x-y-z stage coupled to a video microscopy system (Stereo Investigator; MicroBrightField, Ins., Williston, USA) as previously described (Bondolfi et al., 2002). The investigator who performed analysis was blind towards the different groups.

Electron Microscopy

HSC were immersed in a fixative solution (4% PFA, 0.05 % glutaraldehyde, 15 % saturated picric acid in 0.1M PBS) for 2 hours and then washed, osmicated, dehydrated and flat-embedded in resin (Fluka Durkupan, EMS, Hatfield, USA) on glass slides. Ultrathin sections were cut by an Ultracut (Leica EM UC7, Leica Biosystems Nussloch GmbH, Nussloch, Germany) and collected on single-slot Formvar-coated nickel grids. For immunolabeling a postembedding protocol was used. After etching in 1% periodic acid for 10 min, an incubation in 1% sodium metaperiodate and glycine/sodium borohydrate solution followed (10 min each). Sections were blocked in 2% human serum albumin in TBST for 10 min and incubated with the polyclonal rabbit CN3 antibody to A β (Eisele et al., 2010) (1:100 over night at 4°C. As secondary layer a gold-conjugated (10 nm) anti-rabbit antibody (1:50, British Biocell Interaction, Cardiff, UK) was used. Sections were exposed to lead citrate for 2 min. Digital images were taken by means of a transmission electron microscope (Leo 906 E, Carl Zeiss MicroImaging GmbH, Jena, Germany) equipped with a 2K Sharpeye CCD camera (Tröndle, Moorenweiss, Germany).

Spine Counts at Electron Microscopic Level

For spine count analysis at electron microscopic level 16-week-old untreated wildtype HSCs and HSCs treated with APPPS1 tg brain extract and synthetic A β 1–42 were analyzed (n=3 each). From

each culture 20 panoramic images (each composed of 3x3 attached and non-overlapping photos) at same magnification were taken randomly. The photographed area of each culture was approximately 2450 μm^2 and number of spines per area was manually counted. The investigator performing the analysis was blind towards the two groups. The Student's t-test was used for statistical analysis.

Spine Analysis at Light Microscopic Level

Spine analysis was done on HSC derived from Thy1-GFP mice. A β plaques were visualized by hFTAA staining (see above for details). GFP and hFTAA were both excited using a 488 nm argon laser line. GFP fluorescence emission was collected using a narrow bandpass 505–530 nm filter, whereas the hFTAA emission was collected using a longpass 585 nm filter, ensuring no fluorescence cross-talk between the two dyes. Dendritic spines were quantified in Fiji (public domain software, version 1.84, <http://fiji.sc/Fiji>) using 3D image stacks of side branches of principal apical dendrites (second- or higher-order dendritic segments) of CA1 pyramidal neurons within stratum radiatum. Image stacks were acquired using the Zeiss LSM 510 META (Axiovert 200M; Carl Zeiss MicroImaging GmbH, Jena, Germany) confocal microscope and a 63x/oil objective (1.4 NA, Zeiss). Spine counting was performed blind to experimental conditions on randomly chosen individual dendritic segments within each culture (4 cultures per condition, 3-8 dendritic segments per culture); the length of the dendritic segment was measured in 3D using the Simple Neurite Tracer plugin in Fiji. The number of spines on each segment was recorded using the Cell Counter plugin in Fiji. The average number of spines per μm on a dendritic segment was used as a measure of spine density. Spine density was calculated on all cultures per condition.

Spectral Analysis of A β Morphotypes

Spectra of pFTAA stained amyloid aggregates within HSC sections (for staining details, see above) were acquired on a Zeiss LSM 510 META (Axiovert 200M) confocal microscope (40x oil-immersion objective, 1.3 NA) equipped with a spectral detector. The dye was excited using the 458 nm argon laser line. Emission spectra were acquired from 470 nm to 695 nm at a step of 10.70 nm and normalized to their respective maxima. The ratio of the intensity of emitted light at the blue-shifted portion (502 nm) and red-shifted peak (599 nm) was used as a parameter for spectral distinction of different plaques. These peaks were selected to maximize the spectral differences of the pFTAA-stained A β plaques between HSC treated with brain APP23 or APPS1 extract in combination with synthetic A β 1–40 or A β 1–42. The 599/502 ratio was computed for each plaque by determining the mean of the 599/502 ratio at 3 different regions of interest (ROIs) within one A β

plaque (core). All plaques analysed were from the intermediate sections of the cultures (neither top nor bottom section) and border regions were excluded. In each culture 4–15 A β plaques were analysed and the mean was taken for statistical analysis (n = cultures; 11-13 cultures were analysed per condition).

Microglia Depletion

To deplete microglia in culture (Kohl et al., 2003) the bisphosphonate clodronate (Clodronate disodium salt, Merck KGaA, Darmstadt, Germany) was dissolved in dH₂O (1mg/ml) and applied to the culture medium at 100 μ g/ml. After 24 hours cultures were carefully rinsed with pre-warmed PBS and replaced with fresh culture medium. A β deposition was induced on day 10 as described above. Seven weeks later HSC were fixed in 4% PFA. HSC were sliced on a vibratome (as described above) and immune-stained for Iba-1 (with the secondary antibody conjugated to Alexa 647 fluorochrome) to assess the microglia depletion. Amyloid deposits were stained using polyclonal CN6 antibody (a follow-up version of CN3) with the secondary antibody conjugated to Alexa 546). Images of sectioned cultures were captured on a Zeiss Axioplan 2 microscope, using tile scanning (MosaiX on AxioVision 4.3) and a Zeiss Plan Neofluar x10/0.3 objective. A semi-automated computer analysis was performed using a custom-made macro written for Fiji (public domain software, version 1.84, <http://fiji.sc/Fiji>) in order to quantify the percentage of A β immunostaining and microglia on each section. Gamma values were adjusted to reduce background tissue fluorescence prior to thresholding each channel. The ratio of the thresholded pixels to the total pixels yielded the microglia stained area coverage, expressed as percentage microglia load and the A β stained area coverage, expressed as percentage A β load.

Electrochemiluminescence-Linked Immunoassay for A β

A β (A β _{x-40}, A β _{x-42}) concentrations in brain extracts, culture extracts and synthetic A β preparations were determined with an electrochemiluminescence-linked immunoassay as previously described (Langer et al., 2011) using the new V-PLEX A β peptide panel 1 (6E10) kit according to manufacturer's instructions (Meso Scale Discovery, Gaithersburg, USA). For total A β , A β _{x-40} and A β _{x-42} were combined.

Preparation of Synthetic A β Fibrils

A β ₁₋₄₀ or A β ₁₋₄₂ (American Peptide Company Inc., Sunnyvale, USA) was dissolved in PBS at a concentration of 100 μ M (i.e. 433ng A β ₁₋₄₀/ μ l or 451 ng A β ₁₋₄₂/ μ l), vortexed 3 x 1 min on wet

ice. Solutions were subsequently incubated at 37°C for 5 days on a rotator, as previously described (Meyer-Luehmann et al., 2006). Aliquots were stored at -80°C until use.

Assessing A β Seeding Activity of Brain Extracts and Hippocampal Slice Culture Homogenates

Male and female 4-month-old APP23 tg mice on an *App*-null background (Eisele et al., 2014) served as host mice (gender was matched between the groups). The mice were anaesthetized with a ketamine/xylazine mixture (ketamine 100 mg/kg, xylazine 10 mg/kg) in saline. Bilateral stereotactic injections of 2.5 μ l brain extract or culture homogenate were made with a Hamilton syringe into the hippocampus (AP -2.5 mm, L \pm 2.0 mm, DV -1.8 mm). Injection speed was 1.25 μ l/min and the needle was kept in place for additional 2 min before withdrawal. The surgical area was cleaned with sterile PBS and the incision was sutured. The mice were kept under infrared light and monitored until recovery from anesthesia.

Four months later animals were sacrificed and the brains were removed and immersion-fixed for 48 h in 4% PFA in PBS, followed by cryoprotection in 30% sucrose in PBS for additional 48 h. After freezing, brains were cut into 25 μ m-thick coronal sections using a freezing-sliding microtome (Leica SM 2000R, Leica Biosystems Nussloch GmbH, Nussloch, Germany). Sections were collected in cryoprotectant (35% ethylene glycol, 25% glycerol in PBS) and stored at -20 °C until use. Immunohistochemistry was performed according to standard protocols with the Vectastain Elite ABC Kit (Vector laboratories Inc. Burlingame, USA) using the polyclonal rabbit CN3 antibody to A β and counterstained with Congo red as previously described (Eisele et al., 2010).

Study Approval

Experimental procedures were carried out in accordance with German animal welfare legislation and approved by the local animal welfare officer and/or the local Animal Care and Use Committees.

RESULTS

A β Deposition in HSC is Induced by Seeded Aggregation of Synthetic A β

HSC were prepared from postnatal APP23, APPPS1 and APP23 x APPPS1 double tg mice and cultivated for up to 10 weeks (Fig. 1). After this time the cytoarchitecture was still largely intact. However, no A β deposition was detected in any of the untreated HSC (Fig. 1C) despite robust A β deposition being present in 8-week-old APP23 x APPPS1 tg mice *in vivo* (F. Langer and M. Jucker, unpublished observation). To compensate for the release of the secreted A β from the slices into the medium the latter was supplemented continuously with 1.5 μ M synthetic A β 1–40. Again, no A β deposits emerged in the HSC (Fig. 1D).

Previous work has shown that cerebral β -amyloidosis can be induced in APP tg mice by inoculation with A β -amyloid containing brain extracts (Meyer-Luehmann et al., 2006; Eisele et al., 2010). Inspired by these findings, a small volume (1 μ l) of extract from an aged amyloid-laden APP23 tg mouse brain was applied once onto the top of the HSC on day 10 after establishing the culture. Yet again, no A β deposits were induced even after 9 weeks in culture (Fig. 1E). However, when treatment with brain extract from aged APP23 tg mice (but not from age-matched wildtype control mice) was combined with the continuous application of synthetic human A β 1–40 in the medium, robust A β deposition was induced in the slices (Fig. 1F). Remarkably, this treatment combination also induced A β deposition in HSC derived from wildtype mice (Fig. 1G), suggesting that A β deposits develop also in the absence of transgenic HSC-generated human A β . This was also true for endogenous HSC-derived mouse A β since deposits were also found in HSCs from *App*-null mice using the same conditions (Fig. 1H). Thus, HSC-generated A β is not necessary for the induction of A β deposition; however, if present, HSC-derived murine A β appears to co-deposit with the induced A β deposits (Fig. 1L). Strikingly, when tg brain extract and synthetic A β treatment were applied to formaldehyde-fixed (and thus inactivated) HSC, A β deposition was limited to the rim of the culture (Fig. 2), while in living HSC A β deposition was much stronger and also present in the center of the sections (Fig. 1I, 2B). This argues that living hippocampal slices are mandatory for the development of A β deposits in HSC. Furthermore, in living HSC A β deposition was dependent on time and on concentration of synthetic A β in the medium (Fig 1J, K). With the highest A β concentration tested (1.5 μ M synthetic A β 1–40 in the medium) first A β deposits were detected 1 week after the combined treatment and increased further for up to 10 weeks in culture.

Brain Extract and Synthetic A β Species Determine the Morphotype of HSC A β Deposits

The requirement of adding both amyloid-laden APP tg brain extract on top of the culture and synthetic A β to the medium to induce HSC A β deposition suggests that A β aggregation in culture occurs via seeded conversion. To confirm such a mechanism HSC were treated with brain extracts from either aged APP23 or aged APPPS1 tg mice and were incubated with medium supplemented with either synthetic A β 1–40 or A β 1–42. A β deposits in APP23 tg mice differ in appearance and molecular architecture from deposits in APPPS1 tg mice (Heilbronner et al., 2013). While A β deposits in aged APP23 tg mice are fairly large and contain predominantly A β 40 (i.e. A β ending with amino acid 40), A β plaques in aged APPPS1 tg mice are smaller, more numerous, highly compact, and contain predominantly A β 42. Indeed, HSC treated with APP23 brain extract and synthetic A β 1–40 demonstrated larger plaques while deposits were smaller, more numerous and highly compact when cultures were treated with APPPS1 extract and synthetic A β 1–42 (Fig. 3). Based on morphological criteria, both the brain extract as well as the synthetic A β species in the medium determined the morphotypes of the induced A β deposits. Using the amyloid conformation-specific luminescent conjugated oligothiophene pFTAA (Klingstedt et al., 2011; Fritschi et al., 2014) this morphological observation was quantitatively confirmed (Fig. 3E).

HSC A β Deposits Recapitulate Many Aspects of Cerebral β -Amyloidosis

Electron microscopic analysis of HSC A β deposits revealed anti-A β -immunogold labeled amyloid fibers arranged in typically packed parallel bundles (Fig. 4A) virtually identical as described for A β plaques in APP tg mice (Stalder et al., 1999; Stalder, 2001) and AD patients (Terry et al., 1963). Larger deposits exhibited Congo red-positive staining with the characteristic birefringence under cross-polarized light (Fig. 4B, C).

To study amyloid associated morphological alterations in more detail, HSCs were prepared from tg mice expressing enhanced green fluorescence protein (GFP) in neurons (Thy1-GFP mice) and were treated once with brain extract from aged APPPS1 tg mice while the media was supplemented with synthetic A β 1–42. Numerous GFP-positive dystrophic and neuritic structures were observed in vicinity of A β -plaques (Fig. 4D-F). Also at ultrastructural level dystrophic boutons were observed in the vicinity of A β plaques (Fig. 4G). Some of these dystrophic structures were positive for phosphorylated Tau (AT8 antibody) and neurofilament light chain (Fig. 4H, I). Overall, the dystrophic elements appeared very similar to dystrophic neurites described in aged APP tg mice (Masliah et al., 1996; Phinney et al., 1999; Rupp et al., 2011) and AD brain (Probst et al.,

1983). The same HSCs were then used for dendritic spine counts, which revealed an approximate 50% decrease in the density of GFP-labeled spines (Fig. 4J–L). Spine loss appeared to be strongest in the vicinity of A β deposits, again similar to reports in aged APP tg mice (Spires et al., 2005; Bittner et al., 2010). A general decrease (39%) in the number of spines was also found at the ultrastructural level in wildtype HSCs treated with APPS1 brain extract and synthetic A β 1–42 compared to untreated wildtype HSCs (221.0 ± 31.79 vs 135.7 ± 13.22 spines per counting area, indicated is the mean \pm SEM, see Material and Methods for details; $p < 0.05$). Obvious neuron loss was not apparent in HSC, similar to APP23 and APPS1 mice, where neuron loss is also modest and develops only in aged mice (Calhoun et al., 1998; Rupp et al., 2011).

A β plaques in APP tg mice and human AD brain are surrounded by microglia (Itagaki et al., 1989; Mackenzie et al., 1995; Stalder et al., 1999; Grathwohl et al., 2009). While microglia were evenly distributed in untreated HSC, they were more numerous, hypertrophic, and intensely Iba1-positive in areas with A β deposition (Fig. 5 A, B). Although individual microglia cells were attached to the amyloid deposits with apparent uptake of amyloid-positive material (Fig. 5C), the typical tight clustering of several microglia around a single A β deposit (plaque) as seen in APP tg mice and AD brain was not observed in HSC. When microglia were depleted in HSC, the total A β load was not significantly changed but a significant increase of the more compact LCO-positive amyloid was noted (Fig. 5D).

HSC with Induced A β Deposits Efficiently Seed β -Amyloidosis in APP Tg Animals

To assess whether such HSC harbor β -amyloid inducing activity *in vivo*, 2.5 μ l of homogenates from amyloid-laden cultures (treated with APP23 tg brain extract and synthetic A β 1–40), or the same amount of homogenates from amyloid-free cultures (treated only with APP23 tg brain extract) were injected into the hippocampus of young, 4 month-old APP23 tg mice on an *App*-null background. For comparison, some hosts were intracerebrally injected with APP23 brain extract or with aggregated, synthetic A β 1–40, which have previously been shown to have very potent and very poor *in vivo* β -amyloid-inducing activities, respectively (Meyer-Luehmann et al., 2006) (Fig. 6A, B). Analysis 4 months post-inoculation revealed the expected induction of A β deposition in the hippocampus of mice receiving APP23 brain extract (Fig. 6C). Although less pronounced than for the APP23 extract (approximately 40% less), robust induction of A β deposition was observed with the amyloid-laden HSC (Fig. 6D). In contrast, only minimal A β deposits were found with amyloid-free HSCs that were treated only with the APP23 extract (Fig. 6E). Fibrils of synthetic A β 1–40,

despite 40-fold higher concentration, induced only minimal A β deposition (Fig. 6F). These remarkable observations suggest that A β aggregates in HSC reproduce seeding characteristics of brain-derived A β aggregates that are absent in synthetic *in vitro* aggregated A β .

DISCUSSION

In the present work we demonstrate that HSC promote the seeded aggregation of synthetic A β and the formation of amyloid plaques. Remarkably, the A β aggregates generated in the HSC model are active *in vivo* as seeds for inducing cerebral β -amyloidosis, which emphasizes their similarity to A β seeds formed in brain. A β aggregation has recently been described in APP-overexpressing 3D human neural stem cell cultures, but its *in vivo* activity has not been tested (Shi et al., 2012; Choi et al., 2014). Moreover, according to current insights A β aggregation in the brain spreads along neuroanatomical pathways in a self-propagating non-cell autonomous process (Jucker and Walker, 2013; Raj et al., 2015) and therefore an *in vitro* system more closely mimicking the *in vivo* brain environment (Frotscher and Heimrich, 1993; Bahr, 1995; Frotscher et al., 1995) is required. The development of amyloid plaque associated pathologies in the HSC underlines the similarities of this new *in vitro* model with cerebral β -amyloidosis in a transgenic mouse brain. Of note, the amyloid-associated changes in HSC occur in wildtype brain tissue without APP overexpression and thus make seeded A β aggregation in HSC a unique and valid model of cerebral β -amyloidosis, also for sporadic AD. Pre-fixation of the HSC largely prevented A β aggregation and highlights the contribution of cellular processes to achieve biological active A β aggregates.

HSC prepared from postnatal APP tg mice did not develop A β deposits, even after 10 weeks of cultivation and despite development of robust cerebral β -amyloidosis in the corresponding 8-week-old tg mice. This may be because A β generated in HSC diffuses into the medium precluding the local buildup of sufficiently high A β levels for amyloid deposition (Waters, 2010). The recently reported A β deposition in human cell cultures (Shi et al., 2012; Choi et al., 2014) is probably related to the used Matrigel, a gelatinous mixture of extracellular matrix proteins that should trap A β . However, we achieved amyloid plaque formation in HSC by repeatedly adding synthetic A β to the medium and brain-derived A β seeds once to the culture. This seeded A β aggregation can occur independent of endogenous A β generation and may be initiated at cellular membrane structures (Nagarathinam et al., 2013). Interestingly, however, seeded A β aggregation requires functional, living HSCs (membranes), as inactivation prior to cultivation largely eliminated amyloid deposition. Consistently, in previous work using a variety of cell lines and medium supplemented with A β (albeit in at least 10 fold higher concentration than in the present work), it was found that A β aggregates occurred only in the presence of living cells (Friedrich et al., 2010), although again its *in vivo* activity was not tested.

Our data demonstrate that A β plaque formation occurs via templated conversion of synthetic A β exemplified by the achievement of different A β morphotypes depending on the nature of the synthetic A β species in the medium (A β 1–40 vs A β 1–42) and also on the applied brain extract (APP23 or APPPS1 mice). Polymorphic A β deposits and structural A β variants have also been described in APP tg mouse models (Heilbronner et al., 2013) and AD brain (Lu et al., 2013) and different A β conformers have different biological activities *in vitro* (Petkova et al., 2005; Eisenberg and Jucker, 2012).

Although *in vitro* aggregated synthetic A β can act as an *in vivo* seed in APP tg mice (Stohr et al., 2012), its seeding activity is at least 100x less potent than brain-derived aggregated A β (Meyer-Luehmann et al., 2006; Stohr et al., 2012). In contrast, HSC-derived aggregated A β shows seeding activity within the same order of magnitude as brain-derived aggregated A β . This is consistent with the idea that brain seeds impose their structure on the synthetic A β and render it seeding active. The strong reduction of A β aggregation by fixation prior to treatment suggests a factor in living HSC (and thus the brain) which contributes to the seeded A β aggregation.

A β plaque features (congophilic amyloid, star-like appearance and parallel fibril bundles at ultrastructural level) and associated neural changes in HSC (dystrophic and phosphorylated Tau-positive neurites, loss of dendritic spines) recapitulate largely the amyloid-associated neural changes in APP tg mouse models (Masliah et al., 1996; Phinney et al., 1999; Spires et al., 2005; Bittner et al., 2010; Rupp et al., 2011) and AD brain (Probst et al., 1983). However and most remarkably, these amyloid features and neural changes in HSC occur in response to the induced aggregation of exogenously applied synthetic A β . Equally important and of note, all these changes occur in wildtype tissue and thus avoid the potential confounding overexpression of APP present in transgenic mice (Jucker, 2010).

Microglia in HSCs show a typical ramified morphology (Hailer et al., 1996; Skibo et al., 2000), which was retained throughout the 10 week HSC period. Although microglia were more numerous and hypertrophic in areas with A β plaques (typically around the rim of the culture) indicating that a local inflammatory and phagocytic response was taking place, the tight clustering of microglia observed around A β deposits *in vivo* was not observed in HSC. This may be a result of the disruption of localized signals and microglial chemotaxis due to dilution of chemoattractants and/or the presence of synthetic A β in the culture medium. When microglia were depleted in HSC, the total A β load was not changed but a shift to more dense-cored plaques was found. Interestingly, this finding is

reminiscent of our *in vivo* observations, where in microglia-depleted APP23 animals a small but significant decrease in the diffuse A β load and a tendency towards an increase in the dense-cored amyloid load (albeit not significant) was observed after 4 weeks (Grathwohl et al., 2009). The lack of changes in total A β load after microglia-depletion *in vitro* and *in vivo* may at least partly be explained by overwhelming A β aggregation over (physiological) removal.

In summary, we have demonstrated that A β aggregation and many of the previously described neuronal changes in APP tg mice and AD brain can be achieved by the seeded conversion of synthetic A β in living wildtype brain tissue. HSC combine advantages of *in vitro* tissue culture and *in vivo* analysis of mouse models. This easily accessible system is amenable to experimental manipulation and live imaging. Systems that model the complex brain environment are urgently needed to study the mechanisms governing A β aggregation *in vivo*, the downstream pathological processes of neurodegeneration, and to test therapeutic approaches. The finding of seeded conversion of synthetic A β into biologically active A β aggregates should ease further studies aiming at deciphering the factors responsible for its conversion.

REFERENCES

- Bahr BA (1995) Long-term hippocampal slices: a model system for investigating synaptic mechanisms and pathologic processes. *J Neurosci Res* 42:294-305.
- Bittner T, Fuhrmann M, Burgold S, Ochs SM, Hoffmann N, Mitteregger G, Kretzschmar H, LaFerla FM, Herms J (2010) Multiple events lead to dendritic spine loss in triple transgenic Alzheimer's disease mice. *PLoS One* 5:e15477.
- Bondolfi L, Calhoun M, Ermini F, Kuhn HG, Wiederhold KH, Walker L, Staufenbiel M, Jucker M (2002) Amyloid-associated neuron loss and gliogenesis in the neocortex of amyloid precursor protein transgenic mice. *J Neurosci* 22:515-522.
- Brinks H, Conrad S, Vogt J, Oldekamp J, Sierra A, Deitinghoff L, Bechmann I, Alvarez-Bolado G, Heimrich B, Monnier PP, Mueller BK, Skutella T (2004) The repulsive guidance molecule RGMA is involved in the formation of afferent connections in the dentate gyrus. *J Neurosci* 24:3862-3869.
- Calhoun ME, Wiederhold KH, Abramowski D, Phinney AL, Probst A, Sturchler-Pierrat C, Staufenbiel M, Sommer B, Jucker M (1998) Neuron loss in APP transgenic mice. *Nature* 395:755-756.
- Choi SH, Kim YH, Heisch M, Sliwinski C, Lee S, D'Avanzo C, Chen H, Hooli B, Asselin C, Muffat J, Klee JB, Zhang C, Wainger BJ, Peitz M, Kovacs DM, Wolf CJ, Wagner SL, Tanzi RE, Kim DY (2014) A three-dimensional human neural cell culture model of Alzheimer's disease. *Nature* 515:274-278.
- DaSilva KA, Shaw JE, McLaurin J (2010) Amyloid-beta fibrillogenesis: structural insight and therapeutic intervention. *Exp Neurol* 223:311-321.
- Del Turco D, Deller T (2007) Organotypic entorhino-hippocampal slice cultures--a tool to study the molecular and cellular regulation of axonal regeneration and collateral sprouting in vitro. *Methods Mol Biol* 399:55-66.
- Du D, Murray AN, Cohen E, Kim HE, Simkovsky R, Dillin A, Kelly JW (2011) A kinetic aggregation assay allowing selective and sensitive amyloid-beta quantification in cells and tissues. *Biochemistry* 50:1607-1617.
- Duyckaerts C, Potier MC, Delatour B (2008) Alzheimer disease models and human neuropathology: similarities and differences. *Acta Neuropathol* 115:5-38.
- Eisele YS, Obermuller U, Heilbronner G, Baumann F, Kaeser SA, Wolburg H, Walker LC, Staufenbiel M, Heikenwalder M, Jucker M (2010) Peripherally applied Abeta-containing inoculates induce cerebral beta-amyloidosis. *Science* 330:980-982.
- Eisele YS, Fritschi SK, Hamaguchi T, Obermuller U, Fuger P, Skodras A, Schafer C, Odenthal J, Heikenwalder M, Staufenbiel M, Jucker M (2014) Multiple factors contribute to the peripheral induction of cerebral beta-amyloidosis. *J Neurosci* 34:10264-10273.
- Eisenberg D, Jucker M (2012) The amyloid state of proteins in human diseases. *Cell* 148:1188-1203.

- Feng G, Mellor RH, Bernstein M, Keller-Peck C, Nguyen QT, Wallace M, Nerbonne JM, Lichtman JW, Sanes JR (2000) Imaging neuronal subsets in transgenic mice expressing multiple spectral variants of GFP. *Neuron* 28:41-51.
- Friedrich RP, Tepper K, Ronicke R, Soom M, Westermann M, Reymann K, Kaether C, Fandrich M (2010) Mechanism of amyloid plaque formation suggests an intracellular basis of Abeta pathogenicity. *Proc Natl Acad Sci U S A* 107:1942-1947.
- Fritschy SK, Cintron A, Ye L, Mahler J, Buhler A, Baumann F, Neumann M, Nilsson KP, Hammarstrom P, Walker LC, Jucker M (2014) Abeta seeds resist inactivation by formaldehyde. *Acta Neuropathol* 128:477-484.
- Frotscher M, Heimrich B (1993) Formation of layer-specific fiber projections to the hippocampus in vitro. *Proc Natl Acad Sci U S A* 90:10400-10403.
- Frotscher M, Zafirov S, Heimrich B (1995) Development of identified neuronal types and of specific synaptic connections in slice cultures of rat hippocampus. *Prog Neurobiol* 45:vii-xxviii.
- Games D, Adams D, Alessandrini R, Barbour R, Berthelette P, Blackwell C, Carr T, Clemens J, Donaldson T, Gillespie F, et al. (1995) Alzheimer-type neuropathology in transgenic mice overexpressing V717F beta-amyloid precursor protein. *Nature* 373:523-527.
- Grathwohl SA, Kalin RE, Bolmont T, Prokop S, Winkelmann G, Kaeser SA, Odenthal J, Radde R, Eldh T, Gandy S, Aguzzi A, Staufenbiel M, Mathews PM, Wolburg H, Heppner FL, Jucker M (2009) Formation and maintenance of Alzheimer's disease beta-amyloid plaques in the absence of microglia. *Nat Neurosci* 12:1361-1363.
- Hailer NP, Jarhult JD, Nitsch R (1996) Resting microglial cells in vitro: analysis of morphology and adhesion molecule expression in organotypic hippocampal slice cultures. *Glia* 18:319-331.
- Hardy J, Selkoe DJ (2002) The amyloid hypothesis of Alzheimer's disease: progress and problems on the road to therapeutics. *Science* 297:353-356.
- Harper JD, Lansbury PT, Jr. (1997) Models of amyloid seeding in Alzheimer's disease and scrapie: mechanistic truths and physiological consequences of the time-dependent solubility of amyloid proteins. *Annu Rev Biochem* 66:385-407.
- Harris-White ME, Chu T, Balverde Z, Sigel JJ, Flanders KC, Frautschy SA (1998) Effects of transforming growth factor-beta (isoforms 1-3) on amyloid-beta deposition, inflammation, and cell targeting in organotypic hippocampal slice cultures. *J Neurosci* 18:10366-10374.
- Heilbronner G, Eisele YS, Langer F, Kaeser SA, Novotny R, Nagarathinam A, Aslund A, Hammarstrom P, Nilsson KP, Jucker M (2013) Seeded strain-like transmission of beta-amyloid morphotypes in APP transgenic mice. *EMBO Rep* 14:1017-1022.
- Holtzman DM, Morris JC, Goate AM (2011) Alzheimer's disease: the challenge of the second century. *Sci Transl Med* 3:77sr71.
- Hsiao K, Chapman P, Nilsen S, Eckman C, Harigaya Y, Younkin S, Yang F, Cole G (1996) Correlative memory deficits, abeta elevation, and amyloid plaques in transgenic mice. *Science* 274:99-102.

- Itagaki S, McGeer PL, Akiyama H, Zhu S, Selkoe D (1989) Relationship of microglia and astrocytes to amyloid deposits of Alzheimer disease. *J Neuroimmunol* 24:173-182.
- Johansson S, Radesater AC, Cowburn RF, Thyberg J, Luthman J (2006) Modelling of amyloid beta-peptide induced lesions using roller-drum incubation of hippocampal slice cultures from neonatal rats. *Exp Brain Res* 168:11-24.
- Jucker M (2010) The benefits and limitations of animal models for translational research in neurodegenerative diseases. *Nat Med* 16:1210-1214.
- Jucker M, Walker LC (2013) Self-propagation of pathogenic protein aggregates in neurodegenerative diseases. *Nature* 501:45-51.
- Klingstedt T, Aslund A, Simon RA, Johansson LB, Mason JJ, Nystrom S, Hammarstrom P, Nilsson KP (2011) Synthesis of a library of oligothiophenes and their utilization as fluorescent ligands for spectral assignment of protein aggregates. *Org Biomol Chem* 9:8356-8370.
- Kohl A, Dehghani F, Korf HW, Hailer NP (2003) The bisphosphonate clodronate depletes microglial cells in excitotoxically injured organotypic hippocampal slice cultures. *Exp Neurol* 181:1-11.
- Langer F, Eisele YS, Fritschi SK, Staufenbiel M, Walker LC, Jucker M (2011) Soluble A β seeds are potent inducers of cerebral beta-amyloid deposition. *J Neurosci* 31:14488-14495.
- Lu JX, Qiang W, Yau WM, Schwieters CD, Meredith SC, Tycko R (2013) Molecular structure of beta-amyloid fibrils in Alzheimer's disease brain tissue. *Cell* 154:1257-1268.
- Mackenzie IR, Hao C, Munoz DG (1995) Role of microglia in senile plaque formation. *Neurobiol Aging* 16:797-804.
- Maslah E, Sisk A, Mallory M, Mucke L, Schenk D, Games D (1996) Comparison of neurodegenerative pathology in transgenic mice overexpressing V717F beta-amyloid precursor protein and Alzheimer's disease. *J Neurosci* 16:5795-5811.
- Mayer D, Fischer H, Schneider U, Heimrich B, Schwemmler M (2005) Borna disease virus replication in organotypic hippocampal slice cultures from rats results in selective damage of dentate granule cells. *J Virol* 79:11716-11723.
- Meyer-Luehmann M, Coomaraswamy J, Bolmont T, Kaeser S, Schaefer C, Kilger E, Neuenschwander A, Abramowski D, Frey P, Jaton AL, Vigouret JM, Paganetti P, Walsh DM, Mathews PM, Ghiso J, Staufenbiel M, Walker LC, Jucker M (2006) Exogenous induction of cerebral beta-amyloidogenesis is governed by agent and host. *Science* 313:1781-1784.
- Morales-Corraliza J, Mazzella MJ, Berger JD, Diaz NS, Choi JH, Levy E, Matsuoka Y, Planel E, Mathews PM (2009) In vivo turnover of tau and APP metabolites in the brains of wild-type and Tg2576 mice: greater stability of sAPP in the beta-amyloid depositing mice. *PLoS One* 4:e7134.
- Nagarathinam A, Hoflinger P, Buhler A, Schaefer C, McGovern G, Jeffrey M, Staufenbiel M, Jucker M, Baumann F (2013) Membrane-anchored A β accelerates amyloid formation and exacerbates amyloid-associated toxicity in mice. *J Neurosci* 33:19284-19294.

- Paravastu AK, Qahwash I, Leapman RD, Meredith SC, Tycko R (2009) Seeded growth of beta-amyloid fibrils from Alzheimer's brain-derived fibrils produces a distinct fibril structure. *Proc Natl Acad Sci U S A* 106:7443-7448.
- Petkova AT, Leapman RD, Guo Z, Yau WM, Mattson MP, Tycko R (2005) Self-propagating, molecular-level polymorphism in Alzheimer's beta-amyloid fibrils. *Science* 307:262-265.
- Phinney AL, Deller T, Stalder M, Calhoun ME, Frotscher M, Sommer B, Staufenbiel M, Jucker M (1999) Cerebral amyloid induces aberrant axonal sprouting and ectopic terminal formation in amyloid precursor protein transgenic mice. *J Neurosci* 19:8552-8559.
- Probst A, Basler V, Bron B, Ulrich J (1983) Neuritic plaques in senile dementia of Alzheimer type: a Golgi analysis in the hippocampal region. *Brain Res* 268:249-254.
- Radde R, Bolmont T, Kaeser SA, Coomaraswamy J, Lindau D, Stoltze L, Calhoun ME, Jaggi F, Wolburg H, Gengler S, Haass C, Ghetti B, Czech C, Holscher C, Mathews PM, Jucker M (2006) Abeta42-driven cerebral amyloidosis in transgenic mice reveals early and robust pathology. *EMBO Rep* 7:940-946.
- Raj A, LoCastro E, Kuceyeski A, Tosun D, Relkin N, Weiner M, for the Alzheimer's Disease Neuroimaging I (2015) Network diffusion model of progression predicts longitudinal patterns of atrophy and metabolism in Alzheimer's disease. *Cell Rep* 10:359-369.
- Rupp NJ, Wegenast-Braun BM, Radde R, Calhoun ME, Jucker M (2011) Early onset amyloid lesions lead to severe neuritic abnormalities and local, but not global neuron loss in APPS1 transgenic mice. *Neurobiol Aging* 32:2324 e2321-2326.
- Shi Y, Kirwan P, Smith J, MacLean G, Orkin SH, Livesey FJ (2012) A human stem cell model of early Alzheimer's disease pathology in down syndrome. *Sci Transl Med* 4:124ra129.
- Skibo GG, Nikonenko IR, Savchenko VL, McKanna JA (2000) Microglia in organotypic hippocampal slice culture and effects of hypoxia: ultrastructure and lipocortin-1 immunoreactivity. *Neuroscience* 96:427-438.
- Spires TL, Meyer-Luehmann M, Stern EA, McLean PJ, Skoch J, Nguyen PT, Bacskai BJ, Hyman BT (2005) Dendritic spine abnormalities in amyloid precursor protein transgenic mice demonstrated by gene transfer and intravital multiphoton microscopy. *J Neurosci* 25:7278-7287.
- Stalder M (2001) 3D-Reconstruction of microglia and amyloid in APP23 transgenic mice: no evidence of intracellular amyloid. *Neurobiol Aging* 22:427-434.
- Stalder M, Phinney A, Probst A, Sommer B, Staufenbiel M, Jucker M (1999) Association of microglia with amyloid plaques in brains of APP23 transgenic mice. *Am J Pathol* 154:1673-1684.
- Stohr J, Watts JC, Mensinger ZL, Oehler A, Grillo SK, DeArmond SJ, Prusiner SB, Giles K (2012) Purified and synthetic Alzheimer's amyloid beta (Abeta) prions. *Proc Natl Acad Sci U S A* 109:11025-11030.
- Sturchler-Pierrat C, Abramowski D, Duke M, Wiederhold KH, Mistl C, Rothacher S, Ledermann B, Burki K, Frey P, Paganetti PA, Waridel C, Calhoun ME, Jucker M, Probst A, Staufenbiel M,

Sommer B (1997) Two amyloid precursor protein transgenic mouse models with Alzheimer disease-like pathology. *Proc Natl Acad Sci U S A* 94:13287-13292.

Terry RD, Gonatas NK, Weiss M (1963) Ultrastructural studies in Alzheimer's presenile dementia. *Am J Pathol* 44:269-297.

Vlachos A, Muller-Dahlhaus F, Roskopp J, Lenz M, Ziemann U, Deller T (2012) Repetitive magnetic stimulation induces functional and structural plasticity of excitatory postsynapses in mouse organotypic hippocampal slice cultures. *J Neurosci* 32:17514-17523.

Waters J (2010) The concentration of soluble extracellular amyloid-beta protein in acute brain slices from CRND8 mice. *PLoS One* 5:e15709.

Figures

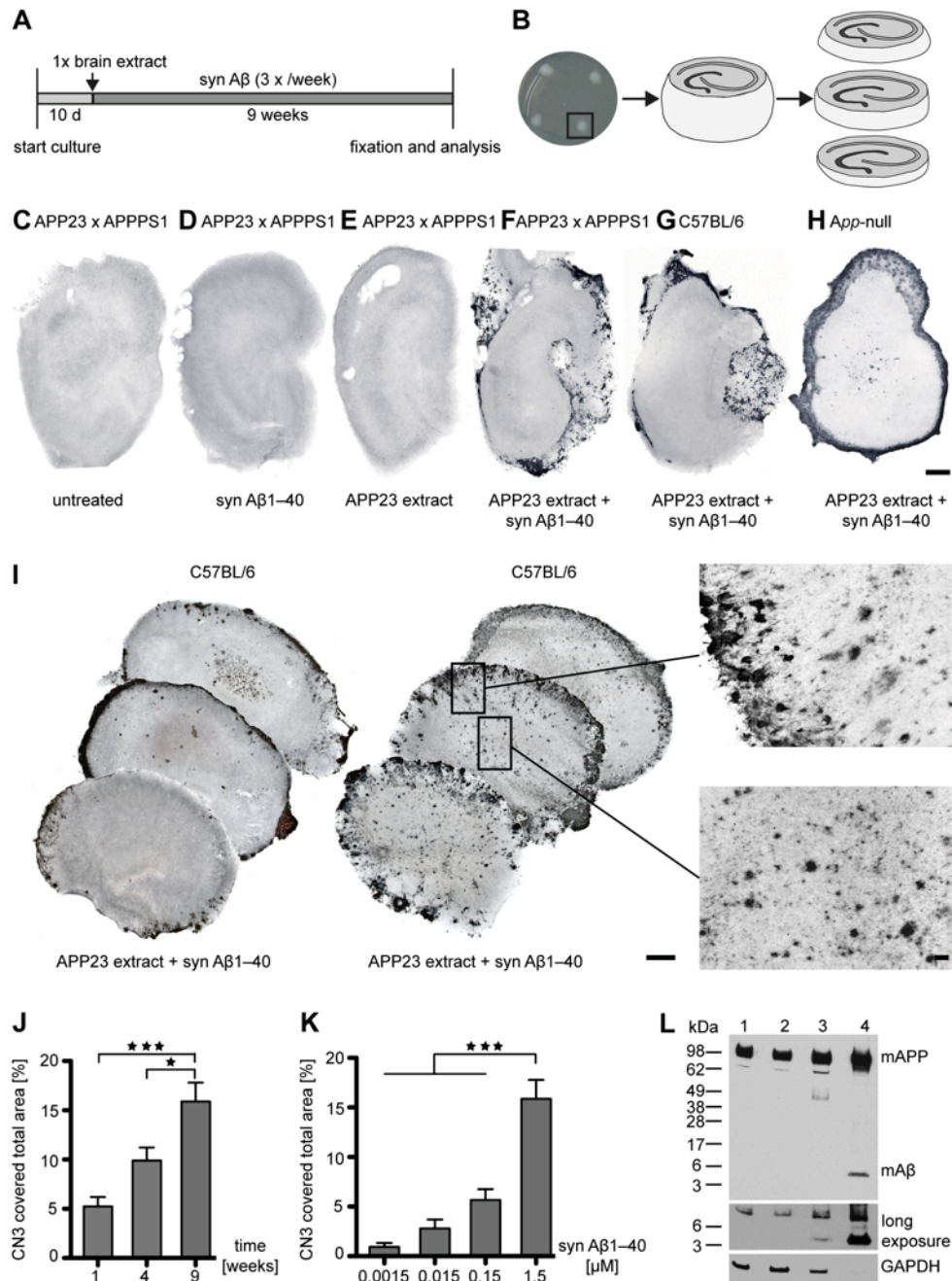


Figure 1. Aβ deposition in HSC is induced by seeded aggregation of synthetic Aβ. (A) Experimental protocol. HSC were kept 10 days to achieve stable culture conditions. Thereafter HSC were treated once with brain extract and the medium was supplemented with synthetic (syn) Aβ during the following 9-week culture period. (B) Image of four HSC placed on a membrane inset and illustration of one 150 μm thick HSC. Slices were fixed and further sectioned into 50 μm thick slices, enabling separate examination of top, intermediate and bottom layers for each slice of the culture. (C) Aβ-immunostained untreated HSC of an APP23 x APPPS1 double tg mouse after 10 weeks of cultivation. No Aβ deposition could be detected. (D, E) Similarly, no Aβ deposition was observed in HSC of APP23 x APPPS1 mice when the medium was supplemented with 1.5 μM human syn Aβ1-

40 (D) or when HSC was treated once with brain extract of an aged APP23 tg mouse (E). (F) In contrast, robust A β -deposition (A β -immunostaining) was observed in HSC of APP23 x APPPS1 mice treated once with APP23 brain extract and medium supplemented with 1.5 μ M human syn A β 1–40. (G, H) A β deposition was also observed in HSC of wildtype (G) and *App*-null mice (H) when treated on top once with brain extract and continuously with human syn A β 1–40 in the medium. (I) Two examples of top, intermediate and bottom layers of wildtype HSC treated with APP23 brain extract and 1.5 μ M A β 1–40 show dominant A β deposits at the rim of all sections but also smaller fibrillar deposits in the center of the culture. Boxed areas are shown at higher magnifications. (J, K) Induced A β deposition in HSC was time-dependent and dependent on the A β concentration in the medium. Quantification of the induced A β load (%) at 1, 4, and 9 weeks with 1.5 μ M syn A β 1–40 in the medium (n=11 cultures/time point; ANOVA, F(2,30)=13.45; p<0.0001; Tukey's post-hoc multiple comparison test, *p<0.05; *** p<0.001) (J). Induced A β load (%)9 weeks after treatment with various concentrations of human syn A β 1–40 in the medium (n=10–13 cultures/concentration; ANOVA, F(3,42)=32.18; p<0.0001; Tukey's post-hoc multiple comparison test, *** p<0.001) (K). (L) Immunoblot analysis with an antibody specific to murine (m) A β revealed a faint A β band in the APP23 brain extract (lane 4) and, upon longer incubation, also in HSC treated with APP23 extract and human syn A β in the medium (lane 3), but not in HSC treated with APP23 brain extract alone (lane 2; lane 1 shows an untreated HSC). This indicates that at least some HSC-derived murine A β is co-deposited with human A β in HSC. GAPDH was used as loading control. Scale bar: 200 μ m (C–H and I), 20 μ m (boxes in I).

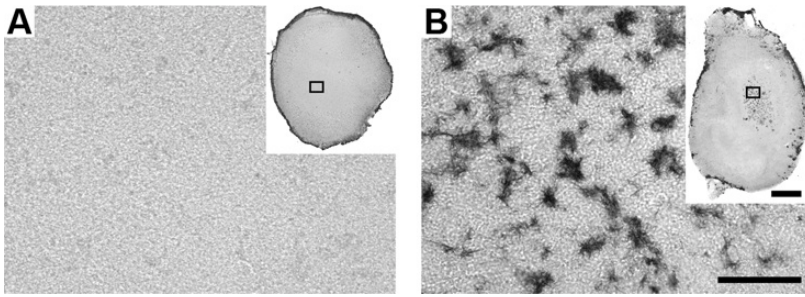


Figure 2. Hippocampal slice cultures fixed prior to treatment reveal only modest A β deposits and only at the rim of the culture. (A) Hippocampal slice cultures were fixed in 4% PFA before treatment with APP23 brain homogenate and synthetic A β 1–40. A β deposits (anti-A β -immunostaining) were only observed at the edge of the HSC (insert a) while no A β deposits were found in the center of the section (A). (B) In contrast numerous A β deposits were found with the same treatment in living HSC (see also Figure 1). Scale bar: 50 μ m (A, B); 200 μ m (inserts).

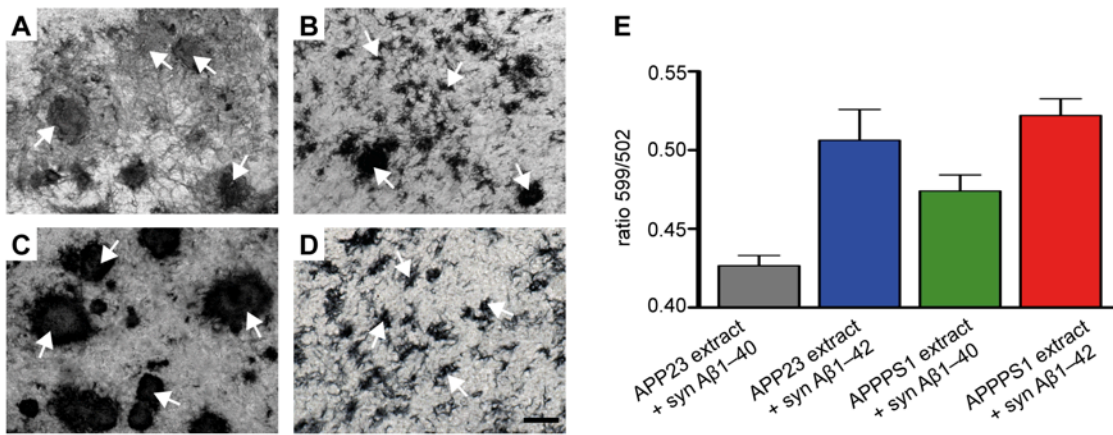


Figure 3. A β morphotypes in HSC depend on the seed and synthetic A β species. (A–D) Differences in structural appearance of induced A β deposits (immunostained with CN3 antibody) in 10-week-old HSC inoculated with different brain extracts and incubated with 1.5 μ M of either synthetic (syn) A β 1–40 or A β 1–42 in the culture medium. (A) Large fibrillary deposits of A β (arrows) were observed with APP23 brain extract and syn A β 1–40. (B) Inoculation with APP23 brain extract and syn A β 1–42 revealed a mixed pattern of small and large fibrillary deposits. (C) APPPS1 brain extract combined with syn A β 1–40 revealed large and compact A β deposits, while (D) numerous small A β deposits (arrows) were seen with APPPS1 brain extract and syn A β 1–42. Scale bar: 20 μ m for A–D. (E) Spectral properties of the induced A β deposits using the conformation-dependent amyloid-specific dye pFTAA. For quantitative comparison the ratio of light emitted at 599 nm and 502 nm was assessed for individual A β deposits and the mean ratio determined per HSC. Per condition 11–13 HSC were analysed and mean and SEM are presented. ANOVA (extract x syn A β) revealed a significant effect for extract ($F(1,43)=6.41$; $p<0.05$) and syn A β ($F(1,43)=26.17$; $p<0.001$) but failed to reach significance for the interaction ($F(1,43)=1.61$; $p>0.05$).

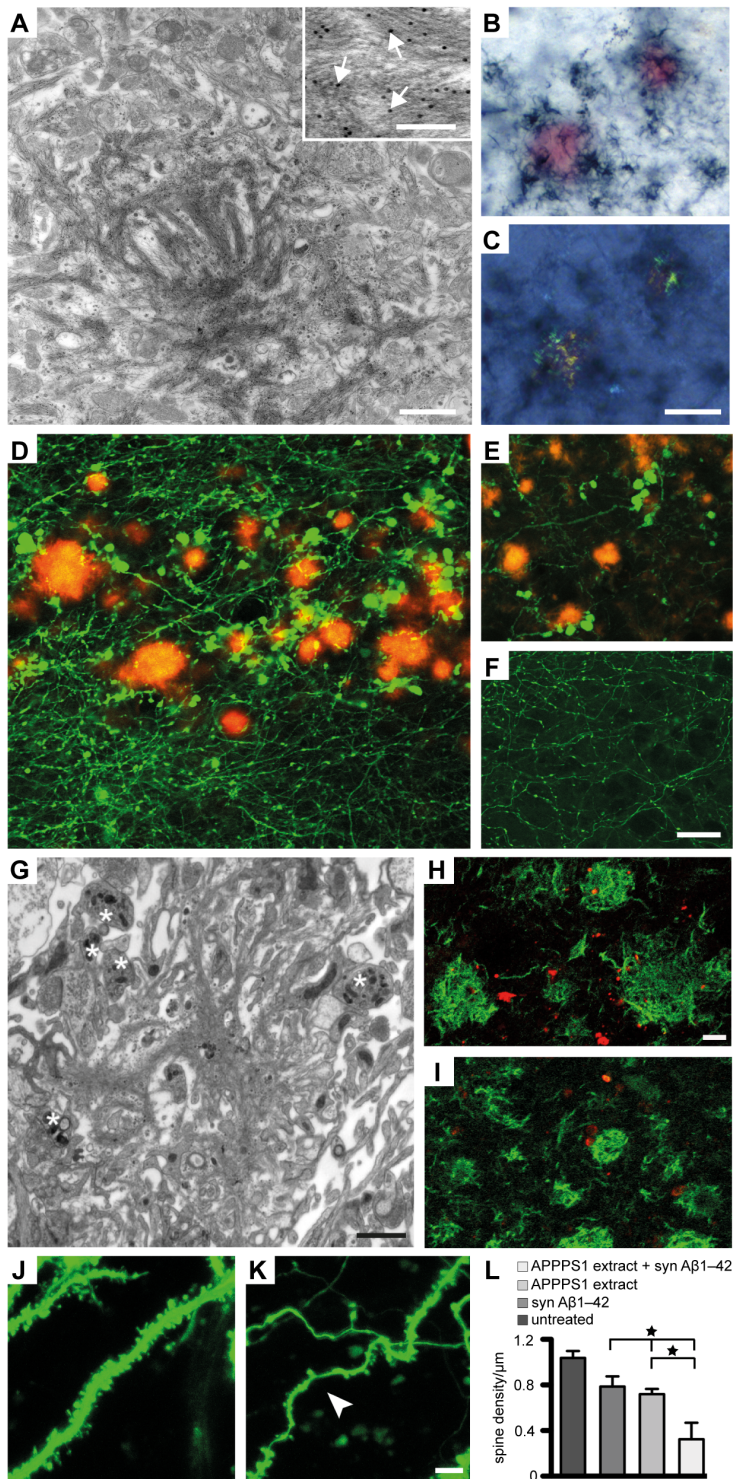


Figure 4. Pathology associated with seeded Aβ deposition in 10-week-old HSC. (A) Immunoelectron microscopy of induced Aβ deposits in wildtype HSC treated with APP23 tg brain extract once on top and continuously supplemented with synthetic Aβ1-40 in the media revealed the typical bundles of amyloid fibrils interdigitated with cellular elements. Insert shows anti-Aβ-immunogold labeled amyloid fibers (arrows) at high magnification. (B, C) Congo red-stained compact Aβ deposits in HSC treated as in (A) combined with Aβ-immunostaining (dark-blue) under normal light (B) and with the characteristic apple-green birefringence between crossed polarizers (C). (D, E) Dystrophic GFP-positive structures in the vicinity of the induced Aβ deposits (Aβ immunostaining, red) in HSC of Thy1-GFP mice treated with APPPS1 brain extract and syn Aβ1-42. Dystrophic

neuritic elements were observed in stratum oriens (D) but they were also found in stratum radiatum and stratum lacunosum-moleculare of CA1 (E). Dystrophic elements were virtually absent in untreated cultures (F), cultures treated only with brain extract or only with syn A β 1–42 (data not shown). Immuno-electron microscopy reveals an amyloid plaque in the stratum oriens (G) surrounded by several dystrophic boutons (asterisk). (H, I) Dystrophic structures and boutons were (at least partly) also immunopositive for hyperphosphorylated tau (AT8 antibody; red in H) and neurofilament light chain (red in I). The A β deposits were visualized with CN3 (green). (J, K) Dendritic spines in HSCs prepared from Thy1-GFP mice. Dendritic segments with numerous spines were observed in untreated HSCs (J). In contrast curved and thinned (arrowhead) dendritic segments with only very few spines were present in HSC treated with APPPS1 extract and syn A β 1–42 (K). The number of dendritic spines/ μ m on side branches of apical dendrites (CA1 pyramidal neurons, stratum radiatum) was significantly reduced in HSC with A β deposits (L) compared to control cultures treated only with syn A β 1–42 or APPPS1 brain extract and compared to untreated cultures (n=4 cultures per group; 3–8 segments analyzed in each culture; ANOVA, F(3,12)=10.21; p<0.001; post-hoc Tukey's Multiple Comparison, *p<0.05). Scale bar: 1 μ m (A), 0.1 μ m (insert), 20 μ m (B, C), 20 μ m (D–F), 1 μ m (G), 5 μ m (H, I), and 5 μ m (J, K).

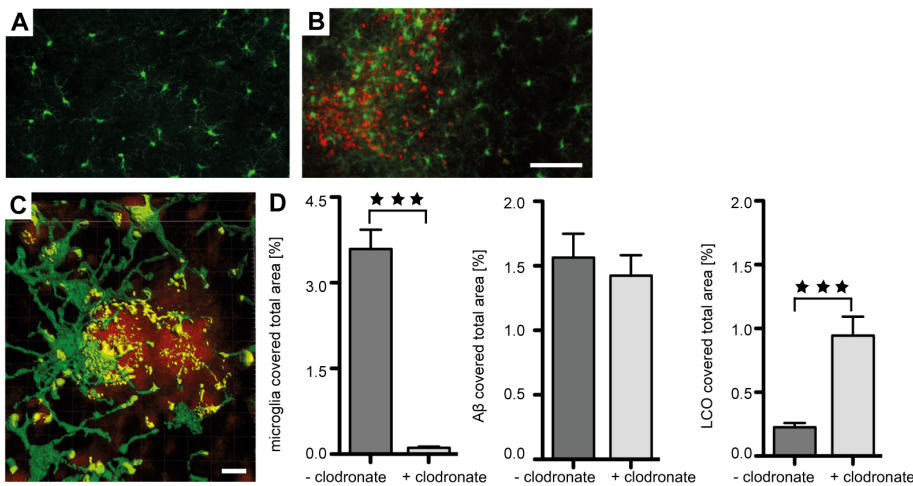


Figure 5. Microglia-amyloid interaction and microglia depletion in HSC. (A, B) Double immuno-labeling of microglia (anti-Iba1, green) and A β (anti-A β , red) revealed the scattered distribution of microglial cells in untreated HSC and thus in the absence of A β deposits (A). In contrast, in HSC treated with APP23 brain extract and synthetic A β 1–40 microglia were more numerous and appeared hypertrophic in areas rich in A β deposits (B). Scale bar: 20 μ m (for A and B). (C) Confocal imaging and 3D surface reconstruction of microglia (Iba-1, green) and amyloid plaques (qFTAA, red) reveals a tight association of microglia processes with the amyloid suggestive of some uptake/interaction with the amyloid (yellow). Scale bar: 100 μ m. (D) Clodronate treatment of HSCs greatly depleted microglia. Shown are 8 week-old HSC (n=29 and 25 cultures/group for depleted and control, respectively; Mann-Whitney U test; ***p<0.001). A similar microglia depletion was already found after 1 week in culture consistent with previous reports (Kohl et al., 2003). Despite the microglia depletion, no significant effect on the induced total A β deposition was found (p=0.640). However, when the amyloid-specific dye qFTAA was used a significant increase was found (p< 0.001). Mean and SEM are shown.

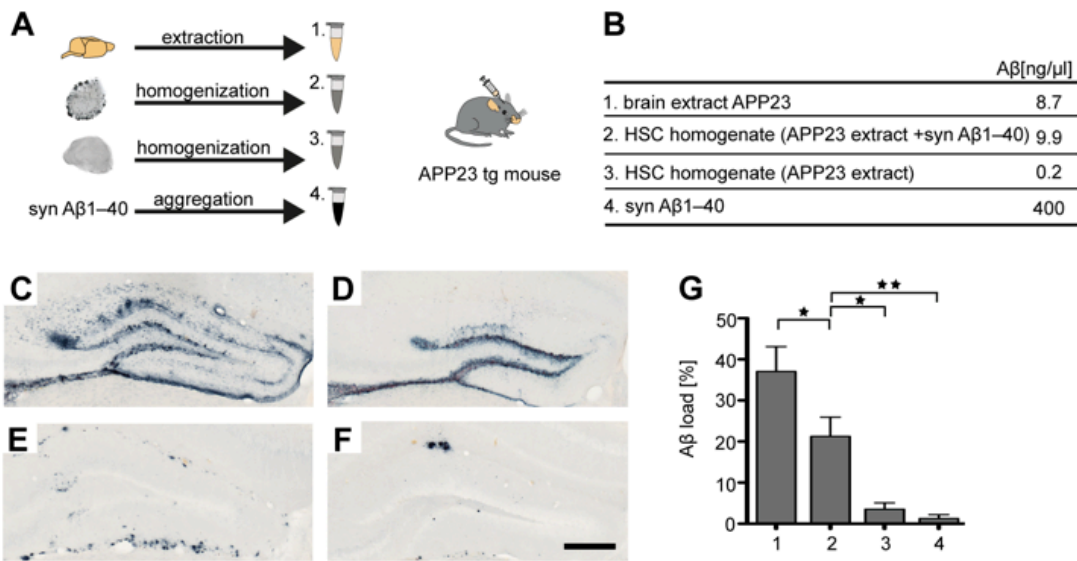


Figure 6. HSC homogenates with A β deposits induce β -amyloidosis upon inoculation in APP tg mice. (A) Preparation of the different inoculates; (1) Brain extract of an aged APP23 tg mouse was used as a control; (2) Homogenates of HSC with abundant A β deposits (induced with APP23 extract and syn A β 1-40); (3) Homogenates of HSC that lack A β deposits (treated only with APP23 extract); (4) preaggregated synthetic A β 1-40. (B) A β concentrations in the different preparations. (C-F) Different preparations were injected into the hippocampus of young, 4-month-old APP23 tg mice on an *App*-null background (abbreviated here as APP23 tg mice). Brains were immunohistochemically analyzed for A β deposition together with Congo red staining 4 months later. The injection of the APP23 brain extract induced the expected A β deposition in hippocampus (dentate gyrus, C). Homogenates of amyloid-laden HSC also induced overt, albeit less, A β deposition (D) while homogenates from HSCs only treated with APP23 extract revealed minor A β deposition (E). Preaggregated synthetic A β only induced sparse and very localized A β deposition (F). (G) Stereological quantification of the induced A β load in the dentate gyrus (n=6-7/group; ANOVA, F(3,21)=19.45; p<0.0001; Tukey's post-hoc multiple comparison test, *p<0.05; **p<0.01). Scale bar 200 μ m (C-F).

3.4 Organotypic hippocampal slice cultures as a new tool to study α -synuclein lesions

Renata Novotny*, Mehtap Bacioglu*, Manuel Schweighauser, Jasmin Mahler, K. Peter R. Nilsson, Bernd Heimrich and Mathias Jucker

unpublished data

Organotypic hippocampal slice cultures as a new tool to study α -synuclein lesions

Renata Novotny^{1,2,3*}, Mehtap Bacioglu^{1,2,3*}, Manuel Schweighauser^{1,2,3}, Jasmin Mahler^{1,2,3}, K.
Peter R. Nilsson⁴, Bernd Heimrich⁵ and Mathias Jucker^{1,2}

¹Department of Cellular Neurology, Hertie Institute for Clinical Brain Research, University of Tübingen, D-72076 Tübingen, Germany; ²DZNE, German Center for Neurodegenerative Diseases, D-72076 Tübingen, Germany; ³Graduate School for Cellular and Molecular Neuroscience, University of Tübingen, D-72076 Tübingen, Germany; ⁴Department of Chemistry, IFM, Linköping University, SE-581 83 Linköping, Sweden; ⁵Institute of Anatomy and Cell Biology, University of Freiburg, D-79104 Freiburg, Germany

*contributed equally

Figures: 1

Number of pages: 9

Number of words: 192 (abstract), 445 (introduction), 588 (results and discussion)

Conflict of interest: none.

Author contribution: R.N., M.B., M.S., J.M. and B.H. performed the experimental work. R.N., M.B. and J.M. carried out the analysis. Experimental design was done by R.N., M.B. and M.J. The preparation of the manuscript was done by R.N. Proofreading was done by M.B. and M.S.

Acknowledgment: We would like to thank Simone Zenker, Aileen Koch and the other members of our laboratories for help and discussions.

Correspondence to: Mathias Jucker: mathias.jucker@uni-tuebingen.de.

Summary

Parkinson's disease (PD), Dementia with Lewy Bodies (DLB) and Multiple System Atrophy (MSA) belong to a cluster of neurodegenerative diseases called α -synucleinopathies – among these PD is the clinically most recognized. The pathological hallmarks in PD are Lewy bodies (LBs) and Lewy neurites (LNs) – mainly composed by intracellular deposits of aggregated α -synuclein (α -syn). The mechanisms underlying the formation of Lewy inclusions are still under investigation, but compelling evidence suggests that α -syn pathology can be transmitted from cell-to-cell via a prion like-mechanism. We aimed to establish a hippocampal slice culture (HSC) model to study α -syn inclusions. Our study shows that untreated HSCs from α -syn transgenic (tg) mice did not develop any inclusions in the given cultivation time while one-time treatment with brain extract from spontaneously ill α -syn tg mice was sufficient to induce LB- and LN-like inclusions. We were able to induce LB- and LN-like inclusions on HSCs from wildtype (wt) mice, but not from α -syn knockout (α -syn KO) mice. Furthermore, we confirmed the amyloidogenic nature of the induced inclusions by applying luminescent conjugated oligothiophenes (LCOs). This work illustrates that HSCs have the potential to become a promising tool to study α -syn inclusions.

Introduction

Parkinson's disease (PD), Dementia with Lewy Bodies (DLB) and Multiple System Atrophy (MSA) are collectively summarized under the term α -synucleinopathy. The aggregation of the α -synuclein (α -syn) protein is central to α -synucleinopathies. The intraneuronal α -syn aggregates that manifest as Lewy bodies (LB) and Lewy neurites (LN) are neuropathological hallmark of the world's second most common neurodegenerative disease, namely PD.

Classically PD has been thought of as a cell-autonomous disease, but this had to be reconsidered after the unexpected discovery of Lewy pathology in grafted embryonic tissue in the postmortem brains of PD patients. To explain this surprising finding, a mechanism of prion-like transmission of α -syn was proposed and the concept of seeded polymerization – a nucleation-dependent process similar to the one described for prions and $A\beta$ – was suggested (Lerner and Bagic, 2008; Olanow and Prusiner, 2009). This concept gained further support by findings from recent *in vitro* studies showing that the exogenous application of α -syn fibrils induces LB-like pathology in cultured neurons (Danzer et al., 2009; Desplats et al., 2009; Volpicelli-Daley et al., 2011). Along the same line, many other groups investigated the putative prion-like behavior of α -syn *in vivo* by performing inoculation studies using α -syn preformed fibrils (PFFs) in α -syn-overexpressing transgenic (tg) mice (Luk et al., 2012b; Sacino et al., 2014) as well as in non-tg animals (Luk et al., 2012a; Masuda-Suzukake et al., 2013). Intriguingly, these experiments do not only indicate that synthetic α -syn PFFs alone are sufficient to induce LB-like pathology but also suggest that α -syn pathology might be transmitted via a mechanism reminiscent of prions. Furthermore, the injection of synthetic α -syn PFFs into α -syn knockout (α -syn KO) mice did not result in any α -syn aggregates, indicating that the recruitment of endogenous α -syn is a critical event (Luk et al., 2012a). Although, synthetic α -syn PFFs can potently induce disease-associated α -syn pathology *in vivo*, the pathological α -syn fibrils originating from brain tissue of spontaneously ill tg mice still have an enhanced templating efficiency (Luk et al., 2012a; Luk et al., 2012b). Hence it is assumed, that additional co-factors are involved, which facilitate the transmissibility of pathological aggregates, in a similar way as it was observed in APP tg mice with synthetic $A\beta$ (Meyer-Luehmann et al., 2006; Stohr et al., 2012; Novotny et al., 2016). The aim of this ongoing work is to induce α -syn inclusions in HSCs and further investigate the cell-to-cell transmission of α -syn in a brain-like cellular environment. Our results reveal that α -syn inclusions can be induced after one-time application of α -syn seed-enriched tg brain extract on HSCs derived from either

wildtype (wt) mice or α -syn tg mice. The preserved three-dimensional structure and cellular connectivity makes HSCs a useful model to study α -synucleinopathies.

Methods

Mice for hippocampal slice cultures

For the preparation of hippocampal slice cultures we used heterozygous Thy1-hA53T α -syn tg pups and non-tg littermates. This mouse line has a 16-fold overexpression of mutant human (A53T) α -syn under the murine Thy1-promoter (van der Putten et al., 2000). Furthermore, we used mouse pups lacking α -syn (α -syn KO) of the same age (Abeliovich et al., 2000).

Preparation of hippocampal slice cultures

HSCs were prepared from pups at postnatal day 4 according to previously published protocols (Mayer et al., 2005; Novotny et al., 2016). After decapitation the brains of postnatal pups were aseptically removed, the hippocampi were dissected and cut perpendicular to the longitudinal axis into 400 μ m sections with a tissue chopper. Intact hippocampal sections were transferred into petri dishes containing ice-cold buffer solution of minimum essential medium (MEM) supplemented with 2 mM GlutaMAX™ at pH 7.3. Four sections were placed onto a humidified porous membrane in a well of a six well plate with 1.2 ml culture medium. The culture medium consisted of heat-inactivated horse serum (25%), Hanks' balanced salt solution (25%) and MEM (50%), complemented with GlutaMAX™ (2 mM) adjusted to pH 7.2. HSCs were kept at 37°C in humidified CO₂-enriched atmosphere. The medium was changed three times per week.

Extract preparation from mouse brain and hippocampal slice culture

Brain extracts were prepared as previously described (Schweighauser et al., 2015). For A53T extract fresh frozen brainstems from spontaneously ill male and female Thy1-hA53T α -syn tg mice (7-8-month-old, n=3) were used. Brainstems were pooled and homogenized at 10% (w/v) in sterile PBS, vortexed and centrifuged at 3000xg for 5 min. Supernatant was collected, aliquoted and stored at -80°C until use, hereafter referred to as hA53T extract. Control extract was prepared from an aged non-tg mouse brain without cerebellum (23-month-old, male), following the same protocol as described above.

Slice culture homogenates were prepared from untreated tg HSCs. Cultures were removed from the membrane, pooled and immediately frozen on dry ice and stored at -80°C until use.

Frozen slice cultures were homogenized with a syringe in 150 μ l sterile PBS, aliquoted and stored at -80°C until use.

Treatment of hippocampal slice cultures

HSCs were kept for 10 days without any experimental treatment. At day 10 after the medium change, 1 μ l of hA53T extract was pipetted on top of each culture and 6 μ l of hA53T extract was added to the medium. Over the following 9-week cultivation period no more extract was added.

Histology and immunohistochemistry of hippocampal slice cultures

HSC were fixed with 4% paraformaldehyde (PFA) in 0.1 M phosphate buffer (PB), pH 7.4 for 2 hours. Cultures were rinsed 3 times with 0.1 M PB for 10 min. The Millipore membrane with the fixed cultures was cut off and cultures were mounted on a planar agar block and sliced into 50 μ m sections with a vibratome. Typically, 2–4 intact sections per culture were obtained and collected in PBS. Immunohistochemistry was performed according to standard protocols on mounted sections using the Vectastain Elite ABC Kit and the goat anti-rabbit secondary antibody. The primary rabbit monoclonal pS129 antibody (1:750) specific to α -syn phosphorylated at ser-129 was used. Sections were counterstained with Nuclear Fast Red according to standard protocols.

Staining with luminescent conjugated oligothiophenes

The luminescent conjugated oligothiophene (LCO) amyloid-binding dye, pentamer formyl acetic acid (pFTAA), was used in order to confirm the amyloidogenic nature of the induced inclusions. For the pFTAA staining, HSC sections were washed in PBS (3 x 10 min) and subsequently mounted on Superfrost slides. Staining with pFTAA (1.5 mM in deionized water, diluted 1:1000 in PBS) was performed similar to a previous description (Klingstedt et al., 2011). Sections were dried for 2 h at RT and then coverslipped with Dako Fluorescence Mounting Medium.

Electrochemiluminescence-linked immunoassay to measure human α -synuclein

The concentration of human α -syn in the sample was determined using the Human α -Synuclein Assay Kit (Meso Scale Diagnostics) according to manufacturer's instructions. Hippocampal slice culture homogenates were diluted 1:100 in PBS to assure measurements within the linear range of the assay.

Results and discussion

In an initial experiment, we used Thy1-hA53T α -syn tg mice and non-tg littermates to prepare HSCs using the same cultivation and fixation protocol as described previously (Novotny et al., 2016). Unfortunately, we were unable to detect any pS129-positive signal in these cultures. In one of the first α -syn inoculation studies by Luk et al., it was reported that a single inoculation event of pathological α -syn aggregates is sufficient to induce widespread α -syn pathology and to accelerate disease progression *in vivo* (Luk et al., 2012b). Based on that finding we applied this seeding paradigm to our HSC model by treating the cultures once with α -syn-laden hA53T extract (Fig. 3a). We found that hA53T extract-treated tg HSCs show LB-like and LN-like inclusions after staining with anti-pS129 α -syn antibody (Fig. 3b), whereas the control extract treated tg HSCs did not develop any α -syn inclusions (data not shown). Surprisingly, the induced inclusions could also be observed in slice cultures prepared from wt mice treated in the same way, but not in HSCs derived from α -syn KO mice. These results indicate that culture-derived α -syn (transgene or endogenous) is necessary for the induction of LB- and LN-like α -syn inclusions. This is in agreement with previously described *in vitro* observations (Volpicelli-Daley et al., 2011). In addition to pS129 immunoreactivity, induced LB- and LN-like α -syn inclusions in HSCs showed properties of amyloid, indicated by the binding of luminescent conjugated oligothiophenes (LCOs) to the β -pleated structures (Fig. 3c). To confirm that the inclusions detected in the HSCs are indeed induced exogenously, i.e. to rule out the possibility that we are detecting only the originally applied extract, we fixed the HSC after different time points (1 week, 5 weeks and 9 weeks) post treatment. In non-tg HSCs the first detectable inclusions appeared after 5 weeks post treatment, suggesting an induction of LB- and LN-like α -syn inclusions in HSCs (Fig. 3d). In contrast, no inclusions could be detected in HSCs prepared from α -syn KO mice at any time point. This result is in support of an induction rather than a simple detection of the applied seed. Nevertheless, even earlier fixation time points (directly after seed application and every second day after application in the first week post treatment) will be chosen to clarify this issue. Strikingly, we did not observe an increase of induced pathology over time (Fig. 3d). A possible explanation could be that HSCs express less α -syn over the cultivation period or progressively release α -syn into the medium due to degenerative processes. An expression analysis of α -syn in HSCs over time might help to explain this unexpected result. However, preliminary data from untreated tg HSCs showed an increase in expression of human α -syn between fresh explanted hippocampi of 4-day-old pups and 10-day-old HSCs. Afterwards the expression levels do not change significantly, indicating a

stable and continuous expression of tg α -syn protein in HSCs during the following cultivation time of 9 weeks (Fig. 3e). An expression analysis of A53T extract treated tg HSCs will be performed to clarify if the treatment itself has an effect on the expression of α -syn protein in HSCs.

Taken together, we demonstrated that α -syn aggregation can be induced after seeding since untreated HSCs did not develop any inclusions in the given cultivation time. The subject of future investigations will be the elucidation of the mechanisms underlying the seeded aggregation of α -syn. The cell-to-cell transmission of α -syn will be investigated by locally injecting labeled α -syn aggregates. Furthermore this novel system can be used as an addition to already existing *in vitro* and *in vivo* approaches.

Figures

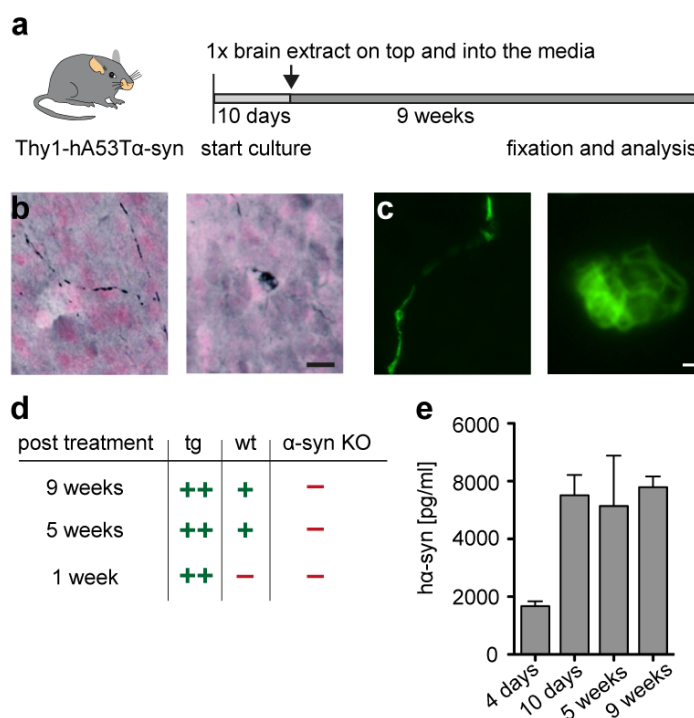


Fig. 1 (a) Experimental treatment protocol. Tg HSCs were kept 10 days to achieve stable culture conditions. Thereafter HSCs were treated once with hA53T extract on top and additionally into the medium. During the remaining cultivation time of 9 weeks, no additional treatment was performed. **(b)** Immunohistological analysis of α -syn inclusions with pS129 antibody. Shown are LN-like (left) and LB-like (right) inclusions. Cell nuclei are counterstained with Nuclear Fast Red. **(c)** Amyloidogenic properties of the induced inclusions visualized by pFTAA staining. Shown are LN-like (left) and LB-like (right) inclusions. **(d)** Qualitative assessment of the amount of induced LB- and LN-like inclusions after pS129 immunostaining on HSCs from either Thy1-hA53T α -syn (tg), non-tg littermates (wt) or α -syn knockout (α -syn KO) mice prepared and treated as described in (a). The + and the ++ reflect the amount of induced inclusions; the - reflects the absence of inclusions (n=3-9 slice cultures/timepoint and genotype). **(e)** Concentration of human α -syn in homogenates prepared from untreated tg HSCs (n=4-5 hippocampi/timepoint). Scale bar: 20 μ m (b); 1 μ m (c).

References

- Abeliovich A, Schmitz Y, Farinas I, Choi-Lundberg D, Ho WH, Castillo PE, et al. Mice lacking alpha-synuclein display functional deficits in the nigrostriatal dopamine system. *Neuron*, 2000; 25: 239-52.
- Danzer KM, Krebs SK, Wolff M, Birk G, Hengerer B. Seeding induced by alpha-synuclein oligomers provides evidence for spreading of alpha-synuclein pathology. *J. Neurochem.*, 2009; 111: 192-203.
- Desplats P, Lee HJ, Bae EJ, Patrick C, Rockenstein E, Crews L, et al. Inclusion formation and neuronal cell death through neuron-to-neuron transmission of alpha-synuclein. *Proc. Natl. Acad. Sci. U. S. A.*, 2009; 106: 13010-5.
- Klingstedt T, Aslund A, Simon RA, Johansson LB, Mason JJ, Nystrom S, et al. Synthesis of a library of oligothiophenes and their utilization as fluorescent ligands for spectral assignment of protein aggregates. *Org. Biomol. Chem.*, 2011; 9: 8356-70.
- Lerner A, Bagic A. Olfactory pathogenesis of idiopathic Parkinson disease revisited. *Mov. Disord.*, 2008; 23: 1076-84.
- Luk KC, Kehm V, Carroll J, Zhang B, O'Brien P, Trojanowski JQ, et al. Pathological alpha-synuclein transmission initiates Parkinson-like neurodegeneration in nontransgenic mice. *Science*, 2012a; 338: 949-53.
- Luk KC, Kehm VM, Zhang B, O'Brien P, Trojanowski JQ, Lee VM. Intracerebral inoculation of pathological alpha-synuclein initiates a rapidly progressive neurodegenerative alpha-synucleinopathy in mice. *J. Exp. Med.*, 2012b; 209: 975-86.
- Masuda-Suzukake M, Nonaka T, Hosokawa M, Oikawa T, Arai T, Akiyama H, et al. Prion-like spreading of pathological alpha-synuclein in brain. *Brain*, 2013; 136: 1128-38.
- Mayer D, Fischer H, Schneider U, Heimrich B, Schwemmler M. Borna disease virus replication in organotypic hippocampal slice cultures from rats results in selective damage of dentate granule cells. *J. Virol.*, 2005; 79: 11716-23.
- Meyer-Luehmann M, Coomaraswamy J, Bolmont T, Kaeser S, Schaefer C, Kilger E, et al. Exogenous induction of cerebral beta-amyloidogenesis is governed by agent and host. *Science*, 2006; 313: 1781-4.
- Novotny R, Langer F, Mahler J, Skodras A, Vlachos A, Wegenast-Braun BM, et al. Conversion of synthetic A β to *in vivo* active seeds and amyloid plaque formation in a hippocampal slice culture model. *J. Neurosci* (in press), 2016.
- Olanow CW, Prusiner SB. Is Parkinson's disease a prion disorder? *Proc. Natl. Acad. Sci. U. S. A.*, 2009; 106: 12571-2.
- Sacino AN, Brooks M, McKinney AB, Thomas MA, Shaw G, Golde TE, et al. Brain injection of alpha-synuclein induces multiple proteinopathies, gliosis, and a neuronal injury marker. *J. Neurosci.*, 2014; 34: 12368-78.
- Schweighauser M, Bacioglu M, Fritschi SK, Shimshek DR, Kahle PJ, Eisele YS, et al. Formaldehyde-fixed brain tissue from spontaneously ill alpha-synuclein transgenic mice induces fatal alpha-synucleinopathy in transgenic hosts. *Acta Neuropathol.*, 2015; 129: 157-9.

Stohr J, Watts JC, Mensinger ZL, Oehler A, Grillo SK, DeArmond SJ, et al. Purified and synthetic Alzheimer's amyloid beta (A β) prions. *Proc. Natl. Acad. Sci. U. S. A.*, 2012; 109: 11025-30.

van der Putten H, Wiederhold KH, Probst A, Barbieri S, Mistl C, Danner S, et al. Neuropathology in mice expressing human alpha-synuclein. *J. Neurosci.*, 2000; 20: 6021-9.

Volpicelli-Daley LA, Luk KC, Patel TP, Tanik SA, Riddle DM, Stieber A, et al. Exogenous alpha-synuclein fibrils induce Lewy body pathology leading to synaptic dysfunction and neuron death. *Neuron*, 2011; 72: 57-71.

4. Appendix

4.1 Abbreviations

A53T	Alanine-to-threonine amino acid substitution at position 53 of the α -synuclein gene
ABCA 7	ATP-binding cassette sub-family A member 7
AD	Alzheimer's disease
ADAM	A disintegrin and metalloprotease
AICD	APP intracellular domain
α -syn	Alpha-synuclein
APOE	Apolipoprotein E
APOE4	E4-allele of the APOE
APP	β -amyloid precursor protein
APP ₆₉₅ , APP ₇₅₁ , APP ₇₇₀	APP isoforms 695, 751, 770 amino acids in length
APP α	APPs generated by α -secretase
APP β	APPs generated by β -secretase
A β	Amyloid- β peptide
A β ₄₀ , A β ₄₂	A β ending at amino acid 40,42
A β ₂₅₋₃₅	A β peptide 36-43 amino acids in length
BACE1	β -site APP cleavage enzyme
BIN1	Bridging integrator protein 1
BSE	Bovine spongiform encephalopathy
C-terminal	Carboxyterminal
CD33	Sialic acid-binding immunoglobulin (Ig)-like lectin
CJD	Creutzfeldt-Jakob disease
CNS	Central nervous system
CR1	Complement receptor 1
CTF α /C83	CTF generated by α -secretase cleavage of APP (83 amino acids in length)
CTF β /C99	CTF generated by β -secretase cleavage of APP (99 amino acids in length)
DLB	Dementia with lewy bodies
EOAD	Early onset Alzheimer's disease
EO-FAD	Early onset familial Alzheimer's disease
FAD	Familial Alzheimer's disease
GWAS	Genome-wide association studies
HC	Hippocampus
HCHWA-D	Human hereditary cerebral hemorrhage with amyloidosis of the Dutch type
HSC	Hippocampal slice cultures
iPSCs	Induced pluripotent stem cells
kDa	Kilo Dalton
KO	Knockout
LB	Lewy body
LCO	Luminescent conjugated oligothiophene
LCP	Luminescent conjugated polythiophene
LN	Lewy neurite
LOAD	Late onset Alzheimer's disease

LO-FAD	Late onset familial Alzheimer's disease
MAPT	Microtubule associated protein tau
MCI	Mild cognitive impairment
MEM	Minimum essential medium
MSA	Multiple system atrophy
NFT	Neurofibrillary tangle
nm	Nanometer
NMR	Nuclear magnetic resonance
OSC	Organotypic slice culture
p3	Product of the APP processing
p4	Postnatal day 4
PB	Phosphate buffer
PBS	Phosphate-buffered saline
PD	Parkinson's disease
PFF	Preformed fibrils
pFTAA	Pentamer formyl acetic acid
PHF	Paired helical filament
PICALM	Phosphatidylinositol-binding clathrin assembly protein
Prion	Proteinaceous infectious particle
PrP	Prion protein
PrP ^C	Cellular PrP
PrP ^{Sc}	PrP scrapie
PS	Presenilin
pS129	Phosphorylation of serine at position 129
PSEN1, PSEN2	Gene encoding presenilin 1,2
RAGE	Receptor for advanced glycation end products
RNA	Ribonucleic acid
tg	Transgene
TREM2	Triggering receptor expressed on myeloid cells 2
TSE	Transmissible spongiform encephalopathy
wt	Wildtype
μl	Microliter

4.2 Bibliography

Publications

Götz Heilbronner, Yvonne S. Eisele, Franziska Langer, Stephan A. Kaeser, **Renata Novotny**, Amudha Nagarathinam, Andreas Åslund, Per Hammarström, K. Peter R. Nilsson & Mathias Jucker (2013). Seeded strain-like transmission of β -amyloid morphotypes in APP transgenic mice. *EMBO Reports*; 14(11):1017-1022.

Renata Novotny*, Franziska Langer*, Jasmin Mahler, Angelos Skodras, Andreas Vlachos, Bettina M. Wegenast-Braun, Stephan A. Kaeser, Jonas J. Neher, Yvonne S. Eisele, Marie J. Pietrowski, K. Peter R. Nilsson, Thomas Deller, Matthias Staufenbiel, Bernd Heimrich and Mathias Jucker (2016). Conversion of synthetic A β to *in vivo* active seeds and amyloid plaque formation in a hippocampal slice culture model. In press in *The Journal of Neuroscience*

*equal contribution, #corresponding authors

Conference proceedings

Renata Novotny*, Franziska Langer*, Jasmin Mahler, Angelos Skodras, Andreas Vlachos, Bettina M. Wegenast-Braun, Stephan A. Kaeser, Jonas J. Neher, Yvonne S. Eisele, Marie J. Pietrowski, K. Peter R. Nilsson, Thomas Deller, Matthias Staufenbiel, Bernd Heimrich and Mathias Jucker. Conversion of synthetic A β to *in vivo* active seeds and amyloid plaque formation in a hippocampal slice culture model (2013). *Alzheimer's Association International Conference, Boston, MA, USA (poster presentation)*.

Renata Novotny*, Franziska Langer*, Jasmin Mahler, Angelos Skodras, Andreas Vlachos, Bettina M. Wegenast-Braun, Stephan A. Kaeser, Jonas J. Neher, Yvonne S. Eisele, Marie J. Pietrowski, K. Peter R. Nilsson, Thomas Deller, Matthias Staufenbiel, Bernd Heimrich and Mathias Jucker. Conversion of synthetic A β to *in vivo* active seeds and amyloid plaque formation in a hippocampal slice culture model (2014). *9th Federation of European Neuroscience Societies, Milan, Italy (poster presentation)*.

Oral presentations

Renata Novotny (2014). Seeded β -amyloidosis in long-term hippocampal slice cultures. *DZNE scientific retreat, Überlingen, Germany*.

Renata Novotny (2014). Organotypische Schnittkulturen als Modell zur Erforschung der Alzheimer Erkrankung. *Statusseminar des BMBF, Berlin, Germany*.

Renata Novotny (2014). Seeded β -amyloidosis in long-term hippocampal slice cultures. *Alternatives to animal testing and research, Tübingen, Germany*.